SEA 8 Technical Report - Hydrography

R. J. Uncles* and J. A. Stephens

PML Applications Ltd., Plymouth Marine Laboratory, Prospect Place, Plymouth, Devon PL1 3DH, UK

April 2007

Technical Summary

The SEA8 region has a cool temperate climate and lies in an area subjected to variable, predominantly westerly winds with frequent gales and storms. The English Channel, St. George's Channel and Bristol Channel open westwards or south-westwards into the prevailing winds, with very long fetches into the Celtic Sea and Atlantic that result in strong wave activity. Tidal ranges at mean spring tides in the SEA8 area vary from less than 2 m on the south coast in the central English Channel to more than 12 m in the Severn Estuary. The oscillatory and predominantly twice-daily tidal currents produce bottom stresses on the seabed that influence the distribution of mobile sediments, their grain sizes and transport. Transient sediment movements result from the suspension of fine material (silt and clay) in the water column and from the bottom traction of coarser material (sand and fine-grained gravel) caused by the tidal current stresses on the seabed. Tidal stresses also produce mixing of the water column, which is an important factor that controls the advance, retreat and extent of seasonal thermal stratification of the water column within the SEA8 area. The frontal areas that separate thermally stratified waters from well-mixed waters move into the western English Channel and northern Celtic Sea in spring and retreat again in autumn. These physical features of the SEA8 region are discussed under various headings. For the broad-scale data, brief discussions and illustrations are given of coastal topography and seabed bathymetry; bed sediment distributions; mean spring tides and the dominant component tides and bed shear stresses; wind-driven currents; storm surges; winds and waves; the turbulent boundary layer on the shelf; salinity and temperature for winter and summer conditions; and the development of the seasonal thermocline across the area. Nearer-to-shore data for the SEA8 area include information on the locations of estuaries and their mean freshwater inputs at gauging stations and, for several segments of the coast between the Dover Strait and St. George's Channel, brief discussions and information on seabed bathymetry and sediments; tides, temperature and salinity; and wind and waves. Recent work is referred to that illustrates the measurement of currents at the boundaries of seasonal (tidal mixing) frontal systems as well as the spatial complexity of these seasonal (and other) frontal systems. The SEA8 region extends to the shelf break and reference is given to some recent work in this environment.

---

*Corresponding author.
E-mail address: rju@pml.ac.uk (R.J. Uncles)

ACKNOWLEDGEMENT

This document was produced as part of the UK Department of Trade and Industry's offshore energy Strategic Environmental Assessment programme. The SEA programme is funded and managed by the DTI and coordinated on their behalf by Geotek Ltd and Hartley Anderson Ltd.

CONTENTS

1. Introduction

2. Broad-scale data for the SEA8 region

2.1. Topography and bathymetry

2.2. Surficial bed sediments

2.3. Mean spring tidal ranges and phases

2.4. Tidal M_2 and S_2 water levels, currents and bed shear stresses

2.4.1. M_2 tidal water levels

2.4.2. S_2 tidal water levels

2.4.3. *Tidal water currents*

2.4.4. *Bed shear stresses and implications*

2.5. Wind-driven currents

2.5.1. Southwest winds

2.5.2. Southeast winds

2.6. Storm surge water level elevations and currents

2.7. Winds and wave heights

2.7.1. Monthly winds and extreme waves

2.7.2. Annual waves

2.8. The turbulent boundary layer on the shelf

2.9. Typical surface and bottom salinity and temperature for winter and summer

2.9.1. Temperature during winter

2.9.2. Temperature during summer

2.9.3. Salinity during winter

2.9.4. Salinity during summer

2.10. Seasonal thermocline development across the area

3. Nearer-to-shore data for the SEA8 area

3.1. Locations of estuaries and their mean freshwater inputs to SEA8

3.2. South coast, Dover Strait

3.2.1. Bathymetry and sediments

3.2.2. Tides, temperature and salinity

3.2.3. Wind and waves

3.3. South coast, eastern English Channel

3.3.1. Bathymetry and sediments
3.3.2. Tides, temperature and salinity
3.3.3. Wind and waves
3.4. Southern England
3.4.1. Bathymetry and sediments
3.4.2. Tides, temperature and salinity
3.4.3. Wind and waves
3.5. South coast of southwest England
3.5.1. Bathymetry and sediments
3.5.2. Tides, temperature and salinity
3.5.3. Wind and waves
3.6. Western Approaches
3.6.1. Bathymetry and sediments
3.6.2. Tides, temperature and salinity
3.6.3. Wind and waves
3.7. Northern Bristol Channel and St. George's Channel
3.7.1. Bathymetry and sediments
3.7.2. Tides, temperature and salinity
3.7.3. Wind and waves
4. Recent data for the SEA8 area
4.1. The DTI atlas (tides, winds and waves)
4.2. The HSE report (winds and waves)
4.3. The OMEX project (dynamics at the shelf break)
4.4. CEFAS drifter studies (density-driven flow)
4.5. PML frontal studies (visualising fronts and eddi*es)*
5. Summary
References
Figure Captions
Figures

1. Introduction

This contracted report is intended to provide a synthesis of the hydrography of the SEA8 area that gives appropriate emphasis on regional and temporal variability. It is neither a scientific review nor a research paper intended for the oceanographic research community and contains no original work. It is a technical report that is meant to convey the essential nature of the hydrography and its forcing in the SEA8 region. The majority of the information is derived from reports and papers published in the 1990s and earlier that we consider to have contributed greatly to knowledge of the region. Recent work is referred to that illustrates the measurement of currents at the boundaries of seasonal (tidal mixing) frontal systems (CEFAS, 2007) as well as the spatial complexity of these seasonal (and other) frontal systems (Miller, in press; Miller, 2007). The SEA8 region extends to the shelf break and reference is given to recent work in this environment (Huthnance et al., 2001; Wollast et al., 2001). For applied offshore applications and feasibility studies it is essential that the latest published quantitative information on tides, winds and waves are utilised (modelled or otherwise). Maps of these variables are available on the web at DTI (2004) for tides, winds and waves, and HSE (2001) for winds and waves; the producers of these maps should be consulted regarding the newest available updates.

Information in the report is given at two regional spatial scales: the broad scale, which provides an overview of the whole SEA8 area, and the local, near-shore scale, which looks at behaviour close to the coastal regions.

The SEA8 region has a cool temperate climate and lies in an area subjected to variable, predominantly westerly winds with frequent gales and storms. The English Channel, St George's Channel and Bristol Channel open westwards or south-westwards into the prevailing winds, with very long fetches into the Celtic

Sea and Atlantic that result in strong wave activity. The effect of waves on the erosion of rock is predominantly confined to a limited zone of wave attack between a few metres below low water and just above high water, leading to erosion of headlands and islands (Tappin, 1994). Less consolidated deposits are affected by wave motions only to modest (roughly 15 m) depths, except during storms. Tidal ranges on spring tides in the SEA8 area vary from less than 2 m on the south coast in the central English Channel to more than 12 m in the Severn Estuary. Wide intertidal areas are restricted to the Severn Estuary and Bristol Channel and the smaller estuaries that lie within the various coastal areas of SEA8 that are influenced by large tides. The oscillatory and predominantly twice-daily tidal currents produce bottom stresses on the seabed that influence the distribution of mobile sediments, their grain sizes and transport. Transient sediment movements result from the suspension of fine material (silt and clay) in the water column and from the bottom traction of coarser material (sand and fine-grained gravel) caused by the tidal-current stresses on the seabed. Tidal stresses also produce mixing of the water column, which is an important factor that controls the advance, retreat and extent of seasonal thermal stratification of the water column within the SEA8 area. The frontal areas that separate thermally stratified waters from well-mixed waters move into the western English Channel and northern Celtic Sea in spring and retreat again in autumn (Pingree, 1980).

These physical features of the SEA8 region are discussed under various headings. For the broad-scale data, brief discussions and illustrations are given of coastal topography and seabed bathymetry; bed sediment distributions; mean spring tides and lunar and solar semidiurnal tides and bed shear stresses; wind-driven currents; storm surges; winds and waves; the turbulent boundary layer on the shelf; salinity and temperature for winter and summer conditions; and the

development of the seasonal thermocline across the area. Nearer-to-shore data for the SEA8 area include information on the locations of estuaries and their mean freshwater inputs and, for several segments of the coast between the Dover Strait and St. George's Channel, brief discussions and information on seabed bathymetry and sediments; tides, temperature and salinity; and wind and waves.

2. Broad-scale data for the SEA8 region

The SEA8 region lies between approximately 48.2°N to 51.7°N and 1.5°E to 10°W (Figure 2.1(A)). The area includes the DTI-UK's Continental Shelf Designated Area from Dover in the eastern English Channel, westward through the English Channel to the edge of the continental shelf in the Celtic Sea, the Celtic Sea north-eastwards to the St. George's Channel entrance to the Irish Sea (but south of Milford Haven) and the Bristol Channel and its estuaries. Between their respective endpoints, the southern limb of the region covers a great-circle distance of roughly 880 km (550 miles) and the northern limb roughly 480 km (300 miles).

2.1. Topography and bathymetry

The nature of the English Channel coastline adjacent to the SEA8 region is very varied (Hamblin et al., 1992). In the west it is typified by rugged cliffs with minimal coastal erosion. In places there are tall cliffs (generally steep because of wave erosion) sometimes with offshore stacks. Softer parts of the strata give rise to low-lying coastlines, which are in places subject to rapid erosion, as in Poole and Christchurch Harbours.

An overall physical description of the seabed can be divided into five elements: offshore shoals, submerged cliff lines, incised valleys, tidal sand ridges and, most extensively, a gently dipping marine planation surface (Hamblin et al., 1992). The marine planation surface covers most of the seabed in the area, and everywhere

slopes directly away from the coast (Figure 2.1(B)). West of 1°W it slopes due south at about 1:1500 to beyond the SEA8 region, whereas east of 1°W it slopes to the south-south-east or southeast at a rather steeper angle, but does not extend more than 20 km offshore because it is interrupted by incised valleys and tidal sand ridges. Within the eastern English Channel, immediately southwest of the Dover Strait, there is a major suite of tidal sand ridges whose formation is related to the present hydrodynamic regime.

The coast surrounding Devon and Cornwall in the western English Channel and Celtic Sea is mostly backed by cliffs which rise steeply to heights in excess of 100 m (Evans, 1990). These cliffs are best developed along the northern coast of the peninsula, whereas along the southern coast they are broken by rias where the sea penetrates along mature valleys. Offshore, away from these valleys, the seabed slopes steeply from the foreshore to a depth of about 50 to 70 m. The near-shore zone is steepest around the major promontories. Adjacent to the cliff coastline, the coastal zone from the foreshore to a depth of about 7 to 20 m is a continuation of the modern cliff slope, though slopes are gentler in bays that lack a cliff surround. The seabed below this depth, down to about 50 to 70 m, continues as a series of cliffs (marking submerged coastlines) separated by near-horizontal benches.

The offshore area surrounding Devon and Cornwall may be divided into five bathymetric zones (Figure 2.1(B)): A narrow, steep coastal zone extending down to 50 or 70 m in depth; a wide, almost featureless inner shelf extending down to about 120 m in depth; the (usually) rugged, rocky shoals that rise above the general level of the inner shelf; a more irregular outer shelf, extending from 120 m down to the shelf-break at 180 to 205 m in depth; and a steep continental slope extending from the shelf-break down to about 4500 m in depth (Evans, 1990).

Five bathymetric types occur in the Bristol Channel to St. George's Channel region (Tappin, 1994): (1), Coastal embayments that comprise embayments and estuaries but exclude the large, open bight comprising the Bristol Channel. The embayments are up to about 10 m deep and include up to approximately 50% intertidal area; (2), Inner shelf platforms that vary in width and exceed 200 km in the Bristol Channel. These have gentle gradients of 1:100 to 1:2000. Water depths on the inner shelves are generally 10 to 60 m; (3), The Celtic Trough, which is an extensive, broad trough of subdued slopes (1:50 or less), part of which runs south-south-westwards through St George's Channel to the southern end of the Celtic Deep (Figure 2.1(B)). It is 60 km wide and depths in the trough are generally approximately 110 m, but reach a maximum of almost 160 m; (4), Rocky prominences, which generally are restricted zones of rough and rugged topography with outcrops of rock. In coastal embayments they occur as rocky headlands, islets, or shoals, whereas on the inner shelf they occur as islets, islands and shoals; (5), Enclosed deeps, which are areas less than 5 km wide, up to 30 km long and 10 to 50 m deeper than the surrounding sea floor.

2.2. Surficial bed sediments

The distribution of bottom sediments has been classified into mud, sand, gravel and mixtures of these grain types for the purposes of illustrating bottom sediments over the broad spatial scale of the SEA8 region (MAFF, 1981). In order to provide a useful comparison with sediments, Figure 2.2(A) shows the main depth zones over the SEA8 area (MAFF, 1981). The seabed sediment distribution shown in Figure 2.2(B) is largely a consequence of waves and tidal currents, especially peak current speeds, acting upon sediments that were laid down during the ice age. Close to the south-western boundary of SEA8, near the shelf break, the bottom sediments are mud and mixtures of mud and sand, with substantial areas

of sand. Smaller areas of mud, sand and mixtures of mud, sand and gravel also occur near the Celtic Deep feature of St. Georges Channel (Figures 2.2(A, B)). Over much of the Celtic Sea and English Channel the sediments comprise mixtures of sand and gravel. There is a large area of gravel in the central and eastern English Channel and for much of the SEA8 region there are large areas of mixed sand, gravel and exposed rock closer to shore where fast currents have scoured the bed of finer sediments.

2.3. Mean spring tidal ranges and phases

The mean spring tidal range at a location, MSTR, is defined as the difference in water levels between mean high-water springs and mean low-water springs. Contours of MSTR are shown on Figure 2.3(A). The range increases from approximately 3 m close to the south western boundary of SEA8, near the shelf break, to more than 12 m in the upper Severn Estuary of the Bristol Channel (Hydrographic Office, 1996). Some of this increase can be attributed to the funnelling of waters that are confined by converging coastlines. The MSTR in the English Channel region of SEA8 can be less than 2 m in the amphidrome (a point in the sea where there is near-zero tidal amplitude due to cancelling of tidal waves) near the Isle of Wight and exceed 6 m in the eastern English Channel and near the Dover Strait (Figure 2.3(A)). These English Channel tides constitute a co-oscillation with those of the North Sea and the Atlantic Ocean and their detailed patterns are greatly influenced by effects resulting from the earth's rotation (Proudman, 1953).

Co-tidal lines are drawn through locations of equal Mean High Water Interval (MHWI) and are shown on Figure 2.3(B). MHWI is defined as the mean time interval between the passage of the moon over the Meridian of Greenwich and the time of the next High Water at the place concerned. MHWI increases from

approximately 3.5 hours close to the south-western boundary of SEA8 to more than 5.5, 7 and 10 hours near the St. George's Channel boundary of SEA8 with the Irish Sea, the upper Severn Estuary of the Bristol Channel, and the eastern English Channel, respectively (Hydrographic Office, 1996, Figure 2.3(B)).

Recently produced maps of spring tidal range in the region also are available on the web (see section 4.1 and DTI, 2004).

2.4. Tidal M_2 and S_2 water levels, currents and bed shear stresses

The M_2 tide is the largest component of tide in the SEA8 region. The amplitudes and phases of the lunar semidiurnal tide (M_2) and the solar semidiurnal tide (S_2) on the northwest European shelf have been computed accurately by Sinha and Pingree (1997) and Pingree and Griffiths (1981), amongst others, using models of the depth-averaged water levels and currents.

2.4.1. M_2 tidal water levels

A numerical simulation of the M_2 tidal amplitudes (half the M_2 tidal ranges) and phases is shown in Figure 2.4.1(A). When compared with the available observations for the whole northwest European Shelf, the root-mean-square errors of the computed amplitudes and phases are estimated to be approximately 4.5 cm (typically 2% of the amplitude) and 3.1° (about 6 minutes), respectively (Sinha and Pingree, 1997). The pattern of M_2 elevations corresponds very closely to that plotted for the mean spring tidal range in the SEA8 region (Figure 2.3(A)), as would be anticipated because of the dominance of M_2 in this area. The pattern of M_2 elevation phases (Figure 2.4.1(B)) also corresponds closely to that for the spring-tide phases (the co-tidal lines on Figure 2.3(B)).

2.4.2. S_2 tidal water levels

The S_2 tide is the next most important tidal constituent over the SEA8 region. The addition of M_2 and S_2 tides produces a spring-neap cycle. Because the patterns of S_2 amplitudes and phases are very similar to those for the M_2 tide, it is more informative to show how the ratio of S_2 to M_2 amplitudes and the difference between their phases (gS_2 - gM_2) varies over the region. When compared with the available observations for the whole northwest European Shelf, the root-mean-square errors of the computed amplitudes and phases of the S_2 tide are estimated to be typically 5% of the amplitude and 8° (about 16 minutes), respectively, although a comparison of computed and observed data shows that S_2 to M_2 amplitude ratios generally are within 2% and phase differences are within 3° (about 6 minutes, Pingree and Griffiths, 1981). Variations in these parameters mainly result from the displacements of the M_2 and S_2 amphidromes and the oceanic M_2 and S_2 inputs to the shelf. The S_2 to M_2 elevation ratio is somewhat less than 35% close to the southwest boundary of SEA8 and remains close to 35% near the St. George's Channel boundary of SEA8 and within the Bristol Channel and for much of the English Channel, although it decreases to 30% in the eastern English Channel and increases to 55% in the amphidrome region near the Isle of Wight (Figure 2.4.2(A)). The S_2 to M_2 ratios tend to be large close to the M_2 amphidrome because M_2 becomes small there. The ratio is smaller in the shallow areas because S_2 is relatively more attenuated by bottom friction than M_2 (Figure 2.4.2(A)). The phase differences (gS_2 - gM_2) generally show that the S_2 elevation phase is roughly 40° - 50° greater than the M_2 phase throughout much of the SEA8 region (Figure 2.4.2(B)), but is smaller near the southwest boundary of SEA8 (33°) and within the English Channel amphidrome (30°).

2.4.3. *Tidal water currents*

Flather (1987) has published a simulation of the depth-averaged, spring tidal currents over the northwest European shelf. The tidal currents are expressed as semi-major and semi-minor axes of the spring-tide, tidal-current ellipses. When the semi-minor axis is zero at a location the ellipse becomes a straight line and the currents are rectilinear, flowing backwards and forwards through the point. When the semi-minor axis is equal to the semi-major axis the ellipse becomes a circle and the current vector rotates about the point and has a constant speed.

Spring tidal currents are expressed in terms of their ellipse semi-major axes in Figure 2.4.3(A). These current speeds are the maximum speeds reached during the spring tidal cycle. Flather (1987) did not specify the overall accuracy of the computed speeds, but they are thought to convey a realistic, broad-scale representation for the SEA8 region. Spring tidal speeds are relatively slack, typically 0.2 m s^{-1} close to the southwest boundary of SEA8 and increase to more than 1.0 m s^{-1} near the St. George's Channel boundary of SEA8, 1.6 m s^{-1} in the upper Bristol Channel and 1.4 m s^{-1} in the English Channel (Figure 2.4.3(A)). Currents can be very variable in space and reflect numerous small-scale features, such as flow around headlands, which are not adequately resolved in Figure 2.4.3(A).

Spring tidal current ellipses are represented by the ratio of semi-minor to semi-major axes over the SEA8 region in Figure 2.4.3(B). The semi-minor axes current speeds are the minimum speeds reached at a location during the spring tidal cycle. A tidal current vector rotates anticlockwise about a point at locations where the ratio of semi-minor to semi-major axes is positive on Figure 2.4.3(B) and conversely when the ratio is negative. The current vectors are quite strongly elliptical and exhibit clockwise rotation in much of the Celtic Sea, but are more

nearly rectilinear and generally possess anticlockwise rotation in most of the English Channel. A substantial area of strong elliptic motion and anticlockwise rotation exists seaward of the Bristol Channel (Figure 2.4.3(B)).

Recent maps of peak spring-tide current speeds also are available on the web (see section 4.1 and DTI, 2004) together with neap-tide current speeds and tidal power densities.

2.4.4. *Bed shear stresses and implications*

Tidal currents produce a shearing stress on the seabed that has an important influence on sediment transport and sediment grain size distributions. The main tidal currents generate higher frequency components of the tide through various hydrodynamic mechanisms. For example, the dominant tide in SEA8 is M_2 (with period 12.4 h) and this will generate an M_4 tide (with period 6.2 h). The M_4 tide is much smaller than M_2 and therefore has little effect on the *magnitude* of the bed shear stress (shown for M_2 and M_4 tidal currents on Figure 2.4.4(A)). This maximum stress has an important influence on bed sediment types because it determines the sizes of sediment grains that are moved and the sizes of those that can remain at a location.

Although the magnitude of the combined M_2 and M_4 bed shear stresses are not much affected by M_4, the direction of the peak stresses are effectively determined by M_4, because this factor introduces a difference between peak flood and peak ebb current speeds and stresses. There is a remarkable similarity between the direction of peak tidal stresses (illustrated in Pingree and Griffiths, 1979) and the direction of sediment transport paths for sand-sized bottom sediments over the northwest European shelf (Stride, 1973) and over the SEA8 region in particular (Figure 2.4.4(B)).

2.5. Wind-driven currents

Currents driven by a steady uniform wind stress on the shelf seas around the British Isles have been modelled by Pingree and Griffiths (1980) and others. Pingree and Griffith's (1980) analysis is particularly useful because it permits an extrapolation to a range of applied wind-stresses, based on modelled results for just two applied, steady-state stresses, which are 1.6 dynes cm^{-2} (0.16 Pa) from the southwest and the southeast. Because the conversion from wind speed to wind stress is not straightforward, the stress rather than the wind speed is used. A typical relationship gives stress as the product of air density, the square of the wind speed at 10 m height above the sea surface and a coefficient, which typically is 0.0013 (but might be as high as 0.0045). Using the former, smaller coefficient gives a wind speed of 10 m s^{-1} corresponding to a stress of 0.16 Pa.

2.5.1. Southwest winds

The numerical model superimposes the wind on an accurate model of the average (M_2) tide, so that the steady, wind-driven currents are estimated when simulated currents computed with and without wind are subtracted. Steady winds from the southwest that correspond to a stress of 0.16 Pa produce depth-averaged residual currents to the southeast (of magnitude a couple of cm s^{-1}) close to the southwest boundary of SEA8 and across the Celtic Sea (Figure 2.5.1(A)). A north-flowing current is formed along the north Cornwall and Devon coasts and across the mouth of the Bristol Channel (typically a few cm s^{-1}) and a south-flowing return flow occurs in the central reaches of the St. George's Channel. The southwest wind stress drives a flow to the north and east along the English Channel with currents exceeding 0.1 m s^{-1} through the Dover Strait (Figure 2.5.1(A)). The water levels that correspond to the southwest wind stress are shown on Figure 2.5.1(B). These are very small close to the southwest

boundary of SEA8 and across the Celtic Sea and show an increase from 0.025 m in the St. George's Channel to over 0.1 m in the Bristol Channel and 0.05 m in the SEA8 region of the English Channel.

2.5.2. Southeast winds

Steady winds from the southeast that correspond to a stress of 0.16 Pa produce depth-averaged residual currents that flow to the northwest (of magnitude a couple of cm s^{-1}) close to the southwest boundary of SEA8 and across the Celtic Sea (Figure 2.5.2(A)). However, a north-flowing current is again formed along the north Cornwall and Devon coasts and across the mouth of the Bristol Channel (typically a few cm s^{-1}) but in this case there is no south-flowing return flow in the central reaches of St. George's Channel. The southeast wind stress, like the southwest wind stress, drives a flow to the north and east along the English Channel, with currents that are of order 0.1 m s^{-1} through the Dover Strait (Figure 2.5.2(A)). The water levels that correspond to the southeast wind stress are shown on Figure 2.5.2(B). These are less than 0.025 m close to the southwest boundary of SEA8 and increase to more than 0.05 m in the St. George's Channel. Levels decrease to zero in the Bristol Channel and decrease to -0.1 m in the SEA8 region of the eastern English Channel.

The numerical model superimposes the wind on an accurate model of the average (M_2) tide and because the tidal flow generally is larger than that due to the wind it largely determines the bottom friction in the model. The wind-driven currents are therefore nearly linear with respect to an applied wind stress, which implies that in reality the wind-driven currents would be greater at neap tides and smaller at spring tides than those shown in Figures 2.5.1(A) and 2.5.2(A).

Although uniform, steady wind conditions may rarely occur in nature, a southwest or west-southwest wind stress approximates to winter conditions on the

northwest European shelf (Figure 2.5.1(A)). According to Pingree and Griffiths (1980), the transport of water due to both wind and tide, Q, in units of 10^4 m^3 s^{-1}, eastward through the English Channel into the North Sea, northward through the St. George's Channel to the Irish Sea, and across the Celtic Sea, can be summarized in terms of the direction of the wind, θ, and the magnitude of the wind stress, τ, in dynes cm^{-2}, by, respectively:

$$Q = 3 + 12\cos(\theta - 187^\circ) \cdot \tau$$

$$Q = 2 + 10\cos(\theta - 140^\circ) \cdot \tau$$

and

$$Q = 6 + 20\cos(\theta - 166^\circ) \cdot \tau$$

The results for a southwest wind stress, illustrated in Figures 2.5.1(A, B), will approximate to the winter pattern of wind-driven residual flows in the SEA8 region. Moreover, provided the wind stress is reasonably uniform over a localised region of interest within the SEA8 area, then the more local circulations will be valid, e.g. within a particular bay, even if the wind stress is not uniform over the whole shelf.

2.6. Storm surge water level elevations and currents

Storm surges are caused by strong winds and associated low atmospheric pressure during storms. The forcing of waters by the traction that occurs between wind and water surface, the response to low and variable atmospheric pressure and the piling-up of water against coastlines can produce high water levels that pose the risk of floods. Storm surges are shallow water waves on the shelf and propagate rather like tides.

A contour map of storm surge elevations in water level for a fifty year return period (Flather, 1987) is shown on Figure 2.6(A). Elevations increase from approximately 0.5 m close to the southwest boundary of SEA8 to between 0.75

and 1.25 m near the St. George's Channel boundary of SEA8 with the Irish Sea and exceed 1.5 m in the Bristol Channel. The surge elevation increases as it propagates from the Celtic Sea and into the English Channel and reaches 2 m near the Dover Strait boundary of SEA8.

A contour map of the maximum storm surge current speeds associated with the surge elevations shown on Figure 2.6(A), i.e. for a fifty year return period (Flather, 1987), is shown on Figure 2.6(B). Maximum speeds increase from approximately 0.2 m s^{-1} close to the southwest boundary of SEA8 to approximately 0.4 m s^{-1} in the central Celtic Sea, before decreasing again to 0.2 m s^{-1} near the St. George's Channel and in the Bristol Channel. The maximum surge speed increases as the surge propagates from the Celtic Sea into the English Channel and typically is 0.6 m s^{-1} in the English Channel coastal regions of SEA8, reaching 1 m s^{-1} in the Dover Strait area (Figure 2.6(B)). The arrows on Figure 2.6(B) indicate the direction of the maximum surge current in those regions that show a directional preference.

2.7. Winds and wave heights

2.7.1. Monthly winds and extreme waves

An illustration of monthly wind data for January over the SEA8 region during 1962 to 1976 (MAFF, 1981) is shown in Figure 2.7.1(A). Each wind rose plot shows wind speed data as 'arms' for the eight primary direction-sectors. The sum of the eight wind rose arms equals 100% and the length of each arm is the percentage of winds in that direction-sector. The length along each arm is divided into four segments of differing thickness that represent the percentage of winds within that direction-sector having Beaufort scales 1 - 3, 4, 5 - 6, and 7 – 12. In the SEA8 region the winds are predominantly from the southwest or west.

The predicted heights of the highest individual waves that are likely to occur in the worst storm in any 50-year interval and also the period of the wave at that time are shown in Figure 2.7.1(B). Data are based on predicted 50-year extreme winds and assume that the storm responsible for the waves will last in its fully-developed state for 12 hours (MAFF, 1981). The effects of wave breaking, bottom friction, shallow water topography or tidal currents on waves are not taken into account. Wave height decreases from approximately 35 m close to the southwest boundary of SEA8 to less than 20 m near the St. George's Channel and the Bristol Channel, and to less than 13 m in the eastern English Channel (Figure 2.7.1(B)). The wave period decreases from greater than approximately 16 s close to the southwest boundary of SEA8 to approximately 14 s near the St. George's Channel and the Bristol Channel, and decreases to less than 10 s in the eastern English Channel.

More recent wind and wave data have been produced using hindcast wind and wave time-series data from the NEXT model for the combined periods January 1977 to December 1979 and January 1989 to December 1994 and the results are available on the web (see section 4.2 and HSE, 2001). There are two grid points in the English Channel and three in the Celtic Sea. The DTI (2004) atlas, available on the web, supplies maps of modelled annual mean significant wave heights, wave power and seasonal variations. Wind data includes maps of annual mean wind speed and wind power density (see section 4.1).

2.7.2. Annual waves

The 'significant' wave height contoured here corresponds approximately to the value estimated from visual observations of the sea's surface by an experienced mariner. Figure 2.7.2(A) shows the significant wave heights that are predicted to be exceeded for 10% of the year (Draper, 1991). These waves are an order of magnitude smaller than the extreme waves contoured on Figure 2.7.1(A). Heights

decrease from greater than 4 m at the southwest limit of SEA8 to less than 2 m in the eastern English Channel, inner Bristol Channel and Severn Estuary, while remaining greater than 3 m in the St. George's Channel.

Figure 2.7.2(B) shows the significant wave heights that are predicted to be exceeded for 75% of the year. Heights decrease from greater than 1.5 m at the southwest limit of SEA8 to less than 0.5 m in the eastern English Channel, inner Bristol Channel and Severn Estuary, while remaining greater than 1 m in the St. George's Channel. Annual wave periods are greater than 6 s and less than 8 s at the southwest limit of SEA8 and reduce to less than 4 s in the eastern English Channel and inner Bristol Channel (Figure 2.7.2(B)). Seasonal variations in wave period are small.

Again, more recent wind and wave data are available on the web (see sections 4.1 and 4.2; DTI, 2004 and HSE, 2001).

2.8. The turbulent boundary layer on the shelf

The southwest boundary of the SEA8 region extends to the shelf break and measurements by Pingree (1974) on the shelf in this general area (located on Figure 2.8(A)) at depths of 180 and 160 m and in much shallower English Channel waters of 55 m depth (Pingree and Griffiths, 1977) illustrate the thermal structure of the water column at these sites (S1, S2, S3, respectively, on Figure 2.8(A)). In the deeper waters (stations S1 and S2) the temperature of the bottom 100 m of water column (beneath the thermocline) increases very slightly but consistently with depth (Figure 2.8(B)). This marginal increase of temperature is approximately adiabatic (i.e. due to compression of the water by pressure at depth and equal to 1.3×10^{-4} °C m^{-1}) and is to be expected of a turbulent boundary layer. The adiabatic gradient is given for comparison on Figure 2.8(B). The in-situ temperature profiles at stations S1, S2, S3 are from different mixing regimes;

strong currents and mixing in the English Channel (station S3) do not permit the development of a pronounced seasonal thermocline, even at the end of July (the time of the profile), whereas a thermocline develops above the bottom-mixed layer at stations S1 and S2 (Figure 2.8(B)). Therefore, intense vertical mixing on the shelf in the south-western approaches to the English Channel produces near-homogeneous temperature and salinity structure beneath the thermocline. Away from the bottom the increasing stability of the thermocline leads to greatly increased temperature gradients. Similarly, in regions of intense tidal mixing where no persistent seasonal thermocline exists, the sea surface will restrict the mixing and lead to greatly increased near-surface temperature gradients under calm conditions of net heat gain at the surface (station S3, Figure 2.8(B)).

The edge of the Celtic Sea shelf is characterised by a band of cold water, roughly 100 km wide, that is about 1 – 2 ℃ colder than the adjacent shelf and oceanic waters (Pingree and Mardell, 1981). The seasonal thermocline at the shelf break tends to be broader in vertical extent than the adjacent waters and, as illustrated in Figure 2.8(B), the shelf waters near the break are characterised by an extensive (> 100 m) near-homogeneous bottom layer due to tidal mixing, which limits the vertical region for thermocline development between the wind-mixed layer and the bottom-mixed layer. The thermocline is characterised by marked internal wave activity and the broadening of the thermocline over the slopes is thought to indicate greater mixing near the shelf break. Mixing caused by internal tides at the thermocline (sometimes 40 m in vertical extent) and generated by the 'surface' tides appear to play a role in shelf break cooling, in addition to wind-induced up-welling of cooler waters and mixing caused by the interaction of bottom roughness (due to canyons and ridges) with trapped waves that propagate along the slope.

More recent work at the shelf break near the SEA8 region was undertaken in the OMEX project (Wollast et al., 2001; Huthnance et al., 2001). This work showed that the along-slope flow typically is of the order of 0.05 m s^{-1} and is reduced or even reversed in spring. Tidal currents typically are of the order of 0.2 m s^{-1} on the adjacent shelf (as shown from earlier work on Figure 2.4.3(A)). Other (wind and eddy-forced) contributions to the currents typically are of the order of 0.1 m s^{-1} or less, except on the shelf, and decrease with depth. Wind-forced, tide-forced and wave-forced currents probably are the most consistent agents of cross-slope water exchange (of the order of 1 m^2 s^{-1}) with topographic effects due to canyons and spurs being locally important.

2.9. Typical surface and bottom salinity and temperature for winter and summer

The data used to illustrate mean salinity and temperature are published and their origins sourced and referenced in MAFF (1981). The mean monthly temperature distribution for February is used to provide a representation of the coldest temperatures that occur on average during the year. The mean monthly temperature distribution for August is used to provide a representation of the warmest temperatures that occur, on average, during the year. The term 'salinity' is used to describe the total weight of dissolved salts present in a known weight of seawater, expressed as g kg^{-1} or parts per thousand. Current usage specifies salinity as a dimensionless quantity. Higher values of salinity (greater than about 35) indicate a very strong presence of Atlantic Ocean waters, whilst lower values indicate the presence of waters influenced to some extent by river runoff.

2.9.1. Temperature during winter

The mean monthly surface temperature for February decreases from approximately 11°C close to the southwest boundary of SEA8 to less than 8.5, 6 and 8.5°C near the St. George's Channel boundary of SEA8, the upper Severn

Estuary of the Bristol Channel, and the eastern and much of the shallow near-shore English Channel, respectively (Figure 2.9.1(A)). The mean bottom temperature distribution in February (Figure 2.9.1(B)) shows marked similarities to the mean surface temperature distribution. The bottom temperature decreases from greater than approximately 10°C close to the southwest boundary of SEA8 to less than approximately 9°C near the St. George's Channel, the upper Severn Estuary of the Bristol Channel, and the central and eastern (and much of the shallow near-shore) English Channel (Figure 2.9.1(B)).

2.9.2. Temperature during summer

The mean surface temperature for August increases from approximately 17°C close to the southwest boundary of SEA8 to less than 15.5°C near the St. George's Channel, and typically 16 °C in the outer Bristol Channel and the English Channel (Figure 2.9.2(A)). The mean bottom temperature distribution in August shows marked differences to the mean surface temperature distribution in August over the SEA8 region. The bottom temperature increases from greater than approximately 11 °C close to the southwest boundary of SEA8 to more than 16 °C in the eastern English Channel, which illustrates a strong, surface to bottom temperature stratification over the Celtic Sea and western English Channel during summer (Figure 2.9.2(B)).

2.9.3. Salinity during winter

The mean monthly salinity distribution for February provides a representation of the salinity that occurs during winter. The surface salinity decreases from greater than approximately 35.6 close to the southwest boundary of SEA8 to less than 35.0 near the St. George's Channel and within the Bristol Channel (Figure 2.9.3(A)). Salinity exceeds 35.0 for much of the SEA8 area of the English Channel, although generally it is less close to the shore, due to the influence of

estuarine outflows that carry waters mixed with freshwater runoff from rivers. The mean bottom and surface salinity distributions in February exhibit similarities over the SEA8 region; in particular, the locations of the 35 and 35.25 bottom contours are very similar to the mean 35 and 35.25 (interpolated) surface contours (Figure 2.9.3(B)).

2.9.4. Salinity during summer

The mean monthly salinity distribution for August provides a representation of the salinity during summer. The mean surface salinity for August decreases from greater than approximately 35.5 close to the southwest boundary of SEA8 to (generally) less than 35.0 in the Bristol Channel, St. Georges Channel and the eastern English Channel and for much of the near-shore region of the English Channel (Figure 2.9.4(A)). A retreat of the surface 35 isohaline occurs during summer months in the English Channel and Celtic Sea, although substantial patches of higher salinity waters, greater than 35, occur in the eastern English Channel and St. Georges Channel (Figure 2.9.4(A)). The mean bottom salinity distribution in August is similar to the mean bottom salinity distribution for the winter over the SEA8 region (Figure 2.9.4(B)). Some retreat of the 35 isohaline is indicated within bottom waters of the English Channel in summer, but this is small compared with that for the surface salinity field, and there is an advance of the 35 isohaline in the Bristol Channel and St. George's Channel.

2.10. Seasonal thermocline development across the area

There is an advance and retreat of the seasonal thermocline across the continental shelf within the SEA8 region during the year. When surface heating becomes sufficiently great, more buoyancy is produced in the water column than can be dissipated by mixing due to wind and tide and the water column stratifies, with well-defined surface and bottom layers separated by a sharp interface (the

thermocline). Because the thermocline does not form simultaneously over the SEA8 region, the water column may be vertically mixed in one area and stratified in a neighbouring area, so that a surface frontal area comprising sharp temperature gradients may occur between them. Pingree (1975) used historical temperature data for the shelf to illustrate the 'mean' movements of the seasonal thermocline. To obtain sufficient coverage, data were averaged over 1 degree squares of latitude and longitude (Pingree, 1975).

The 'mean' development (advance) of the seasonal thermocline is shown by means of weekly frontal plots on Figure 2.10(A). The thermocline first forms south of Ireland near the western boundary of the SEA8 region and then spreads eastward into the region across the Celtic Sea, towards the mouth of the Bristol Channel, and less than a month later penetrates the English Channel. The basic pattern of the 'mean' breakdown (retreat) of the seasonal thermocline is essentially the reverse of its advance (Figure 2.10(B)). By November the English Channel waters of SEA8 are vertically mixed, although it is not until well into December that the thermocline is completely eroded from the Celtic Sea.

Although this early work is important, it could not convey the spatial and temporal complexity of frontal development that is now routinely displayed by satellite images that depict sea-surface temperature and other variables (e.g. view work of the Remote Sensing Group, Plymouth Marine Laboratory, at www.pml.ac.uk). An example of a composite-front map of sea surface temperature that shows the complexity and short-term evolution of the frontal situation for the UK Western Approaches and much of the SEA8 region during 18 – 22 July 2000 is given in section 4.5 and illustrated in Figure (4.5).

The earlier work did not map the residual (non-tidal) currents that are driven by density gradients associated with the seasonal fronts. That such currents must

exist has been known from theoretical analysis for many years. Recent measurements by CEFAS (2007) has shown that relatively strong, residual circulations can arise from the density contrasts that exist between areas that are thermally stratified (layered) in summer and those that are thermally mixed (see section 4.4).

CEFAS drifter surveys in the Celtic Sea and St. George's Channel during summer yielded a mean residual speed of 0.065 m s^{-1} for all drifters and speeds in excess of 0.3 m s^{-1} for drifters in the St. Georges Channel (CEFAS, 2007). It was concluded that the residual circulation of the Celtic Sea in summer, in the areas studies, is dominated by intense and predictable cyclonic (anticlockwise) baroclinic flows associated with bottom density fronts. CEFAS surveys in the Western English Channel during summer similarly led them to conclude that under these summer frontal conditions a transport pathway exists between the coasts of Brittany to the southern English coast and then around the southern and western Irish coast.

3. Nearer-to-shore data for the SEA8 area

The near-shore information on freshwater inflow to be presented in Section 3.1 relies heavily on data from IH(1998) and the detailed information to be presented in Sections 3.2 to 3.7 relies heavily on data and graphics presented in the volumes edited by Barne et al. (1995; 1996a, b, c; 1998a, b) and especially chapters within those volumes by Evans (1995a, b) and by British Geological Survey (1996a - f; 1998a, b) and British Geological Survey et al. (1998a, b). The plotted wind speeds in the volumes edited by Barne et al. (1995; 1996a, b, c; 1998a, b) correspond to data given by Caton (1976), the plotted wave data to those in Draper (1991), and plotted tidal current data to those in Sager and

Sammler (1968). More recent data for some of these variables are available on the web at DTI (2004) and HSE (2001).

The morphology of the seabed in these near-shore areas is influenced by the nature of their bedrock, their exposure to wave attack and their supply of mobile sediments. Seabed sediments considered here are the unconsolidated, surficial sediments that have been transported and deposited since the sea transgressed across the area following the last ice age.

Mean sea surface water temperatures for summer and winter are shown for August and February, the months of highest and lowest sea temperatures on average. The mean surface salinity values shown for summer and winter also are based on data for August and February, respectively (MAFF, 1981). These data are averaged for each month, which has the effect of smoothing out the salinity gradients in some areas. Wave data are presented for the various regions, although close to the coast and especially within the surf zone the apparent period may be less than that plotted for offshore areas (Draper, 1991).

3.1. Locations of estuaries and their mean freshwater inputs to SEA8

Numerous estuaries enter the SEA8 region and contribute substantial quantities of freshwater, sediments, nutrients and, potentially, pollutants. Estuaries that enter the eastern English Channel part of SEA8 are listed as numbers 5 (the Rother) to 20 (the Yar) on Figure 3.1(A). These estuaries often have several tributaries, which may be tidal or non-tidal, but are not listed separately here. The mean, long-term average rates of freshwater river flow measured at the seaward-most gauging stations are listed on Figure 3.1(A). The sum of the freshwater flow rates over all these stations is approximately 40 $m^3 s^{-1}$.

In Southwest England there are 28 estuarine systems (not counting their various tributaries) many of which are rias (Figure 3.1(B)). Plymouth Sound

(number 16) is the largest in terms of freshwater flow, and receives inputs from the Plym and the Tamar (and its sub-estuaries of the Tavy and Lynher), which are not listed separately. The mean, long-term average rates of freshwater flow at the seaward-most gauging stations are listed on Figure 3.1(B), except for Poole and Christchurch Harbours, Plymouth Sound and the Fal system, where the freshwater flow rates to the coastal sea are estimated and listed. The sum of these freshwater flow rates is approximately 250 $m^3 s^{-1}$.

There are 19 estuarine systems that enter SEA8 along the northern coastline of the Severn Estuary and Bristol Channel, including the River Severn itself (Figure 3.1(C)). The largest average freshwater flow rate is from the River Severn (109 $m^3 s^{-1}$) and the sum of inputs from the seaward-most river gauging stations (numbers 1 to 19 on Figure 3.1(C)) is approximately 350 $m^3 s^{-1}$, which is greater than the combined inputs from the other two coastal regions that comprise SEA8.

3.2. South coast, Dover Strait

3.2.1. Bathymetry and sediments

Water depths in the Dover Strait increase from the Kent coast to more than 40 m in the centre of the strait (Figure 3.2.1(A)). The inshore part of the region is shallow, usually less than 10 m in depth, with variations that include sand-bank bathymetry and sand-bank movement. Seabed sediments are shown on Figure 3.2.1(B). The seabed sediments of this region are mostly relict and offshore sediments generally are thin. North-south oriented linear sand banks occur in deeper water north of the Dover Strait.

3.2.2. Tides, temperature and salinity

Figure 3.2.2(A) shows the tidal ranges at mean spring tides. Tidal range reaches 7.0 m in the Dover Strait. Fluctuations in atmospheric pressure can raise

or lower water levels. Storm surges of raised water levels occur fairly frequently in the North Sea and increase in height towards the south. The maximum 50-year surge levels along the east coast of Kent are 2.25 m at Ramsgate, north Dover Strait, falling to 2 m at Dungeness, south Dover Strait.

Tidal streams can vary greatly, depending on coastline shape and near-shore bathymetry (Figure 3.2.2(B)). Tidal current speeds in the eastern English Channel increase in the Dover Strait, reaching 1.75 m s^{-1}, because of the restriction of the channel and the presence of tidal sand ridges aligned with the direction of flow.

Variations in temperature occur across the region during winter and summer (Figure 3.2.2(C)). Relatively warm waters in the English Channel serve to prevent water temperatures in the region dropping below 5 °C during winter.

The salinity of seawater off the coast is slightly below that of Atlantic oceanic water (approximately 35.5) owing to the mixing of Atlantic water with low-salinity coastal waters (Figure 3.2.2(D)). Salinity increases southwards from the southern North Sea into the English Channel during both summer and winter.

3.2.3. Wind and waves

Contours of the hourly wind speeds exceeded for 75% and 0.1% of the time are shown on Figures 3.2.3(A, B), respectively. This region is relatively sheltered from the strongest winds and wind speeds that exceed 15 - 16 m s^{-1} occur for only 0.1% of the time (Figures 3.2.3(A, B)). Usually, wind speeds exceed about 3.5 m s^{-1} for 75% of the time and are consistently stronger than those further inland. Local wind conditions are affected by local topography although gales can occur throughout the area and during strong winds the Dover Strait can become very rough. In the English Channel, the coastline shape steers winds so that they tend to blow from either the southwest or the northeast. Figure 3.2.3(C) shows the

frequency of winds from different directions at Felixstowe in the southern North Sea and Margate, north of the Dover Strait.

Significant wave heights that can be expected to be exceeded for 10% and 75% for the year are shown in Figure 3.2.3(D). For example, the significant wave height off-shore of Folkestone (Figure 3.2.1(B)) is 1.5 m or more for 10% of the year and approximately 0.5 m or more for 75% of the year. Significant wave heights in the Dover Strait region are amongst the lowest for open waters in the British Isles.

3.3. South coast, eastern English Channel

3.3.1. Bathymetry and sediments

The seabed forms a regular submarine erosion surface in this part of the English Channel that is cut in places by a submerged cliff line that roughly follows the 40 m depth contour (Figure 3.3.1(A)). Areas of bedrock outcrop at the seabed in places. The seabed is shallow and gently shelving closer to shore and extensive shallow areas, less than 5 m deep, occur in the bay to the west of Dungeness and to the west of Selsey Bill (Figure 3.3.1(A)).

Seabed sediments in this area are shown on Figure 3.3.1(B). East of Beachy Head there is a cover of mobile sediments, generally in the form of tidal sand ridges. Muddy sands occur nearer the coastline and the seabed of the Bay to the west of Dungeness has a cover of muddy fine sand. Southwest of Beachy Head an extensive area of sand waves covers a layer of sandy sediments up to 20 m thick. Further to the southwest sand waves reduce in size and grade into irregular sand patches, sand ribbons and a smooth, flat seabed. Still further offshore the seabed sediments consist of a discontinuous cover of coarse lag deposits less than 0.5 m thick. West of Selsey Bill a variety of sediment types occur, with muddy sands and sandy mud in the intertidal areas passing into sand and gravelly

sand further offshore and sandy lag gravel exposed locally. Sand ripples, sand waves and even gravel waves occur in areas of strong tidal currents.

3.3.2. Tides, temperature and salinity

Tidal ranges in the area at mean spring tides are shown on Figure 3.3.2(A). Ranges decrease westwards from 7.0 m near Dungeness to less than 4.5 m west of Selsey Bill. The maximum tidal-current speed lies between 0.75 m s^{-1} and 1.25 m s^{-1} in the central part of the English Channel (Figure 3.3.2(B)). Maximum current speeds decrease both eastwards and in the bays but increase close to headlands (e.g. 1.25 m s^{-1} off Beachy Head).

Figure 3.3.2(C) shows mean sea surface temperatures for summer and winter. Sea surface temperatures in this region are strongly influenced by the movement and mixing of English Channel waters. In winter, relatively warm waters occur in the English Channel and average February temperatures range between 6.5° and 8°C (Figure 3.3.2(C)), which is substantially warmer than the coastal waters of Holland, Belgium and Germany. Surface water temperatures in the central English Channel are, on average, 16 - 16.5 °C in August, with temperatures increasing progressively toward both shores.

The mean surface salinity values for summer and winter are shown on Figure 3.3.2(D), based on data for August and February, respectively. Salinity is high along the central English Channel in winter and decreases toward the coast, although it exceeds 34.5 except near the mouths of estuaries (a consequence of their river inputs). In summer, values in the central English Channel are lower, but along the coast they remain similar to those of the winter season.

3.3.3. Wind and waves

Contours of the wind speeds exceeded for 75% and 0.1% of the time are shown on Figures 3.3.3(A, B), respectively. Southwest and west winds are

prevalent over the year (Figure 3.3.3(C)) and strongest winds occur in winter. The south coast is very exposed when there are strong southerly winds. Winds of 80 knots (in excess of 40 m s^{-1}) have been recorded in this area during westerly gales.

Much of this coastline is subjected to waves generated by south-westerly winds and the long fetch from the Western Approaches of the English Channel causes large waves during periods of strong winds. The significant wave heights that can be expected to be exceeded for 10% and 75% for the year are shown on Figure 3.3.3(D). For example, south of Selsey Bill the significant wave height exceeds 1.5 m for 10% of the year and 0.5 m for 75% of the year.

3.4. Southern England

3.4.1. Bathymetry and sediments

Poole Bay, Christchurch Bay and much of the Solent have extensive shallows less than 10 m deep (Figure 3.4.1(A)). Depths exceed 20 m south of the Isle of Wight and the seabed forms part of the submarine erosion surface, which is cut locally by a submerged cliff line that approximately follows the 40 m contour. The near-coast seabed shelves more steeply further west and the 20 m contour is relatively close to shore.

The seabed sediments consist of a discontinuous cover of coarse deposits, mostly gravels and sandy gravels, less than 0.5 m thick over much of the region (Figure 3.4.1(B)). Longitudinal gravel furrows, parallel to the direction of tidal currents, occur in some areas. The lag deposits are locally overlain by sand ribbons, sand waves and rippled sand patches. Nearer shore, thicker sands can occur and muddier sediments in the inshore areas with weakest tidal currents.

3.4.2. Tides, temperature and salinity

Tidal range is greatest in the east of the region (> 4 m, Figure 3.4.2(A)). The smallest tidal ranges in the UK occur in this area (less than 2 m at spring tides). These smaller tides exhibit a double low water in the west and a double high water in the east. The maximum storm surge level expected to occur once in 50 years in this area exceeds 1 m in height, which is comparable with the tidal water level variation, and maximum surge-induced currents can be faster than 0.6 m s^{-1}. Despite the small tidal range, tidal currents can be fast in this area, especially in the entrances and channels of the major tidal inlets and off headlands, where speeds can be faster than 1 m s^{-1} (Figure 3.4.2(B)) and slow in the shallow waters of the main bays.

The mean sea surface temperatures for summer and winter are shown on Figure 3.4.2(C). In winter, average sea surface temperatures increase progressively to the west, from less than 7°C to over 8°C, reflecting the presence of relatively warm Atlantic waters in the English Channel. In summer, temperatures increase from the deeper waters of the offshore English Channel to the coast. The mean surface salinity values for summer and winter are shown on Figure 3.4.2(D). Although lower than in winter, salinity remains relatively high along the centre of the English Channel in summer. Salinity decreases toward the coast both in summer and winter but normally remains above 34.5 except locally near the mouths of estuaries. Rivers carry freshwater into the estuaries, where there is dilution of saltwater due to mixing and subsequent seaward transport into the coastal waters by ebb currents (Figure 3.1).

3.4.3. Wind and waves

Figures 3.4.3(A, B) show, respectively, contours of the wind speeds exceeded for 75% and 0.1% of the time. The prevailing winds throughout the year are from

the southwest (Figure 3.4.3(C)), with the strongest winds occurring in winter. Winds from the southeast are less frequent and usually less persistent. Spring is the most common season for northeast winds. In winter, strong winds may persist for several days. The coastal waters, estuaries and harbours are subject to local variations in wind conditions compared with the open sea.

Figure 3.4.3(D) shows the significant wave heights that can be expected to be exceeded for 10% and 75% for the year. Waves are generated by the prevailing south-westerly winds, which have a long fetch from the Western Approaches of the English Channel. However the western parts of the larger bays are sheltered from these waves by headlands (Figure 3.4.3(D)). For example, the significant wave height offshore is greater than about 2 m for 10% of the year and less than 1.5 m in the sheltered bays and harbours of much of the region.

3.5. South coast of southwest England

3.5.1. Bathymetry and sediments

The near-shore zone is steepest around major promontories and gentlest in the large bays, where depths are less than 60 m (Figure 3.5.1(A)). The cliff coastline is indented by rias, where the sea floods into drowned river valleys. Below 20 m the seabed slopes relatively steeply to a depth of about 50 m. A series of cliffs mark the submerged coast lines and are separated by nearly horizontal submerged ‘beaches’. The seabed is part of the planar submarine erosion surface below about 50 m depth. The seabed rises to less than 20 m depth around the erosion-resistant Eddystone Rocks (Figure 3.5.1(A)).

Areas of nearly sediment-free rock occur in some parts of the region and generally the sediment cover is thin, so that the form of the seabed approximates that of the bedrock erosion surface (Figure 3.5.1(B)). However, in some near-shore areas sediment thicknesses greater than 5 m can occur. Over much of the

region the seabed sediments consist of a discontinuous cover of coarse deposits, less than 0.5 m thick. In some areas longitudinal gravel furrows have formed parallel to the direction of tidal currents. The lag deposits are locally overlain by mobile bodies of sand, in the form of ribbons, sand waves and rippled sand patches. Near shore, thicker sands can occur and sandy mud and muddy sand deposits occur in the areas of weak tidal currents. The sands tend to become cleaner and finer in the west of the region and contain more carbonate in the form of finely-broken shell material.

3.5.2. Tides, temperature and salinity

Mean spring tidal ranges for the region are shown on Figure 3.5.2(A). Ranges decrease from more than 4.5 m to less than 4 m progressing east along the English Channel coast.

Mean spring tidal current speeds (Figure 3.5.2(B)) are increased by the constriction of area between South Devon and the Cotentin Peninsula on the French coast and again tend to be greater near to headlands. Maximum tidal current speeds of less than 0.5 m s^{-1} occur in parts of the larger bays.

The mean sea surface temperatures for summer and winter are shown on Figure 3.5.2(C). In winter, relatively warm Atlantic waters elevate average sea surface temperatures in this region, particularly to the west, which are then the warmest waters in Britain, at nearly 9 °C. In summer, temperatures typically are about 16 °C.

The mean surface salinities for summer and winter are shown on Figure 3.5.2(D). The salinity of waters in this region generally is high (more than 35), mainly because of the movement of Atlantic waters into the English Channel. The mixing of Atlantic waters with coastal freshwater discharges from estuaries decreases salinity toward the coast, both in summer and winter.

3.5.3. Wind and waves

Figures 3.5.3(A, B) show, respectively, contours of the wind speeds exceeded for 75% and 0.1% of the time. Wind speeds of greater than 45 m sec^{-1} (90 knots) have been recorded at various places in this region. The prevailing winds throughout the year are from the southwest, Figure 3.5.3(C). Strong winds occur in winter, when a series of gales, lasting on average 4 - 6 hours each, may persist for several days. Small depressions develop rapidly and move quickly eastwards causing frequent changes in wind conditions but not in wind direction. Winds from the southeast are less frequent and usually less persistent. Spring is the most common season for northeast winds. Estuaries, harbours and the inner parts of bays are particularly subject to local variations in wind conditions, due to the sheltering effect of headlands and other topography as well as steering of winds along steeply-sided estuary valleys.

Figure 3.5.3(D) shows the significant wave heights that can be expected to be exceeded for 10% and 75% for the year in this region. Large waves are generated by the prevailing south-westerly winds, which have a long 'fetch' from the Western Approaches of the English Channel onto the south-westerly facing coasts of the region (Figure 3.5.3(D)). Again, the western parts of the larger bays are sheltered from these waves by headlands (Figure 3.5.3(D)). For example, the significant wave height offshore is greater than about 2.5 m for 10% of the year and less than 1.5 m in the sheltered parts of major bays.

3.6. Western Approaches

3.6.1. Bathymetry and sediments

The seabed of most of this region slopes steeply and regularly down to a depth of about 60 m, levelling out onto the westward-sloping continental shelf (Figure 3.6.1(A)). Much of it is covered in thin, mobile sediments and reflects the shape of

the bedrock surface. Submerged cliffs occur down to a depth of about 70 m around the coast of Cornwall and the Isles of Scilly.

The majority of the seabed sediments in the southwest of the region are sands or thin spreads of gravel, generally less than one metre thick. Extensive areas of bedrock are exposed at the seabed near the coast (Figure 3.6.1(B)). A major sand wave field covers a large area northwest of Lundy in which individual waves can rise to over 20 m above the level of the surrounding seabed. Generally, the thickness of the seabed sediment decreases eastwards within the inner Bristol Channel and the Severn Estuary as tidal current speeds increase. Much of the inner Bristol Channel has bare rock at the seabed, with mobile sediment restricted to isolated linear banks near the coast. Bridgwater Bay (Figure 3.6.1(B)) is underlain by an extensive mud sheet, locally over 20 m thick, that displays a sharp seaward termination. Similar mud flats are found in other parts of the Severn, but generally the mud is only a few metres thick. The upper part of the Severn Estuary is in-filled with sand banks.

3.6.2. Tides, temperature and salinity

The mean springs tidal range along the coast of the region shows a steady increase north-eastwards from 5 m in the southwest to 12.3 m in the upper Severn (Figure 3.6.2(A)). Water levels can be further raised by more than 1.5 m during large storm surges that can occur in the inner Bristol Channel and Severn Estuary (e.g. Figure 2.6(A)). Large spring tides often lead to the formation of a tidal bore in the Severn that can be seen as one or more waves, sometimes 2 m in height, that flood into the River Severn, breaking in the shallows at the banks of the tidal river.

Maximum spring-tide tidal currents in the region exceed 1 m s^{-1} near headlands and in the channel between the Isles of Scilly and the mainland (Figure 3.6.2(B)).

Speeds increase progressively going eastwards into the Bristol Channel and within the Severn Estuary. Computer modelling of the tides in the area by Uncles (1983) indicates maximum current speeds that are somewhat slower than those plotted here and with distributions that are much more complex. Nevertheless, Figure 3.6.2(B) does provide a qualitative illustration of currents and emphasises that current speeds are fast and increasing progressing into the Severn Estuary.

Figure 3.6.2(C) shows the mean sea surface temperatures for summer and winter. The southwest of the region has a temperature of about 9.0 - 9.5 °C in February, compared with 10.5° C at the edge of the continental shelf. Water temperatures decrease in the shallower waters to the northeast, and the mean in the inner Severn Estuary is less than 6°C. Temperatures are at a maximum for the year in August on average, attaining approximately 16 °C throughout the region. Thermal stratification of the water column develops in the Celtic Sea by late spring and spreads eastwards along the north Cornwall coast, whereas the Bristol Channel and Severn remain vertically well-mixed throughout the year.

The mean surface salinity in the southern part of the region is 35 or more, which is typical of Atlantic Ocean waters (Figure 3.6.2(D)). Salinity decreases north-eastwards into the Bristol Channel as the influence of freshwater input from the Severn and various Bristol Channel estuaries increases (Figure 3.1). Variations in the salinity of the Severn Estuary and inner Bristol Channel follow changes in the river flow, with generally lower salinities in winter (when river flows are greater) than in summer. Salinity values in the upper estuary in winter may be less than 20 (Collins & Williams 1981) and approach zero in the tidal river where the influence of fast ebb-directed river currents exceeds the ability of flood-directed tidal currents and mixing of water masses to transport saltwater further into the estuary.

3.6.3. Wind and waves

Figures 3.6.3(A, B) show, respectively, contours of the wind speeds exceeded for 75% and 0.1% of the time. Maximum wind speeds occur across western parts of the region and most of the coast is exposed to the prevailing winds, which are mainly from the west (Figure 3.6.3(C)). Wind speeds decrease eastwards in the Bristol Channel. There are an average of 25 days of gales per year in the southwest of the region, most of which occur in the winter months (Hydrographic Department 1960b).

Figure 3.6.3(D) shows the significant wave heights that can be expected to be exceeded for 10% and 75% for the year in this region. Large waves are generated on the open coasts of the region because of the long fetch across the Atlantic Ocean and the prevailing westerly winds. The relatively steep near-shore bathymetric gradient and cliff coastline results in high waves approaching close to the coast. The significant wave height in the outer reaches of the Bristol Channel is greater than about 3 m for 10% of the year (compared with a predicted 50-year extreme of 18 m) and decreases to less than 1 m in the upper Severn Estuary (Figure 3.6.3(D)). Wave data from the southwest of the region show that significant wave heights have increased progressively between 1962 and 1984, indicating an increase in storminess in the North Atlantic over this time (Draper, 1991).

3.7. Northern Bristol Channel and St. George's Channel

3.7.1. Bathymetry and sediments

The wide trough that runs the length of St George's Channel (maximum depth greater than 100 m) is the dominant bathymetric feature in the region (Figure 3.7.1(A)). The Bristol Channel is less than 60 m deep and shallows to the east.

Because of the fast tidal currents in the Bristol Channel, the seabed sediments become coarser grained and thinner towards the east (Figure 3.7.1(B)). The major bays of the northern Bristol Channel (Swansea Bay and Carmarthen Bay) have thicker deposits of sandy sediments within them. Sediments generally are coarse grained and thinly spread off the western-most (Pembrokeshire) coast.

3.7.2. Tides, temperature and salinity

The mean spring-tide tidal range along the region's coastlines generally is high (Figure 3.7.2(A)), ranging from more than 8 m in the north-eastern parts of the Bristol Channel to about 4 m or less northeast of the St. George's Channel. The tidal water levels may be modified further by storm surges, which are predicted to increase levels by over 1.5 m as an extreme value during a 50-year period. Tidal currents during mean spring tides (Figure 3.7.2(B)) are at their maximum of over 2 m s^{-1} in the Bristol Channel but also are fast in the vicinity of the headlands.

The surface temperature of the seawater (Figure 3.7.2(C)) varies between 6.5 to 8.5 °C in winter (February/March) and 14 to 16 °C in summer (August/September). In winter, coastal waters are cooler than those offshore, and in summer they are warmer. The seawater salinity varies slightly with the seasons, generally being greater in the summer than in the winter (Figure 3.7.2(D)). Greater variation occurs near the coast, especially near river mouths, where Atlantic water is diluted by river water.

3.7.3. Wind and waves

Parts of the coast of this region are among the windiest in the UK. Wind speeds exceed about 3.5 m s^{-1} (about Force 3) at the coast for 75% of the time and exceed 19 m s^{-1} (Gale) for 0.1% of the time (Figures 3.7.3(A, B)). These data are mean hourly speeds, but for shorter intervals the maximum speed may be much faster. Dominant winds are from the southwest and blow for approximately 20% of

the time, whereas winds from the eastern sector blow for about 9% of the time (Figures 3.7.3(C)). As one would anticipate, gales are more common in winter than in summer.

Figure 3.7.3(D) shows the significant wave heights that can be expected to be exceeded for 10% and 75% for the year in this region. Much of the coast is open to the prevailing south-westerly winds and where deep water occurs close to the coast, it is subject to severe wave attack during storms. The significant wave height in the outer reaches of the Bristol Channel and St. George's Channel is greater than about 3 m for 10% of the year (compared with a predicted 50-year extreme of 18 m) and decreases progressing into the Bristol Channel (Figure 3.6.3(D)).

4. Recent data for the SEA8 area

4.1. The DTI Atlas (tides, winds and waves)

The UK Department of Trade and Industry (DTI) has funded an atlas (the UK Atlas of Offshore Renewable Energy) produced by ABPmer, the Met Office, Garrard Hassan and Proudman Oceanographic Laboratory that was published in December 2004 (DTI, 2004).

The Atlas supplies considerable quantitative information on the tidal, wave and wind regimes of the northwest European shelf and the SEA8 area in particular. Tidal data includes maps of spring tidal range, peak spring-tide and neap-tide current speeds and power densities. Wave data includes maps of annual mean significant wave heights, wave power and seasonal variations. Wind data includes maps of annual mean wind speed and wind power density. All of the graphics utilise output-data from the latest UK tide, wave and wind models of their time (2004) and as such the Atlas supplies an easy-to-access source of the most

recent quantitative, highly spatially-resolved physical and hydrographical data for the SEA8 area.

4.2. The HSE Report (winds and waves)

The UK Health and Safety Executive (HSE) have funded an Offshore Technology Report produced by Fugro GEOS (HSE, 2001) that presents wind and wave frequency distributions and roses for 40 sites around the British Isles. These distributions have been produced using hindcast wind and wave time-series data from the NEXT model (HSE, 2001) for the combined periods January 1977 to December 1979 and January 1989 to December 1994. There are two grid points in the English Channel and three in the Celtic Sea, and as such the Report supplies an important source of relatively recent wind and wave data for the SEA8 area. The stated intention of the Report is to supply a decision-making tool, primarily for those persons concerned with offshore operations.

4.3. The OMEX project (dynamics at the shelf break)

The SEA8 region extends to the shelf break and the OMEX project (Wollast et al., 2001; Huthnance et al., 2001) collected valuable oceanographic data at the shelf break near the southwest boundary of the SEA8 region. Many of the physical data published from OMEX-1 apply to the Goban Spur area near 49º N, 11º W, somewhat outside the SEA8 region, but they may nevertheless contribute to the understanding of processes at the boundary of SEA8. The major conclusions for the physical data are (Huthnance, 2001):

- The along-slope flow (typically of the order of 0.05 m s^{-1}) is reduced or even reversed in spring and generally is weaker than at some other margin sectors owing to the non-meridional alignment and indentations in the Celtic Sea

slope, and may sometimes overshoot rather than follow the depth contours around the Goban Spur.

- Tidal currents typically are of the order of 0.2 m s^{-1} on the adjacent shelf and 0.1 m s^{-1} or less over most of the Goban Spur; they increase to the southeast.
- Other (wind and eddy-forced) contributions to the currents typically are of the order of 0.1 m s^{-1} or less, except on the shelf, and decrease with depth.
- Wind-forced, tide-forced and wave-forced currents probably are the most consistent agents of cross-slope water exchange (of the order of 1 m^2 s^{-1}) with topographic effects due to canyons and spurs being locally important.
- Water-column stratification starts intermittently until early June, becomes shallower through June and deepens by September. One storm, on 5 – 8 September 1995, roughly doubled the upper mixed-layer depth to greater than 40 m.
- Vertical mixing is intermittent, dominated by surface inputs due to winds and waves; towards the southeast, internal waves of tidal origin are increasingly important for mixing across the thermocline.

4.4. CEFAS drifter studies (density-driven flow)

Work by the UK Centre for Environment, Fisheries & Aquaculture Science (CEFAS, 2007) in recent years has shown that relatively strong, residual (non-tidal, baroclinic) circulations can arise from the density contrasts that exist between areas that are thermally stratified (layered) in summer and those that are thermally mixed. In the stratified areas, dense 'pools' of colder (and saltier) bottom waters occur, potentially from spring to autumn. At the edges of these regions, where strong horizontal density-gradients exist in the form of bottom fronts, density forces generate along-frontal, residual flows (Horsburgh et al., 1998).

CEFAS surveys in the Celtic Sea and St. George's Channel during summer 1998 showed the dominance of temperature in determining water column structure over the stratified regions. Computed geostrophic flows (i.e. obtained assuming a balance between the dynamical effects caused by density and the Earth's rotation) showed jets of residual flow associated with bottom fronts, with current speeds in excess of 0.1 m s^{-1}. Drifter studies yielded a mean residual speed of 0.065 m s^{-1} for all drifters and speeds in excess of 0.3 m s^{-1} for drifters in the St. Georges Channel. It was concluded that the residual circulation of the Celtic Sea in summer, in the areas studies, is dominated by intense and predictable cyclonic (anticlockwise) baroclinic flows associated with bottom density fronts. They conclude that the circulations limit exchange of waters between the Irish Sea and Celtic Sea and are likely to enhance transport from the Bristol Channel into the Celtic Sea, with a component passing westward around Ireland.

CEFAS surveys in the Western English Channel during summer 2003 similarly showed the importance of seasonal thermal stratification and associated strong frontal boundaries (CEFAS, 2007). Drifter tracks were correlated against wind and showed three groupings: those tracks in the main frontal regions where wind effects were not statistically significant and residual current speeds typically were 0.1 – 0.2 m s^{-1}; those in the central Channel that were wind-driven and had residual current speeds that typically were 0.05 m s^{-1} and those along the south Cornish coast that had current speeds that typically were 0.1 m s^{-1}. They conclude that under these frontal conditions a transport pathway exists between the coasts of Brittany to the southern English coast and then around the southern and western Irish coast.

4.5. PML frontal studies (visualising fronts and eddies)

Novel techniques have been developed at the Plymouth Marine Laboratory (PML) for increasing the value of cloud-affected sequences of Advanced Very High Resolution Radiometer (AVHRR) sea-surface temperature (SST) data and Sea-viewing Wide Field-of-view Sensor (SeaWiFS) ocean colour data for visualising dynamic physical and biological oceanic processes such as fronts, eddies and blooms (Miller, in press). The proposed composite-front-map approach combines the location, strength and persistence of all fronts observed over several days into a single map, which allows the intuitive interpretation of mesoscale structures. This method achieves a synoptic view without blurring dynamic features, which is an inherent problem with conventional time-averaging compositing methods. Objective validation confirms a significant improvement in feature visibility on composite maps compared to individual front maps. A further novel aspect is the automated detection of ocean colour fronts, correctly locating 96% of chlorophyll fronts in a test data set. Front-map animations provide a unique insight into the evolution of upwelling and eddy movements (Miller, 2007).

An example of a composite-front map of sea surface temperature that shows the frontal situation for the UK Western Approaches and much of the SEA8 region during 18 – 22 July 2000 is shown in Figure (4.5). The marked, seasonal, tidal-mixing fronts are very clearly delineated and illustrate a complexity of shape and short-term evolution that could not be obtained in the earlier work (see Figure 2.10 (A, B)).

5. Summary

On a broad scale, the seabed bathymetry that typifies the SEA8 region away from the inner Bristol Channel and eastern English Channel comprises: a narrow, steep coastal zone extending down to 50 or 70 m in depth; a wide, almost

featureless inner shelf extending down to about 120 m in depth; the (usually) rugged, rocky shoals that rise above the general level of the inner shelf; and a more irregular outer shelf, extending from 120 m down to the shelf-break at 180 to 205 m in depth. Thereafter, a steep continental slope extends from the shelf-break down to about 4500 m in depth. The seabed sediment distribution is largely determined by the sediment supply and waves and tidal currents, especially peak current speeds, acting upon sediments that were laid down during the ice age. Close to the south-western boundary of SEA8, near the shelf break, the bottom sediments are mud and mixtures of mud and sand, with substantial areas of sand. Over much of the Celtic Sea and English Channel the sediments comprise mixtures of sand and gravel. There is a large area of gravel in the central and eastern English Channel and large areas of mixed sand, gravel and exposed rock closer to shore, where fast currents have scoured the bed of finer sediments.

The mean spring tidal range in water level increases from approximately 3 m close to the south-western boundary of SEA8 to more than 12 m in the upper Severn Estuary. Spring tidal range in the English Channel can be less than 2 m near the Isle of Wight and exceed 6 m in the eastern English Channel and near the Dover Strait. The time of mean high-water springs relative to the moon's transit over the Meridian of Greenwich increases from approximately 3.5 hours close to the south-western boundary of SEA8 to more than 5.5, 7 and 10 hours near the St. George's Channel, the upper Severn Estuary, and the eastern English Channel, respectively.

M_2 (principal lunar semidiurnal tide) is the largest component of tide in the SEA8 region. The pattern of M_2 water-level elevations corresponds very closely to that of the mean spring tidal range in the region. The pattern of M_2 water-level elevation phases also corresponds closely to that for the spring tide phases. S_2

(principal solar semidiurnal tide) is the next most important tidal constituent over the SEA8 region. The addition of M_2 and S_2 tides produces a spring-neap cycle. The ratio of S_2 to M_2 water-level amplitudes (or ranges) is somewhat less than 35% close to the southwest boundary of SEA8 and remains close to 35% near the St. George's Channel boundary and within the Bristol Channel and for much of the English Channel, although it decreases to 30% in the eastern English Channel and locally increases to 55% near the Isle of Wight. The phase differences between S_2 and M_2 elevations generally show that the S_2 elevation phases are roughly 40° - 50° greater than the M_2 phases throughout much of the SEA8 region, but that differences are smaller both near the southwest boundary of SEA8 (33%) and within the area of small tides in the English Channel (30%).

Spring tidal speeds are relatively slack close to the southwest boundary of SEA8, typically 0.2 m s^{-1}, and increase to more than 1.0 m s^{-1} near the St. George's Channel, 1.6 m s^{-1} in the upper Bristol Channel and 1.4 m s^{-1} in the English Channel. However, currents can be very variable in space as they reflect local features such as bays and headlands. The maximum stress on the seabed due to tidal currents has an important influence on bed sediment types because it determines the sizes of sediment grains that are moved and the sizes of those that can remain at a location. There is a remarkable similarity between the direction of peak tidal stresses and the direction of sediment transport paths for sand-sized bottom sediments over the northwest European shelf and over the SEA8 region in particular

Steady winds from the southwest drive depth-averaged residual currents to the southeast close to the southwest boundary of SEA8 and across the Celtic Sea. A north-flowing current is formed along the north Cornwall and Devon coasts and across the mouth of the Bristol Channel, and a south-flowing return current occurs

in the central reaches of the St. George's Channel. Currents flow to the north and east along the English Channel and through the Dover Strait. Steady winds from the southeast produce depth-averaged residual currents to the northwest close to the southwest boundary of SEA8 and across the Celtic Sea. However, a north-flowing current is again formed along the north Cornwall and Devon coasts and across the mouth of the Bristol Channel, but in this case there is no south-flowing return flow in the central reaches of St. George's Channel. The southeast wind stress again drives a flow to the north and east along the English Channel and through the Dover Strait.

Storm surge elevations in water level for a simulated fifty year return period show that elevations increase from approximately 0.5 m close to the southwest boundary of SEA8 to between 0.75 and 1.25 m near the St. George's Channel and exceed 1.5 m in the Bristol Channel. The surge elevation increases as it propagates from the Celtic Sea and into the English Channel and reaches 2 m near the Dover Strait. Storm surge current speeds associated with the surge elevations show maximum speeds that increase from approximately 0.2 m s^{-1} close to the southwest boundary of SEA8 to approximately 0.4 m s^{-1} in the central Celtic Sea, before decreasing again to 0.2 m s^{-1} near the St. George's Channel and in the Bristol Channel. The maximum surge speed increases as the surge propagates from the Celtic Sea into the English Channel and typically is 0.6 m s^{-1} in the coastal English Channel regions of SEA8, reaching 1 m s^{-1} in the Dover Strait area.

Winds are predominantly from the southwest or west in the SEA8 region. The predicted heights of the highest individual waves that are likely to occur in the worst storm in any 50-year interval have wave heights that decrease from approximately 35 m close to the southwest boundary of SEA8 to less than 20 m

near the St. George's Channel and the Bristol Channel, and to less than 13 m in the eastern English Channel. The associated wave periods decrease from greater than approximately 16 s close to the southwest boundary of SEA8 to approximately 14 s near the St. George's Channel and the Bristol Channel, and decrease to less than 10 s in the eastern English Channel.

The significant wave heights that are predicted to be exceeded for 10% of the year decrease from greater than 4 m at the southwest limit of SEA8 to less than 2 m in the eastern English Channel, inner Bristol Channel and Severn Estuary, while remaining greater than 3 m in the St. George's Channel. The significant wave heights that are predicted to be exceeded for 75% of the year decrease from greater than 1.5 m at the southwest limit of SEA8 to less than 0.5 m in the eastern English Channel, inner Bristol Channel and Severn Estuary, while remaining greater than 1 m in the St. George's Channel. Annual wave periods (seasonal variations in wave period are small) are greater than 6 s and less than 8 s at the southwest limit of SEA8 and reduce to less than 4 s in the eastern English Channel and inner Bristol Channel.

Fast currents and strong mixing in the English and Bristol Channels do not allow the development of a pronounced seasonal thermocline, whereas a thermocline develops above the bottom-mixed layer at stations in the deeper shelf waters. The edge of the Celtic Sea shelf is characterised by a band of cold water, roughly 100 km wide, that is about 1 – 2 °C colder than the adjacent shelf and oceanic waters. The shelf waters near the break are characterised by an extensive (> 100 m) near-homogeneous bottom layer due to tidal mixing, which limits the vertical region for thermocline development between the wind-mixed layer and the bottom-mixed layer. The thermocline is characterised by marked

internal wave activity and the broadening of the thermocline over the slopes is thought to indicate greater mixing near the shelf break.

On average, the mean monthly surface temperature for February decreases from approximately 11 °C close to the southwest boundary of SEA8 to less than 8.5, 6 and 8.5 °C near the St. George's Channel, the upper Severn Estuary of the Bristol Channel, and the eastern and much of the shallow near-shore English Channel. On average, the mean surface temperature for August decreases from approximately 17 °C close to the southwest boundary of SEA8 to less than 15.5 °C near the St. George's Channel and (typically) 16 °C in the outer Bristol Channel and English Channel. There is an advance and retreat of the seasonal thermocline across the continental shelf within the SEA8 region during the year. When surface heating becomes sufficiently great, more buoyancy is produced in the water column than can be dissipated by mixing due to wind and tide and the water column stratifies, with well-defined surface and bottom layers separated by the thermocline. Because the thermocline does not form simultaneously over the SEA8 region, the water column may be vertically mixed in one area and stratified in a neighbouring area, so that a surface frontal area comprising sharp temperature gradients may occur between them.

Numerous estuaries enter the SEA8 region and contribute freshwater, sediments, nutrients and, potentially, pollutants to the coastal zone. In the SEA8 region the mean, long-term average rate of freshwater river inputs (as measured at the seaward-most gauging stations) is approximately 640 $m^3 s^{-1}$. When the additional drainage-basin areas between gauging station locations and estuary mouths are taken into account the flow rate is substantially greater (e.g. for the southwest of England roughly 40% greater). These freshwater inputs influence coastal salinity. The mean monthly surface salinity distribution for February, on

average, decreases from greater than approximately 35.6 close to the southwest boundary of SEA8 to less than 35.0 near the St. George's Channel and within the Bristol Channel. Salinity exceeds 35.0 for much of the SEA8 area of the English Channel, although generally it is less close to the shore, due to the influence of estuarine outflows. On average, the mean monthly surface salinity distribution for August decreases from greater than approximately 35.5 close to the southwest boundary of SEA8 to (generally) less than 35.0 in the Bristol Channel, St. Georges Channel and the eastern English Channel and for much of the near-shore region of the English Channel.

Recent work in the region includes the measurement of currents at the boundaries of seasonal (tidal mixing) frontal systems as well as investigations into the spatial complexity of these seasonal (and other) frontal systems. The SEA8 region extends to the shelf break and reference has been given to recent work in this environment. The data and discussions presented in our report should be used in conjunction with maps of environmental variables available on the web at DTI (2004) for tides, winds and waves, and HSE (2001) for winds and waves; the producers of these maps should be consulted regarding the newest available updates.

References

Barne, J.H., Robson, C.F., Kaznowska, S.S., & Doody, J.P., eds. 1995. Coasts and seas of the United Kingdom. Region 12 Wales: Margam to Little Orme. Peterborough, Joint Nature Conservation Committee. (Coastal Directories Series.)

Barne, J.H., Robson, C.F., Kaznowska, S.S., Doody, J.P, & Davidson, N.C., eds. 1996a. Coasts and seas of the United Kingdom. Region 9 Southern England:

Hayling Island to Lyme Regis. Peterborough, Joint Nature Conservation Committee. (Coastal Directories Series.)

Barne, J.H., Robson, C.F., Kaznowska, S.S., Doody, J.P, Davidson, N.C., & Buck, A.L., eds. 1996b. Coasts and seas of the United Kingdom. Region 10 Southwest England: Seaton to the Roseland Peninsula. Peterborough, Joint Nature Conservation Committee. (Coastal Directories Series.)

Barne, J.H., Robson, C.F., Kaznowska, S.S., Doody, J.P, Davidson, N.C., & Buck, A.L., eds. 1996c. Coasts and seas of the United Kingdom. Region 11 The Western Approaches: Falmouth Bay to KenFigure Peterborough, Joint Nature Conservation Committee. (Coastal Directories Series.)

Barne, J.H., Robson, C.F., Kaznowska, S.S., Doody, J.P, Davidson, N.C., & Buck, A.L., eds. 1998a. Coasts and seas of the United Kingdom. Region 7 South-east England: Lowestoft to Dungeness. Peterborough, Joint Nature Conservation Committee. (Coastal Directories Series.)

Barne, J.H., Robson, C.F., Kaznowska, S.S., Doody, J.P, Davidson, N.C., & Buck, A.L., eds. 1998b. Coasts and seas of the United Kingdom. Region 8 Sussex: Rye Bay to Chichester Harbour. Peterborough, Joint Nature Conservation Committee. (Coastal Directories Series.)

British Geological Survey. 1987. Sea-bed sediments around the United Kingdom (North and South sheets). 1:1,000,000 scale. Keyworth, British Geological Survey.

British Geological Survey. 1991. Geology of the United Kingdom, Ireland and the adjacent continental shelf. 1:1,000,000 scale. Keyworth, British Geological Survey.

British Geological Survey. 1996a. Chapter 2.2 Offshore geology. In: Coasts and seas of the United Kingdom. Region 9 Southern England: Hayling Island to

Lyme Regis, ed. by J.H. Barne, C.F. Robson, S.S. Kaznowska, J.P. Doody & N.C. Davidson, 24-26. Peterborough, Joint Nature Conservation Committee. (Coastal Directories Series.)

British Geological Survey. 1996b. Chapter 2.3 Wind and water. In: Coasts and seas of the United Kingdom. Region 9 Southern England: Hayling Island to Lyme Regis, ed. by J.H. Barne, C.F. Robson, S.S. Kaznowska, J.P. Doody & N.C. Davidson, 27-30. Peterborough, Joint Nature Conservation Committee. (Coastal Directories Series.)

British Geological Survey. 1996c. Chapter 2.2 Offshore geology. In: Coasts and seas of the United Kingdom. Region 10 South-west England: Seaton to the Roseland Peninsula, ed. by J.H. Barne, C.F. Robson, S.S. Kaznowska, J.P. Doody, N.C. Davidson & A.L. Buck, 20-22. Peterborough, Joint Nature Conservation Committee. (Coastal Directories Series.)

British Geological Survey. 1996d. Chapter 2.3 Wind and water. In: Coasts and seas of the United Kingdom. Region 10 South-west England: Seaton to the Roseland Peninsula, ed. by J.H. Barne, C.F. Robson, S.S. Kaznowska, J.P. Doody, N.C. Davidson & A.L. Buck, 23-25. Peterborough, Joint Nature Conservation Committee. (Coastal Directories Series.)

British Geological Survey. 1996e. Chapter 2.2 Offshore geology. In: Coasts and seas of the United Kingdom. Region 11 The Western Approaches: Falmouth Bay to Kenfig, ed. by J.H. Barne, C.F. Robson, S.S. Kaznowska, J.P. Doody, N.C. Davidson & A.L. Buck, 23-26. Peterborough, Joint Nature Conservation Committee. (Coastal Directories Series.)

British Geological Survey. 1996f. Chapter 2.3 Wind and water. In: Coasts and seas of the United Kingdom. Region 11 The Western Approaches: Falmouth Bay to Kenfig, ed. by J.H. Barne, C.F. Robson, S.S. Kaznowska, J.P. Doody,

N.C. Davidson & A.L. Buck, 27-30. Peterborough, Joint Nature Conservation Committee. (Coastal Directories Series.)

British Geological Survey. 1998a. Chapter 2.2 Offshore geology. In: Coasts and seas of the United Kingdom. Region 7 South-east England: Lowestoft to Dungeness, ed. by J.H. Barne, C.F. Robson, S.S. Kaznowska, J.P. Doody, N.C. Davidson & A.L. Buck, 23-27. Peterborough, Joint Nature Conservation Committee. (Coastal Directories Series.)

British Geological Survey. 1998b. Chapter 2.2 Offshore geology. In: Coasts and seas of the United Kingdom. Region 8 Sussex: Rye Bay to Chichester Harbour, ed. by J.H. Barne, C.F. Robson, S.S. Kaznowska, J.P Doody, N.C. Davidson & A.L. Buck, 22-24. Peterborough, Joint Nature Conservation Committee. (Coastal Directories Series.)

British Geological Survey, Dales, D., and Gilbert, K. 1998a. Chapter 2.3 Wind and water. In: Coasts and seas of the United Kingdom. Region 7 South-east England: Lowestoft to Dungeness, ed. by J.H. Barne, C.F. Robson, S.S. Kaznowska, J.P Doody, N.C. Davidson & A.L. Buck, 28-32. Peterborough, Joint Nature Conservation Committee. (Coastal Directories Series.)

British Geological Survey, Dales, D., and Gilbert, K. 1998b. Chapter 2.3 Wind and water. In: Coasts and seas of the United Kingdom. Region 8 Sussex: Rye Bay to Chichester Harbour, ed. by J.H. Barne, C.F. Robson, S.S. Kaznowska, J.P Doody, N.C. Davidson & A.L. Buck, 25-28. Peterborough, Joint Nature Conservation Committee. (Coastal Directories Series.)

Caton, P.G. 1976. Maps of hourly wind speed over the UK 1965 - 73. Bracknell, Meteorological Office. (Climatological Memorandum No. 79.)

CEFAS. 2007. Web-posted presentations on drifter studies in the Celtic Sea, St. George's Channel and the western English Channel by various Cefas staff and colleagues at www.cefas.co.uk/projects/.

Collins, N.R., & Williams, R. 1981. Zooplankton of the Bristol Channel and Severn Estuary. The distribution of four copepods in relation to salinity. Marine Biology, 64: 273-283.

Draper, L. 1991. Wave climate atlas of the British Isles. London, HMSO.

DTI. 2004. UK Atlas of Offshore Renewable Energy. Produced by ABPmer, the Met Office, Garrard Hassan and Proudman Oceanographic Laboratory and posted at www.dti.gov.uk/.

Evans, C.D.R. 1990. United Kingdom offshore regional report: the geology of the western English Channel and its western approaches. (London: HMSO for the British Geological Survey.)

Evans, C.D.R. 1995a. Chapter 2.2 Offshore environment. In: Barne, J.H., Robson, C.F., Kaznowska, S.S., & Doody, J.P, eds. 1995. Coasts and seas of the United Kingdom. Region 12 Wales: Margam to Little Orme. 23-28. Peterborough, Joint Nature Conservation Committee. (Coastal Directories Series.)

Evans, C.D.R. 1995b. Chapter 2.3 Wind and water. In: Barne, J.H., Robson, C.F., Kaznowska, S.S., & Doody, J.P, eds. 1995. Coasts and seas of the United Kingdom. Region 12 Wales: Margam to Little Orme. 29-33. Peterborough, Joint Nature Conservation Committee. (Coastal Directories Series.)

Flather, R. A. 1987. Estimates of extreme conditions of tide and surge using a numerical model of the north-west European continental shelf. Estuarine, Coastal and Shelf Science 24, 69-93.

Folk, R.L. 1954. The distinction between grain-size and mineral composition in sedimentary rock nomenclature. Journal of Geology, 62, 344359.

Hamblin, R.J.O, Crosby, A., Balson, P.S., Jones, S.M., Chadwick, R.A., Penn, I.E., and Arthur, M.J. 1992. United Kingdom offshore regional report: the geology of the English Channel. (London: HMSO for the British Geological Survey.)

Horsburgh, K.J., Hill, A.E., and Brown, J. 1998. A summer jet in the St. George's Channel of the Irish Sea. Estuarine, Coastal and Shelf Science 47, 285-294.

HSE. 2001. Wind and wave frequency distributions for sites around the British Isles. Produced as Offshore Technology Report 2001/030 by Fugro GEOS and posted at www.hse.gov.uk/research/otopdf/2001/oto01030.pdf.

Huthnance, J.M., Coelho, H., Griffiths, C.R., Knight, P.J., Rees, A.P., Sinha, B., Vangriesheim, A., White, M., and Chatwin, P.G. 2001. Physical structures, advection and mixing in the region of Goban Spur. Deep Sea Research II 48, 2979 – 3021.

Hydrographic Department. 1960a. Admiralty North Sea Pilot, volume III. Taunton, British Admiralty.

Hydrographic Department. 1960b. West coast of England pilot. London, Hydrographic Department.

Hydrographic Department. 1984. Channel Pilot. Isles of Scilly and south coast of England, from Cape Cornwall to Bognor Regis. NP 27. London, Hydrographic Office.

Hydrographic Department. 1985. Dover Strait Pilot. South-east coast of England: Bognor Regis to Southwold, and north-west coast of Europe: Cap d'Antifer to Schevenigen. Taunton, Hydrographic Department. (NP 28.)

Hydrographic Office. 1996. Co-tidal and Co-range lines: British Isles and Adjacent waters. Admiralty Chart No. 5058, UK Hydrographic Office, Taunton, UK.

IH, 1998. Hydrological data United Kingdom. Institute of Hydrology, Wallingford, Oxon OX10 8BB. 207 pp.

Lee, A.J., & Ramster, J.W. 1981. Atlas of the seas around the British Isles. Lowestoft, Ministry of Agriculture, Fisheries and Food.

MAFF. 1981. Atlas of the seas around the British Isles. Ministry of Agriculture Fisheries and Food, MAFF Atlas Office, Fisheries Laboratory, Pakefield Road, Lowestoft, Suffolk NR33 0HT.

Miller, P. in press. Composite front maps for improved visibility of dynamic sea-surface features on cloudy SeaWiFS and AVHRR data. Journal of Marine Systems.

Miller, P. 2007. Examples of remote sensing studies at Plymouth Marine Laboratory can be viewed via its web site at: www.pml.ac.uk/ and the animations described in the preceding 'in press' paper may be viewed at: www.npm.ac.uk/papers/miller_jms2007www.npm.ac.uk/papers/miller_jms2007.

Pingree, R.D. 1974. The turbulent boundary layer on the continental shelf. Nature 250, 720-722.

Pingree, R.D. 1975. The advance and retreat of the thermocline on the continental shelf. Journal of the Marine Biological Association of the United Kingdom 55, 965-974.

Pingree, R.D. 1980. Physical oceanography of the Celtic Sea and English Channel. In: The north-west European shelf seas: the sea bed and the sea in motion. Vol. 2. Physical and chemical oceanography and physical resources, ed. by F.T. Banner, M.B. Collins & K.S. Massie, 415-465. Amsterdam, Elsevier. (Oceanography Series.)

Pingree, R.D. and Griffiths, D.K. 1977. The bottom mixed layer on the continental shelf. Estuarine and Coastal Marine Science 5, 399-413.

Pingree, R.D. and Griffiths, D.K. 1979. Sand transport paths around the British Isles resulting from M_2 and M_4 tidal interactions. Journal of the Marine Biological Association of the United Kingdom 59, 497-513.

Pingree, R.D. and Griffiths, D.K. 1980. Currents driven by a steady uniform wind stress on the shelf seas around the British Isles. Oceanologica Acta 3, 227-236.

Pingree, R.D. and Griffiths, D.K. 1981. S_2 tidal simulations on the northwest European Shelf. Journal of the Marine Biological Association of the United Kingdom 61, 609-616.

Pingree, R.D., and Mardell, G.T. 1981. Slope turbulence, internal waves and phytoplankton growth at the Celtic Sea shelf break. Philosophical Transactions of the Royal Society of London, A, 302 663-682.

Proudman, J., 1953. Dynamical Oceanography. Methuen, London. 409 pp.

Sager, G., and Sammler, R. 1968. Atlas der Gezeitenstrome fur die Nordsee, den Kanal and die Irische See. Rostock, Seehydrographischer Dienst der DDR.

Shellard, H.C. 1968. Tables of surface wind speed and direction over the United Kingdom. London, HMSO.

Sinha, B., and Pingree, R.D. 1997. The principal lunar semidiurnal tide and its harmonics: baseline solutions for M_2 and M_4 constituents on the northwest European Continental Shelf. Continental Shelf Research 17, 1321-1365.

Stride, A.H., 1973. Sediment transport by the North Sea. In: North Sea Science (ed. E.D. Goldberg). The MIT Press, pp. 101-130.

Tappin, D.R., Chadwick, R.A., Jackson, A.A., Wingfield, R.T.R., and Smith, N.J.P., 1994. United Kingdom offshore regional report: the geology of Cardigan

Bay and the Bristol Channel. (London: HMSO for the British Geological Survey.)

Uncles, R. 1983. Hydrodynamics of the Bristol Channel. Marine Pollution Bulletin 15(2), 47-53.

Wollast, R., and Chou, L. 2001. Ocean Margin Exchange in the Northern Gulf of Biscay: OMEX I. An introduction. Deep Sea Research II 48, 2971 – 2978.

Figure Captions

Figure 2.1 (A), Location of SEA8 region; (B), Bathymetry of SEA8 region (Redrawn with modifications from MAFF, 1981).

Figure 2.2 (A), Bathymetry of SEA8 region; (B), Bed sediment distribution; (Redrawn with modifications from MAFF, 1981).

Figure 2.3 (A), Mean spring tidal range at a location; (B), Co-tidal lines, drawn through locations of equal Mean High Water Interval (Redrawn with modifications from Chart 5058, Hydrographic Office, 1996).

Figure 2.4.1 (A), Semi-range (amplitude) of the M_2 tidal constituent of water level; (B), Phase of the M_2 tidal constituent of water level. Data obtained by Fourier analysis of depth-averaged, numerical model output (Redrawn with modifications from Sinha and Pingree, 1997).

Figure 2.4.2 (A), Ratio of the S_2 to M_2 tidal-elevation constituents of water level; (B), Phase (g) differences between the S_2 and M_2 tidal-elevation constituents of water level ($gS_2 - gM_2$) in degrees. Data obtained by analysis of depth-averaged, numerical model output (Redrawn with modifications from Pingree and Griffiths, 1981).

Figure 2.4.3 (A), Spring tide semi-major axes of the tidal current ellipse (maximum current speeds during a tide); (B), Ratio of the spring tide semi-minor to semi-major axes of the tidal current ellipse (%, a positive rotation is anticlockwise, a negative rotation is clockwise). Data obtained by analysis of depth-averaged, numerical model output (Redrawn with modifications from Flather, 1987).

Figure 2.4.4 (A), Magnitude of the maximum bottom shear stresses for M_2 and M_4 tidal currents (Redrawn with modifications from Pingree and Griffiths, 1979); (B), Sand transport paths in the SEA8 region (Redrawn with modifications from Stride, 1973).

Figure 2.5.1 (A), Wind-driven residual currents resulting from a uniform southwest wind stress of 1.6 dynes cm^{-2}. The length of a current vector determines the strength of the current at its central point. The current arrows are slightly curved to conform to the direction of current flow. Only about one tenth of the current vectors have been drawn and values less than 1.25 cm s^{-1} have been omitted; (B), The sea level (in m) corresponding to the southwest wind residuals shown in (A) (Redrawn with modifications from Pingree and Griffiths, 1980).

Figure 2.5.2 (A), The wind-driven residual currents resulting from a uniform southeast wind stress of 1.6 dynes cm^{-2} (arrows drawn as for Figure 2.5.1(A)); (B), The sea level (in m) corresponding to the southeast wind residuals shown in (A) (Redrawn with modifications from Pingree and Griffiths, 1980).

Figure 2.6 (A), Storm surge water-level elevations (in m) and (B), maximum expected storm surge current speeds (in m s^{-1}) for a 50 year return period (Redrawn with modifications from Flather, 1987).

Figure 2.7.1 (A), Monthly wind data for January over the SEA8 region during 1962 to 1976; (B), Predicted heights of the highest individual waves that are likely to occur in the worst storm in any 50-year interval and the mean zero-up-crossing period of the wave at that time (Redrawn with modifications from MAFF, 1981).

Figure 2.7.2 (A), Significant wave height (m) exceeded for 10% of the year; (B), Significant wave height (m) exceeded for 75% of the year and the zero-up-crossing wave period in seconds, shown as the dashed line (Redrawn with modifications from Draper, 1991).

Figure 2.8 (A), Chart showing station locations S1, S2 and S3 used to illustrate the bottom mixed layer in areas representative of the SEA8 region; (B), Typical temperature profiles obtained near the shelf edge region of the Celtic Sea

during June 1972 (S1 and S2) and near the Channel Isles during July 1973 (S3) (Redrawn with modifications from Pingree and Griffiths, 1977).

Figure 2.9.1 (A), Mean surface temperature for February; (B), Mean bottom temperature in February (Redrawn with modifications from MAFF, 1981).

Figure 2.9.2 (A), Mean surface temperature for August; (B), Mean bottom temperature in August (Redrawn with modifications from MAFF, 1981).

Figure 2.9.3 (A), Mean surface salinity for February; (B), Mean bottom salinity in February (Redrawn with modifications from MAFF, 1981).

Figure 2.9.4 (A), Mean surface salinity for August; (B), Mean bottom salinity in August (Redrawn with modifications from MAFF, 1981).

Figure 2.10 (A), Schematic showing the 'mean' development (advance) of the seasonal thermocline, which is illustrated using weekly frontal plots and, (B), the 'mean' dissipation (retreat) of the seasonal thermocline, which is illustrated using monthly frontal plots (Redrawn with modifications from Pingree, 1975).

Figure 3.1 The locations of estuaries and their long-term, averaged rate of freshwater flow at seaward-most gauging stations; (A), Central and eastern English Channel; (B), the coast of southwest England; (C), Northern Bristol Channel and Severn Estuary.

Figure 3.2.1 (A), Bathymetry; Source: British Geological Survey (1987); (B), Sea-bed sediments; Source: British Geological Survey (1987); sediment classification modified after Folk (1954). These contours are redrawn with modifications from Barne et al. (1998a).

Figure 3.2.2 (A), Tidal range (m) at mean spring tides (Source: Lee & Ramster (1981) © Crown copyright); (B), Maximum tidal current speed (in m s^{-1}) at mean spring tides (Source: Sager & Sammler (1968)); (C), Mean surface water temperature in summer and winter, ℃ (Source: Lee & Ramster (1981) ©

Crown copyright); (D), Mean surface salinity of seawater in summer and winter (Source: Lee & Ramster (1981) © Crown copyright). These contours are redrawn with modifications from Barne et al. (1998a).

Figure 3.2.3 (A), Hourly means of wind speed (in m s^{-1}) exceeded for 75% of the time: 1965-1973 (Source: Caton (1976)); (B), Hourly means of wind speed (in m s^{-1}) exceeded for 0.1% of the time: 1965-1973 (Source: Caton (1976)); (C), Wind directions at Felixstowe and Margate (Sources: Hydrographic Department (1985)); (D), Significant wave height (m) exceeded for 10% and 75% of the year (Source: Draper (1991)). These contours are redrawn from Barne et al. (1998a).

Figure 3.3.1 (A), Bathymetry (Source: British Geological Survey (1987)); (B), Sea-bed sediments (Source: British Geological Survey (1987); sediment classification modified after Folk (1954)). These contours are redrawn with modifications from Barne et al. (1998b).

Figure 3.3.2 (A), Tidal range (m) at mean spring tides (Source: Lee & Ramster (1981) © Crown copyright); (B), Maximum tidal current speed (in m s^{-1}) at mean spring tides (Source: Sager & Sammler (1968)); (C), Mean surface water temperature in summer and winter, ℃ (Source: Lee & Ramster (1981) © Crown copyright); (D), Mean surface salinity of seawater in summer and winter (Source: Lee & Ramster (1981) © Crown copyright). These contours are redrawn with modifications from Barne et al. (1998b).

Figure 3.3.3 (A), Hourly-mean wind speed (in m s^{-1}) exceeded for 75% of the time; (B), Hourly-mean wind speed (in m s^{-1}) exceeded for 0.1% of the time: 1965-1973 (Source: Caton (1976)); (C), Wind directions at Dungeness (1941-1970) and Thorney Island (1943-1959) (Sources: Hydrographic Department (1985), Shellard (1968)); (D), Significant wave height (m) exceeded for 10% and 75%

of the year (Source: Draper (1991)). These contours are redrawn with modifications from Barne et al. (1998b).

Figure 3.4.1 (A), Bathymetry - 10 m contour not shown where it lies close to the shore (Source: British Geological Survey (1987)); (B), Sea-bed sediments (Source: British Geological Survey (1991); sediment classification modified after Folk (1954)). These contours are redrawn with modifications from Barne et al. (1996a).

Figure 3.4.2 (A), Tidal range (m) at mean spring tides (Source: Lee & Ramster (1981) © Crown copyright); (B), Maximum tidal current speed (in m s^{-1}) at mean spring tides (Source: Sager & Sammler (1968)); (C), Mean surface water temperature in summer and winter, ℃ (Source: Lee & Ramster (1981) © Crown copyright); (D), Mean surface salinity of seawater in summer and winter (Source: Lee & Ramster (1981) © Crown copyright). These contours are redrawn with modifications from Barne et al. (1996a).

Figure 3.4.3 (A), Hourly-mean wind speed (in m s^{-1}) exceeded for 75% of the time: 1965-1973; (B), Hourly mean wind speed (in m s^{-1}) exceeded for 0.1% of the time: 1965-1973 (Source: Caton (1976)); (C), Wind directions at Portland Bill and Southampton (1916-1950) (Source: Hydrographic Department (1960a)); (D), Significant wave height (m) exceeded for 10% and 75% of the year (Source: Draper (1991)). These contours are redrawn with modifications from Barne et al. (1996a).

Figure 3.5.1 (A), Bathymetry (Source: British Geological Survey (1991)); (B), Sea-bed sediments (Source: British Geological Survey (1991), sediment classification modified after Folk (1954)). These contours are redrawn with modifications from Barne et al. (1996b).

Figure 3.5.2 (A), Tidal range (m) at mean spring tides (Source: Lee & Ramster (1981) © Crown copyright); (B), Maximum tidal current speed (in m s^{-1}) at mean spring tides (Source: Sager & Sammler (1968)); (C) Mean surface water temperature in summer and winter, ℃ (Source: Lee & Ramster (1981) © Crown copyright); (D), Mean surface salinity of seawater in summer and winter (Source: Lee & Ramster (1981) © Crown copyright). These contours are redrawn with modifications from Barne et al. (1996b).

Figure 3.5.3 (A), Hourly-mean wind speed (in m s^{-1}) exceeded for 75% of the time: 1965-1973; (B), Hourly-mean wind speed (in m s^{-1}) exceeded for 0.1% of the time: 1965-1973 (Source: Caton (1976)); (C), Wind directions at Plymouth and Falmouth (1913-1950) (Source: Hydrographic Department (1984)); (D), Significant wave height (m) exceeded for 10% and 75% of the year (Source: Draper (1991)). These contours are redrawn with modifications from Barne et al. (1996b).

Figure 3.6.1 (A), Bathymetry (Source: British Geological Survey (1987)); (B), Sea-bed sediments (Source: British Geological Survey (1987), sediment classification modified after Folk (1954)). These contours are redrawn with modifications from Barne et al. (1996c).

Figure 3.6.2 (A), Tidal range (m) at mean spring tides (Source: Lee & Ramster (1981) © Crown copyright); (B), Maximum tidal current speed (in m s^{-1}) at mean spring tides (Source: Sager & Sammler (1968)); (C), Mean surface water temperature in summer and winter, ℃ (Source: Lee & Ramster (1981) © Crown copyright); (D), Mean surface salinity of seawater in summer and winter (Source: Lee & Ramster (1981) © Crown copyright). These contours are redrawn with modifications from Barne et al. (1996c).

Figure 3.6.3 (A), Hourly-mean wind speed (in m s^{-1}) exceeded for 75% of the time: 1965-1973; (B), Hourly-mean wind speed (in m s^{-1}) exceeded for 0.1% of the time: 1965-1973 (Source: Caton (1976)); (C), Wind directions at Cardiff and on the Isles of Scilly shown as % of observations during the years 1916 - 1950. Flat calm (% of observations) = Cardiff (13.5%); Isles of Scilly (18%) (Source: Hydrographic Department (1960b)); (D), Significant wave height (m) exceeded for 10% and 75% of the year (Source: Draper (1991)). These contours are redrawn from Barne et al. (1996c).

Figure 3.7.1 (A), Bathymetry (Source: British Geological Survey (1987)); (B), Sea-bed sediments (Source: British Geological Survey (1991), sediment classification modified after Folk (1954)). These contours are redrawn from Barne et al. (1995).

Figure 3.7.2 (A), Tidal range (m) at mean spring tides (Source: Lee & Ramster (1981) © Crown copyright); (B), Maximum tidal current speed (in m s^{-1}) at mean spring tides (Source: Sager & Sammler (1968)); (C), Mean surface water temperature in summer and winter, ℃ (Source: Lee & Ramster (1981) © Crown copyright); (D), Mean surface salinity of seawater in summer and winter (Source: Lee & Ramster (1981) © Crown copyright). These contours are redrawn from Barne et al. (1995).

Figure 3.7.3 (A), Hourly-mean wind speed (in m s^{-1}) exceeded for 75% of the time: 1965-1973; (B), Hourly-mean wind speed (in m s^{-1}) exceeded for 0.1% of the time: 1965-1973 (Source: Caton (1976)); (C), Wind directions at St Ann's Head shown as % of observations through the years 1916 -1950 (Source: Hydrographic Office (1960b)); (D), Significant wave height (m) exceeded for 10% and 75% of the year (Source: Draper (1991)). These contours are redrawn from Barne et al. (1995).

Figure 4.5, An example of a composite-front map of sea surface temperature that shows the frontal situation for the UK Western Approaches and much of the SEA8 region during 18 – 22 July 2000. (See also Figure 2.10 (A, B)). Reproduced by courtesy of Dr. Peter Miller, Remote Sensing Group, Plymouth Marine Laboratory, Plymouth PL1 3DH, UK.

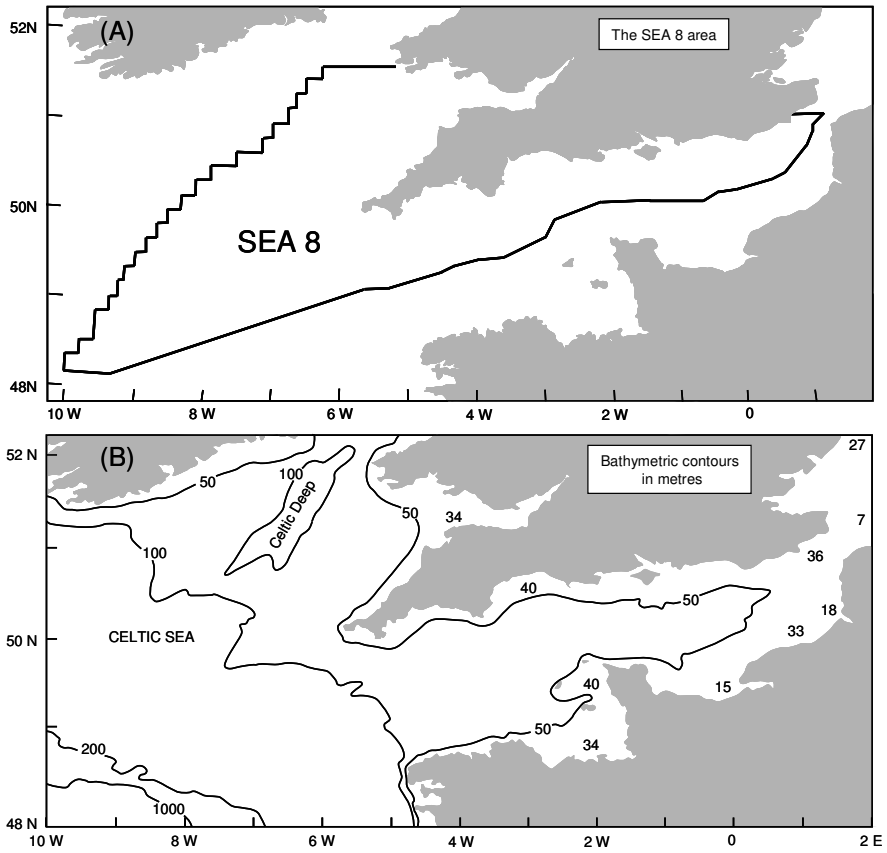

Figure 2.1 (A), Location of SEA8 region; (B), Bathymetry of SEA8 region (Redrawn with modifications from MAFF, 1981).

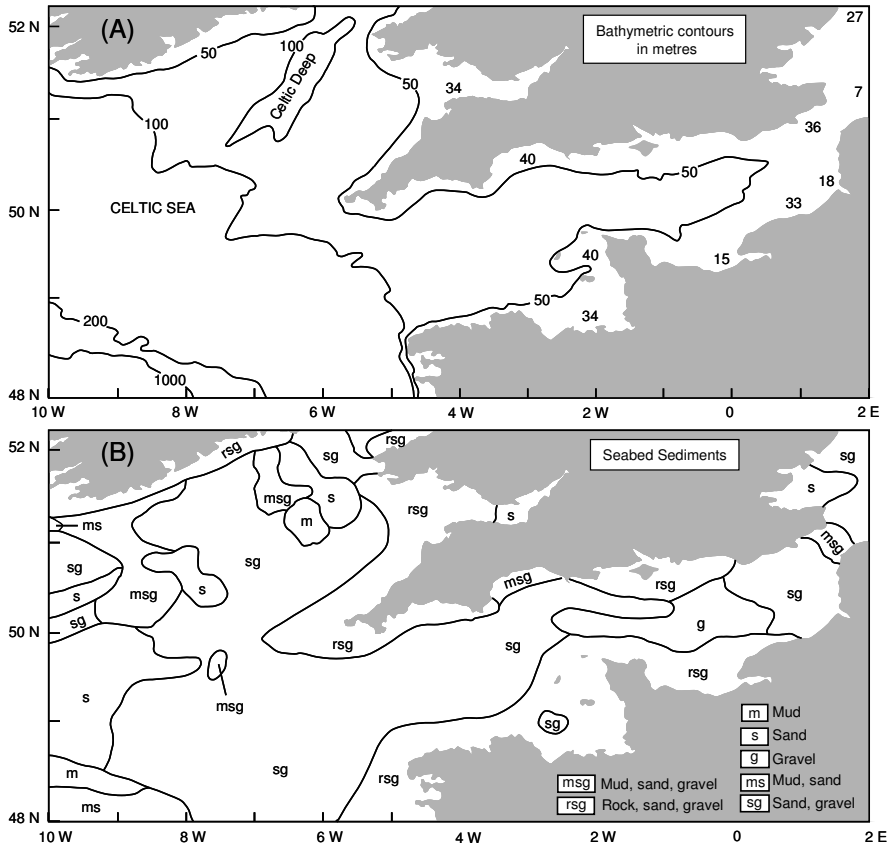

Figure 2.2 (A), Bathymetry of SEA8 region; (B), Bed sediment distribution; (Redrawn with modifications from MAFF, 1981).

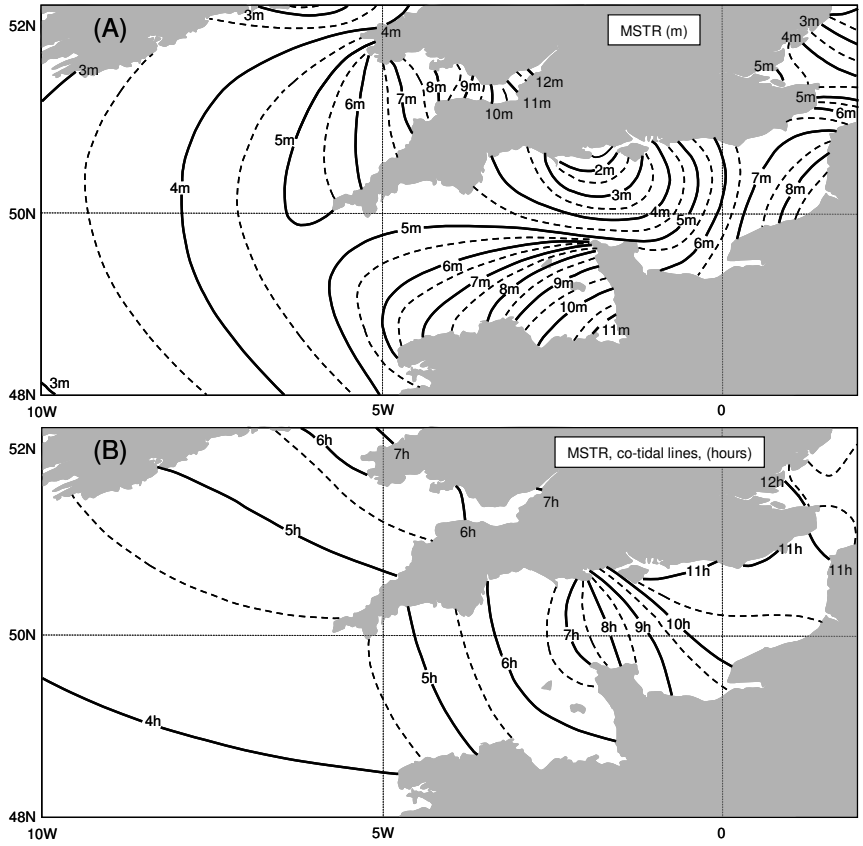

Figure 2.3 (A), Mean spring tidal range at a location; (B), Co-tidal lines, drawn through locations of equal Mean High Water Interval (Redrawn with modifications from Chart 5058, Hydrographic Office, 1996).

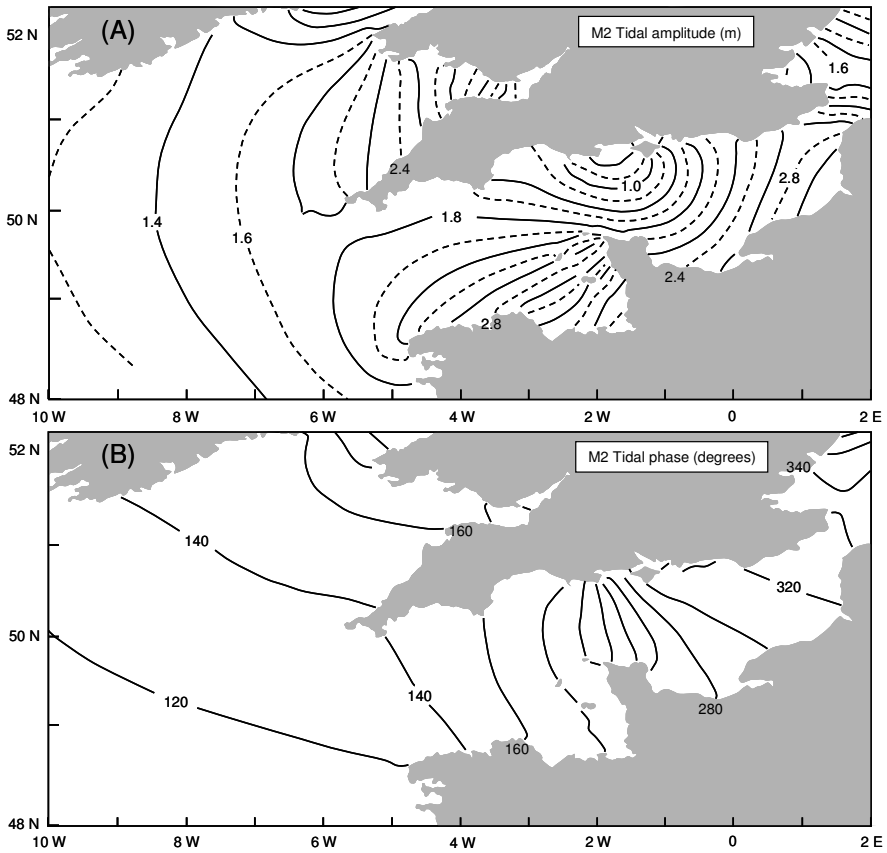

Figure 2.4.1 (A), Semi-range (amplitude) of the M_2 tidal constituent of water level; (B), Phase of the M_2 tidal constituent of water level. Data obtained by Fourier analysis of depth-averaged, numerical model output (Redrawn with modifications from Sinha and Pingree, 1997).

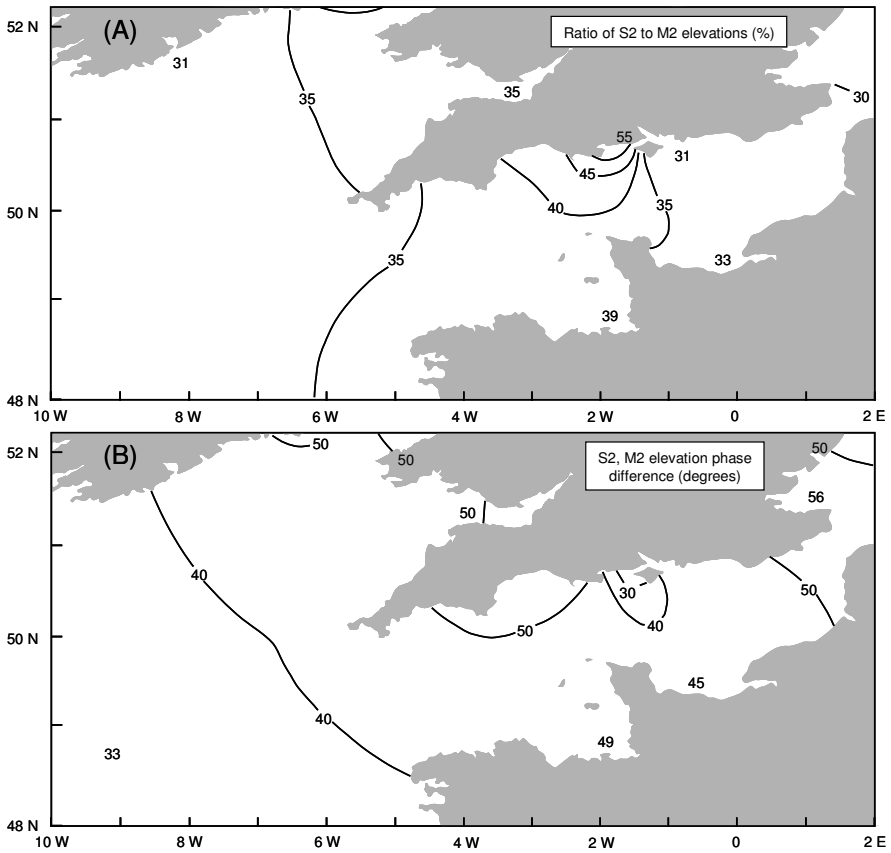

Figure 2.4.2 (A), Ratio of the S_2 to M_2 tidal-elevation constituents of water level; (B), Phase (g) differences between the S_2 and M_2 tidal-elevation constituents of water level (gS_2 - gM_2) in degrees. Data obtained by analysis of depth-averaged, numerical model output (Redrawn with modifications from Pingree and Griffiths, 1981).

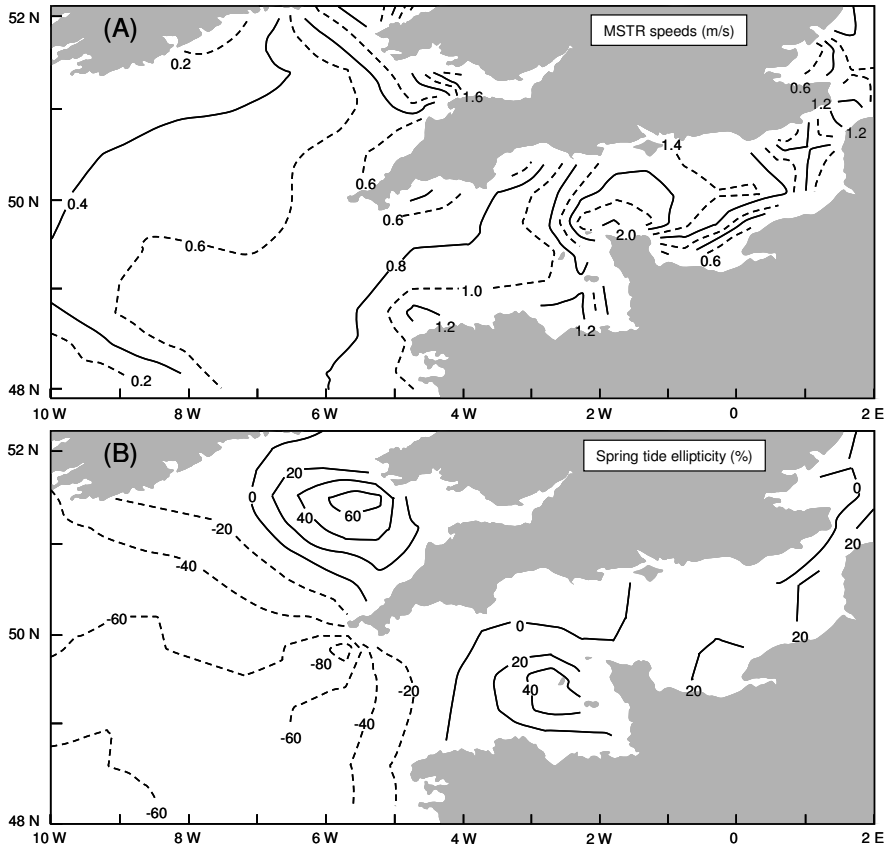

Figure 2.4.3 (A), Spring tide semi-major axes of the tidal current ellipse (maximum current speeds during a tide); (B), Ratio of the spring tide semi-minor to semi-major axes of the tidal current ellipse (%, a positive rotation is anticlockwise, a negative rotation is clockwise). Data obtained by analysis of depth-averaged, numerical model output (Redrawn with modifications from Flather, 1987).

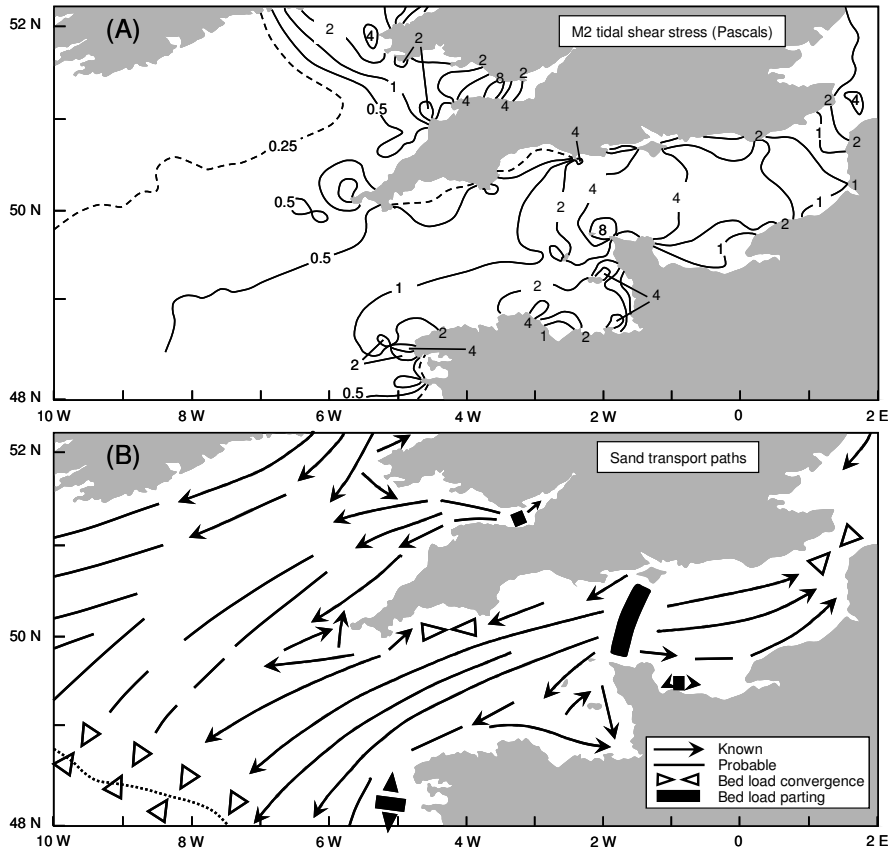

Figure 2.4.4 (A), Magnitude of the maximum bottom shear stresses for M_2 and M_4 tidal currents (Redrawn with modifications from Pingree and Griffiths, 1979); (B), Sand transport paths in the SEA8 region (Redrawn with modifications from Stride, 1973).

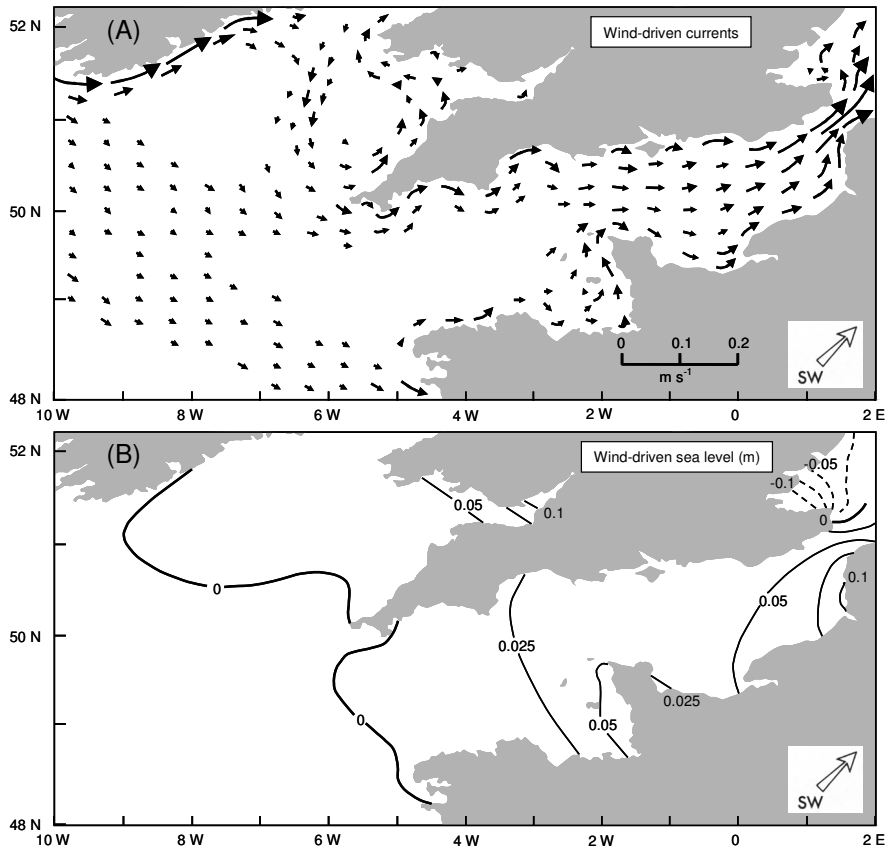

Figure 2.5.1 (A), Wind-driven residual currents resulting from a uniform southwest wind stress of 1.6 dynes cm^{-2}. The length of a current vector determines the strength of the current at its central point. The current arrows are slightly curved to conform to the direction of current flow. Only about one tenth of the current vectors have been drawn and values less than 1.25 cm s^{-1} have been omitted; (B), The sea level (in m) corresponding to the southwest wind residuals shown in (A) (Redrawn with modifications from Pingree and Griffiths, 1980).

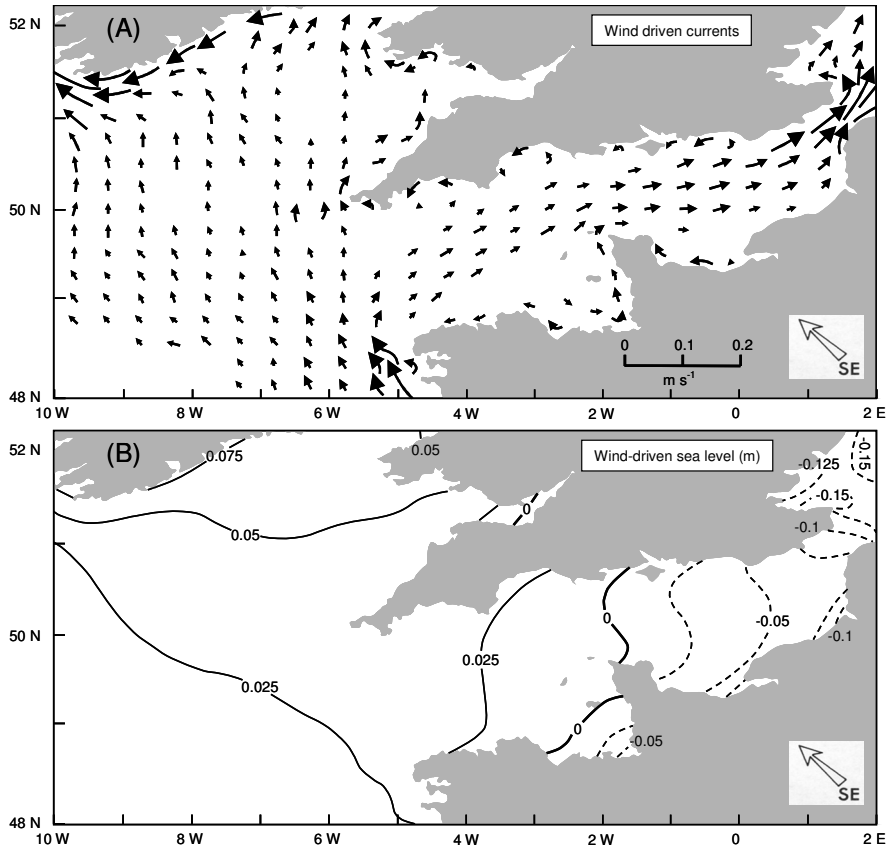

Figure 2.5.2 (A), The wind-driven residual currents resulting from a uniform southeast wind stress of 1.6 dynes cm^{-2} (arrows drawn as for Figure 2.5.1(A)); (B), The sea level (in m) corresponding to the southeast wind residuals shown in (A) (Redrawn with modifications from Pingree and Griffiths, 1980).

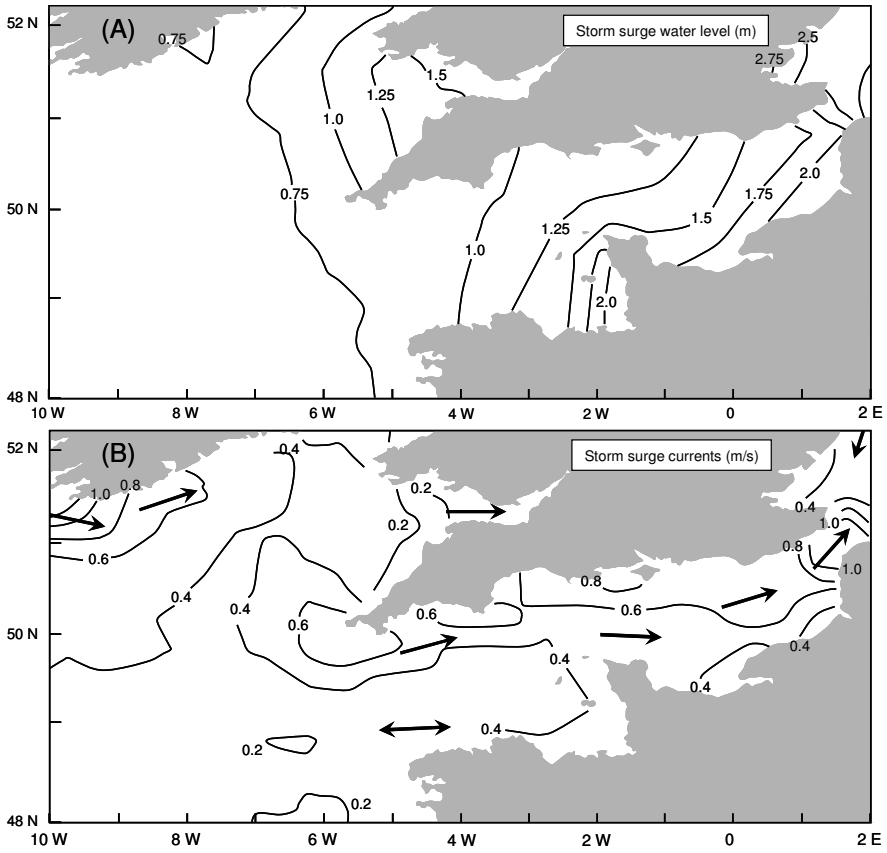

Figure 2.6 (A), Storm surge water-level elevations (in m) and (B), maximum expected storm surge current speeds (in m s^{-1}) for a 50 year return period (Redrawn with modifications from Flather, 1987).

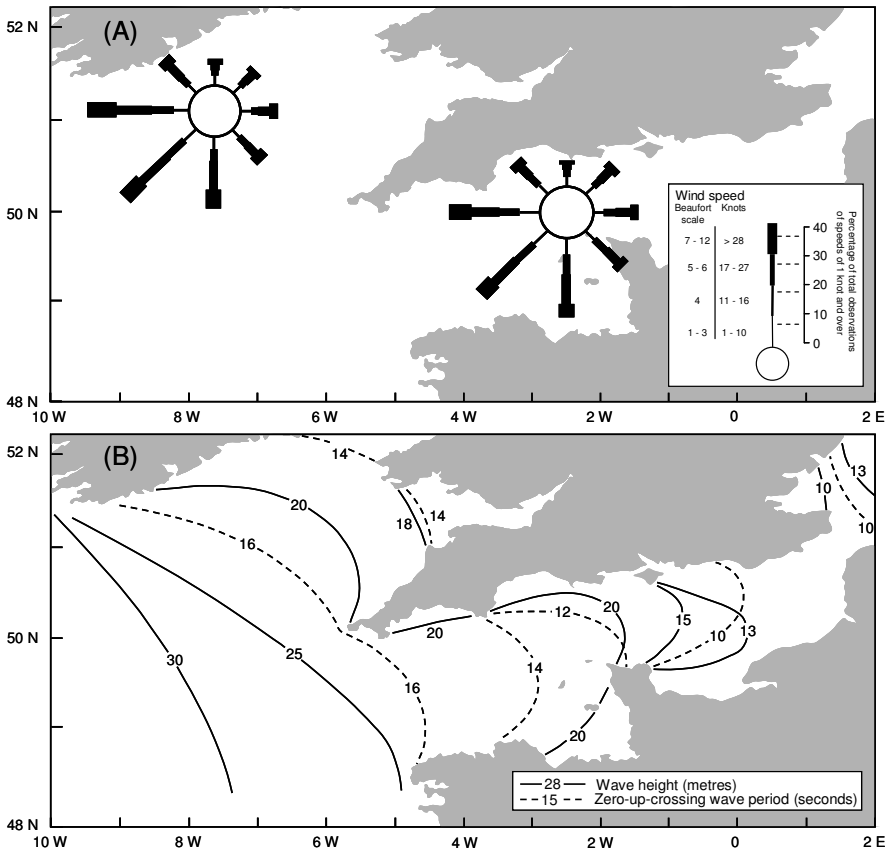

Figure 2.7.1 (A), Monthly wind data for January over the SEA8 region during 1962 to 1976; (B), Predicted heights of the highest individual waves that are likely to occur in the worst storm in any 50-year interval and the mean zero-up-crossing period of the wave at that time (Redrawn with modifications from MAFF, 1981).

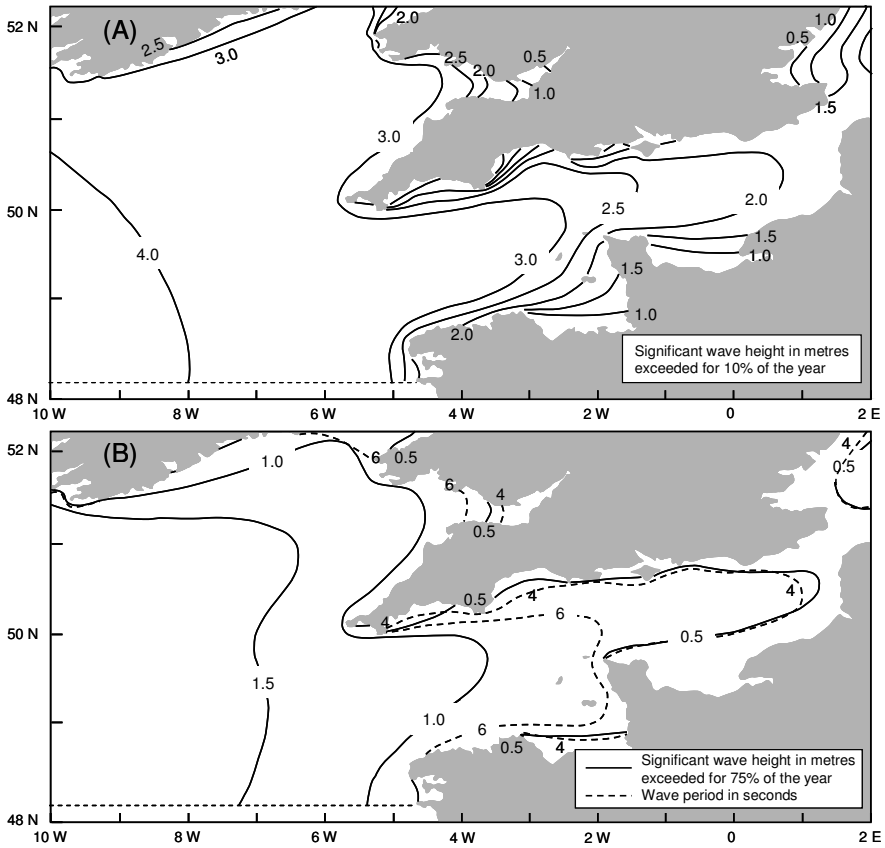

Figure 2.7.2 (A), Significant wave height (m) exceeded for 10% of the year; (B), Significant wave height (m) exceeded for 75% of the year and the zero-up-crossing wave period in seconds, shown as the dashed line (Redrawn with modifications from Draper, 1991).

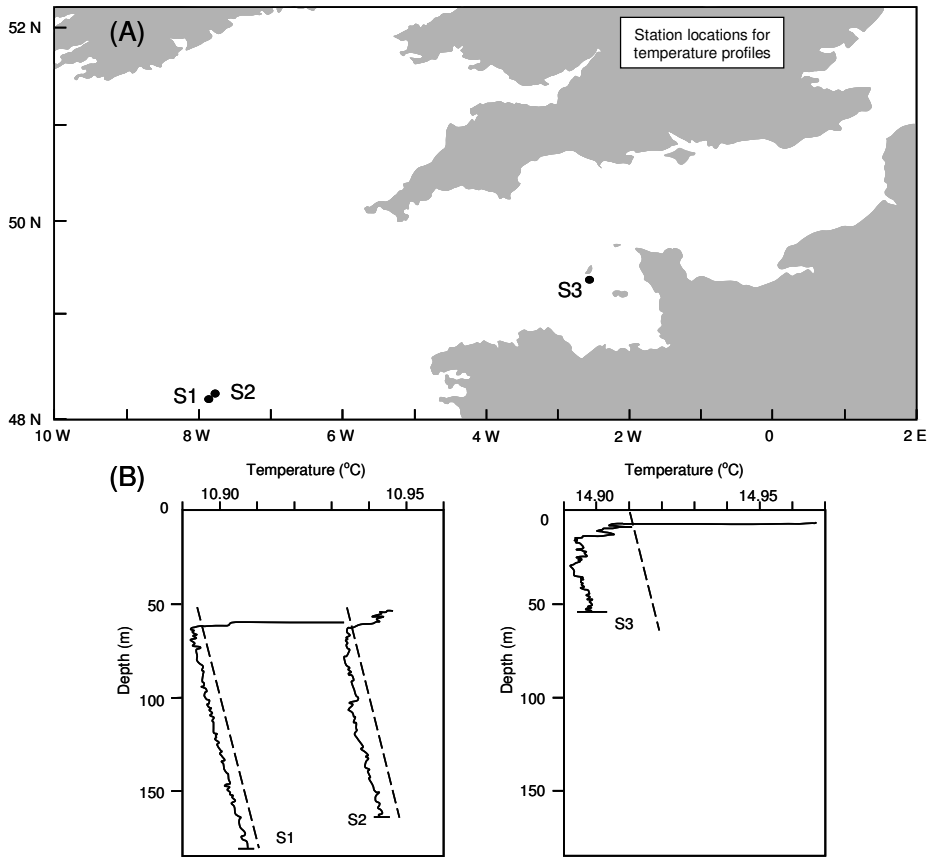

Figure 2.8 (A), Chart showing station locations S1, S2 and S3 used to illustrate the bottom mixed layer in areas representative of the SEA8 region; (B), Typical temperature profiles obtained near the shelf edge region of the Celtic Sea during June 1972 (S1 and S2) and near the Channel Isles during July 1973 (S3) (Redrawn with modifications from Pingree and Griffiths, 1977).

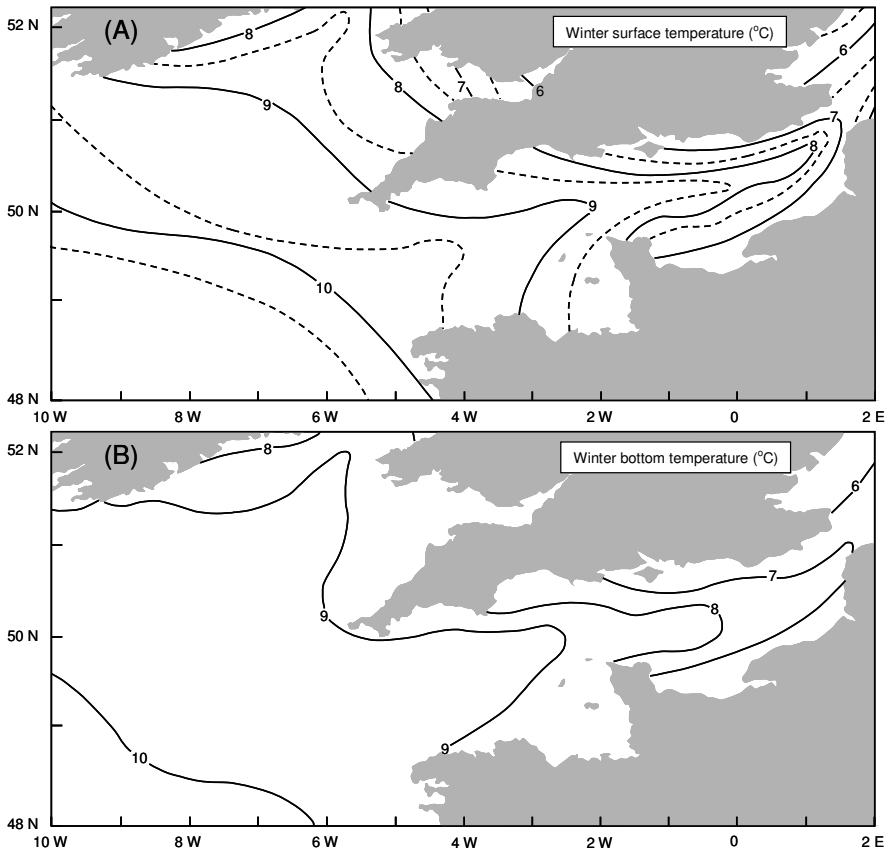

Figure 2.9.1 (A), Mean surface temperature for February; (B), Mean bottom temperature in February (Redrawn with modifications from MAFF, 1981).

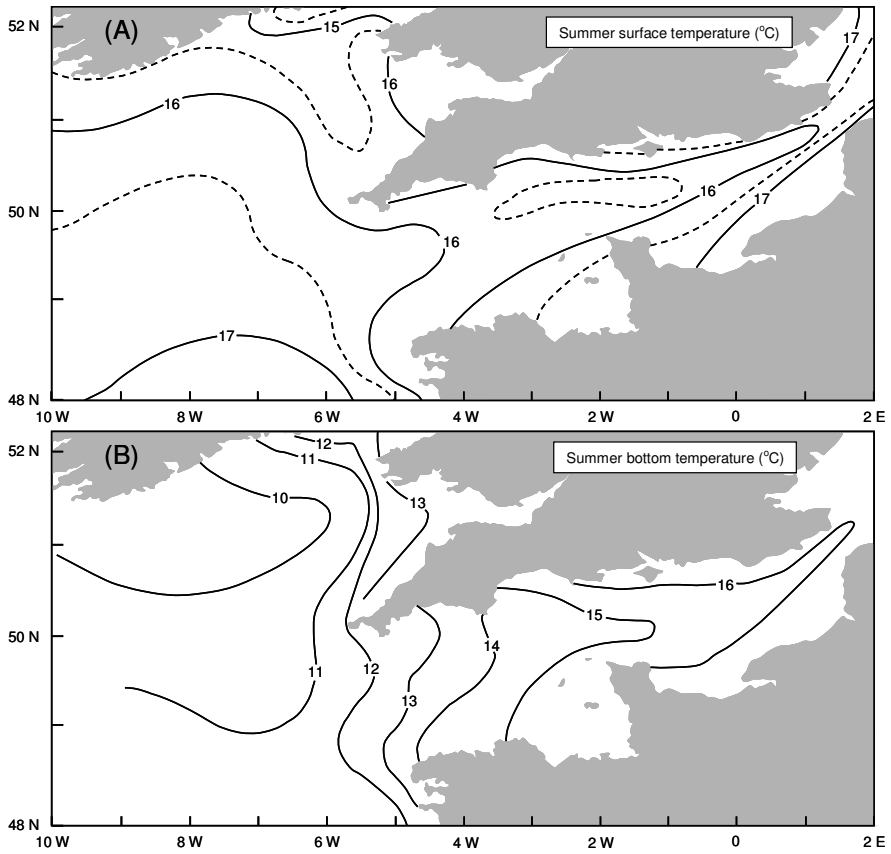

Figure 2.9.2 (A), Mean surface temperature for August; (B), Mean bottom temperature in August (Redrawn with modifications from MAFF, 1981).

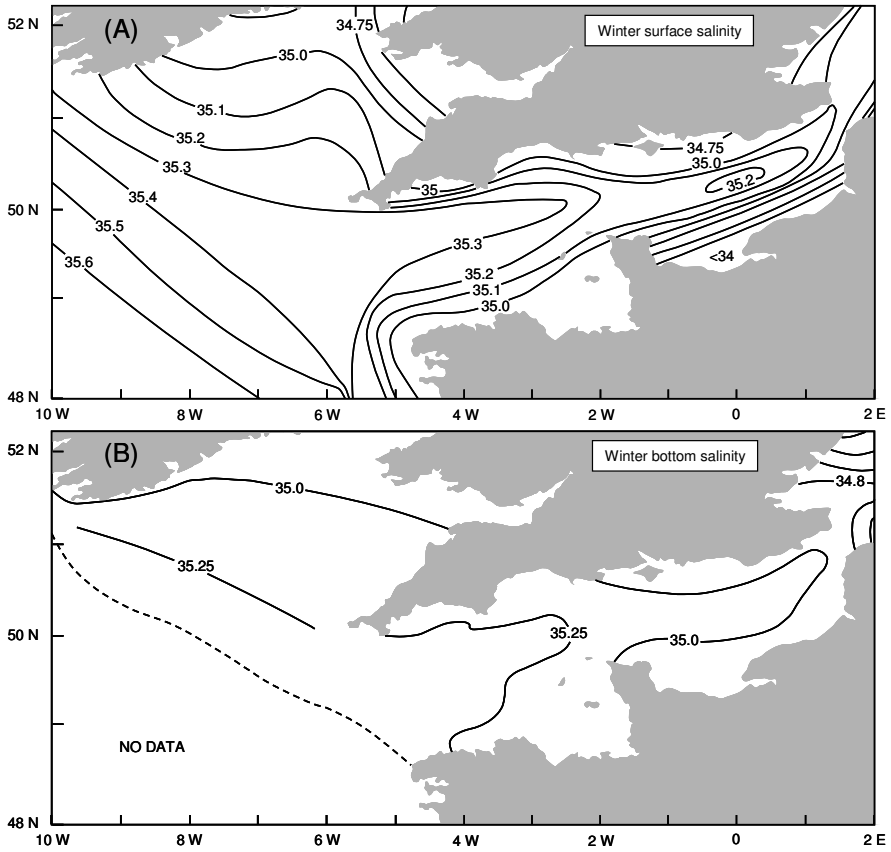

Figure 2.9.3 (A), Mean surface salinity for February; (B), Mean bottom salinity in February (Redrawn with modifications from MAFF, 1981).

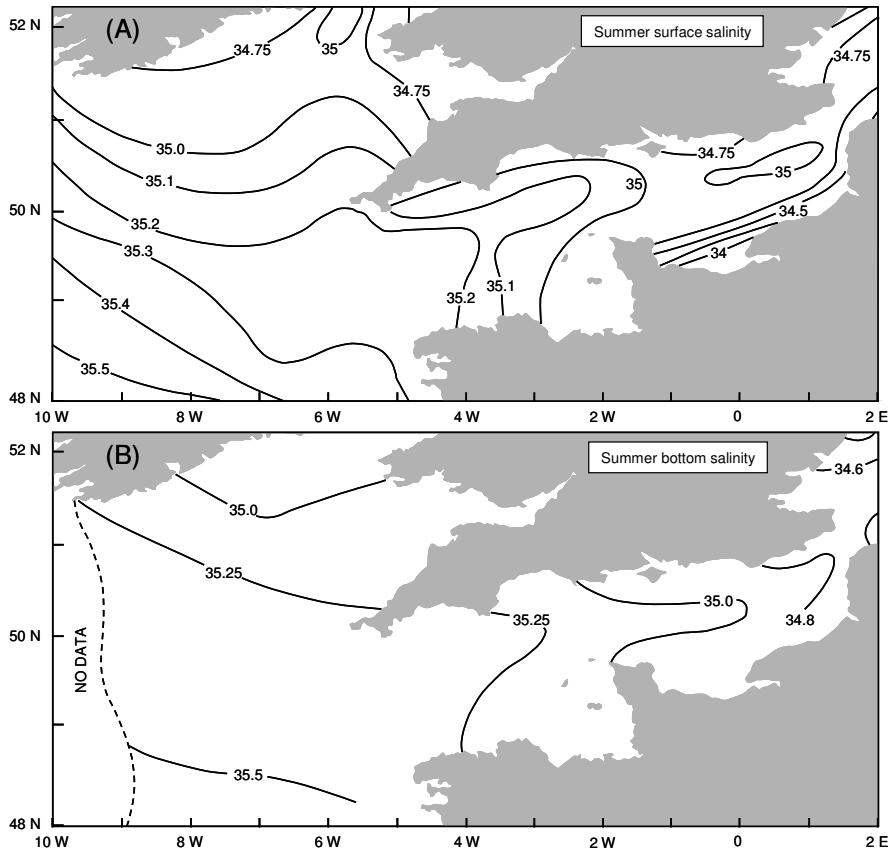

Figure 2.9.4 (A), Mean surface salinity for August; (B), Mean bottom salinity in August (Redrawn with modifications from MAFF, 1981).

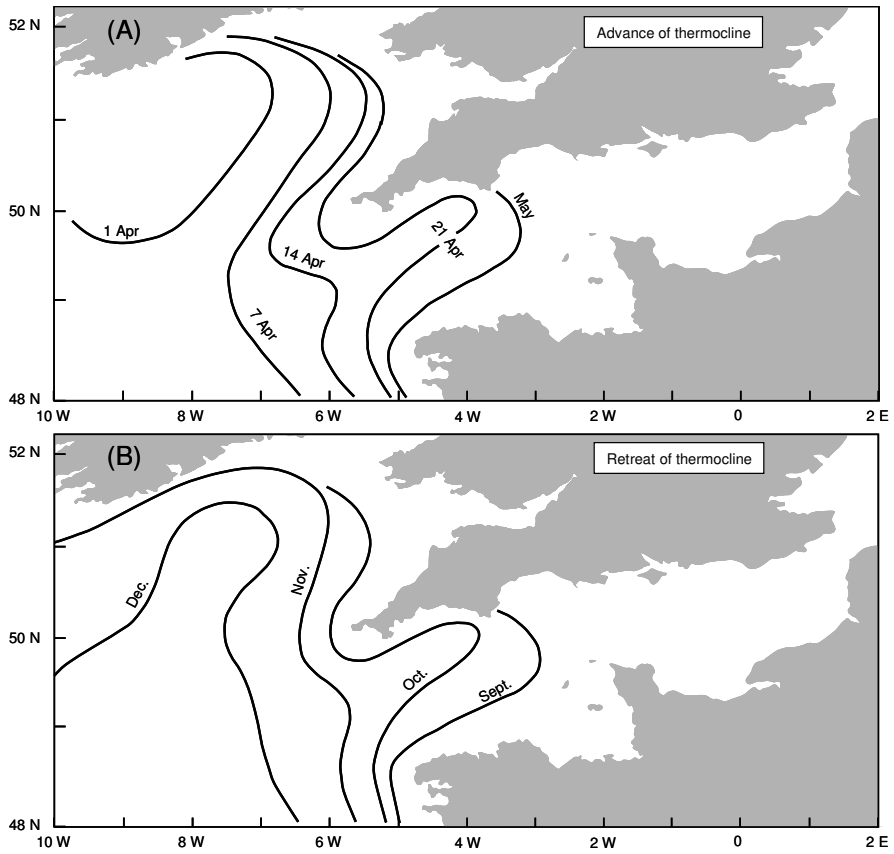

Figure 2.10 (A), Schematic showing the 'mean' development (advance) of the seasonal thermocline, which is illustrated using weekly frontal plots and, (B), the 'mean' dissipation (retreat) of the seasonal thermocline, which is illustrated using monthly frontal plots (Redrawn with modifications from Pingree, 1975).

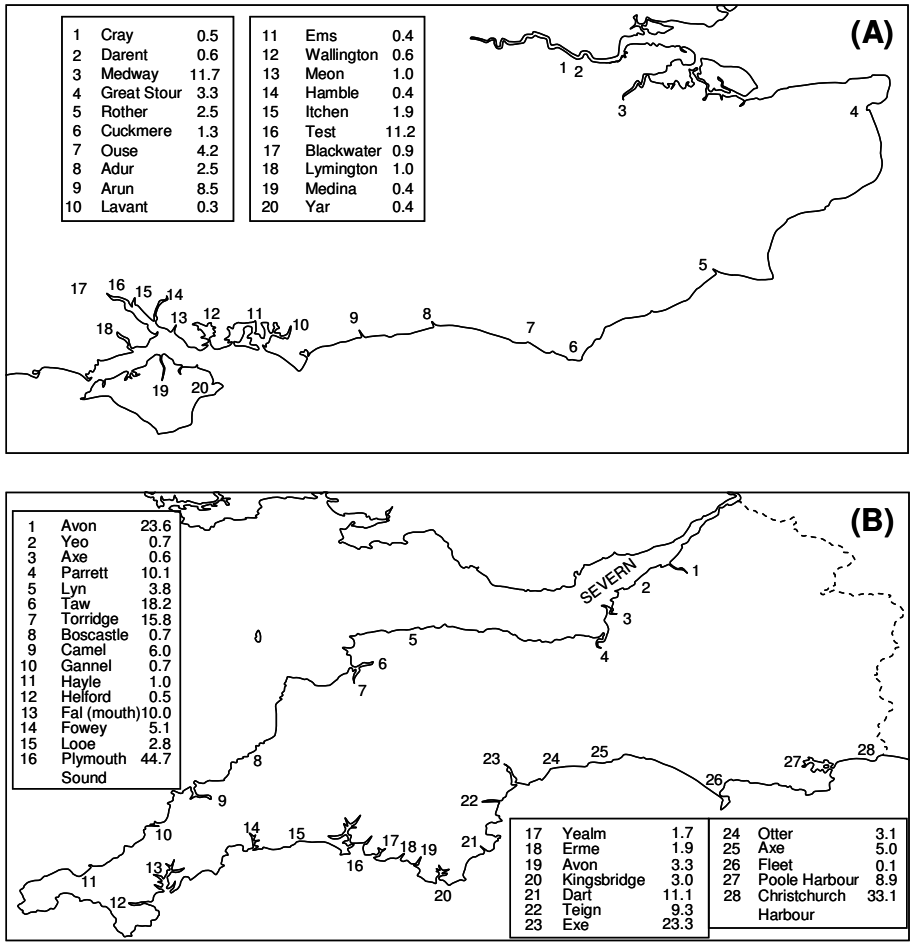

Figure 3.1 The locations of estuaries and their long-term, averaged rate of freshwater flow at seaward-most gauging stations; (A), Central and eastern English Channel; (B), the coast of southwest England.

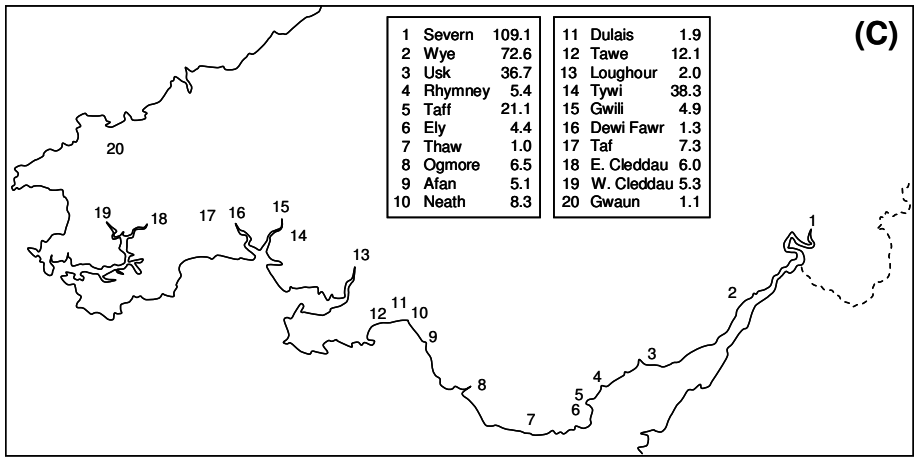

Figure 3.1 The locations of estuaries and their long-term, averaged rate of freshwater flow at seaward-most gauging stations; (C), Northern Bristol Channel and Severn Estuary.

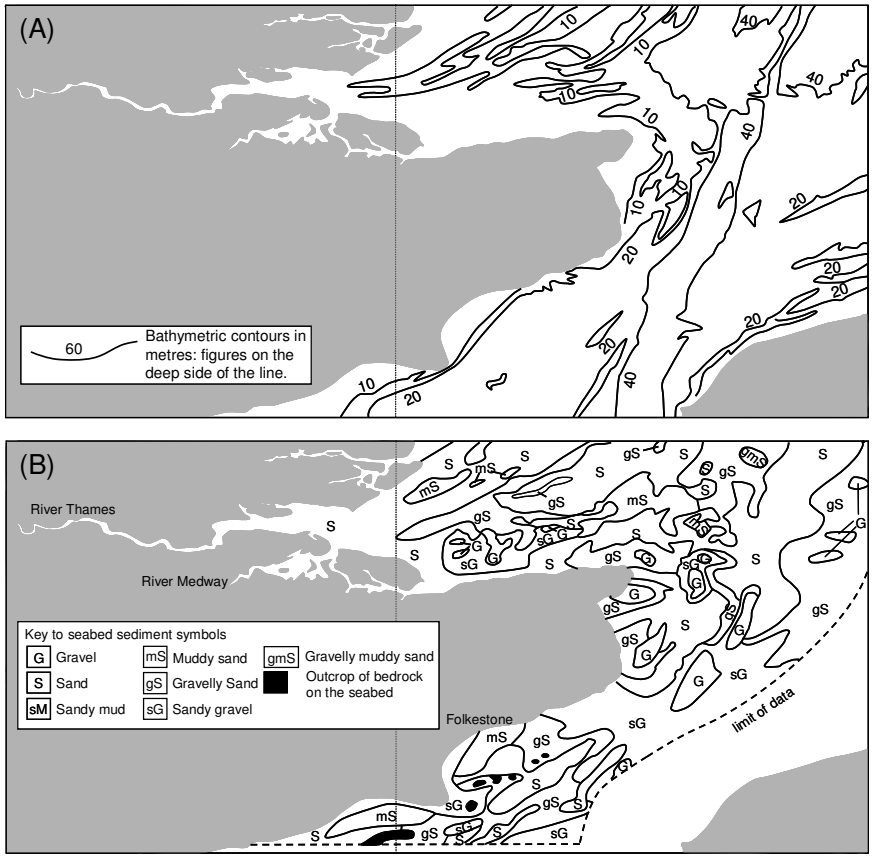

Figure 3.2.1 (A), Bathymetry; Source: British Geological Survey (1987); (B), Seabed sediments; Source: British Geological Survey (1987); sediment classification modified after Folk (1954). These contours are redrawn with modifications from Barne et al. (1998a).

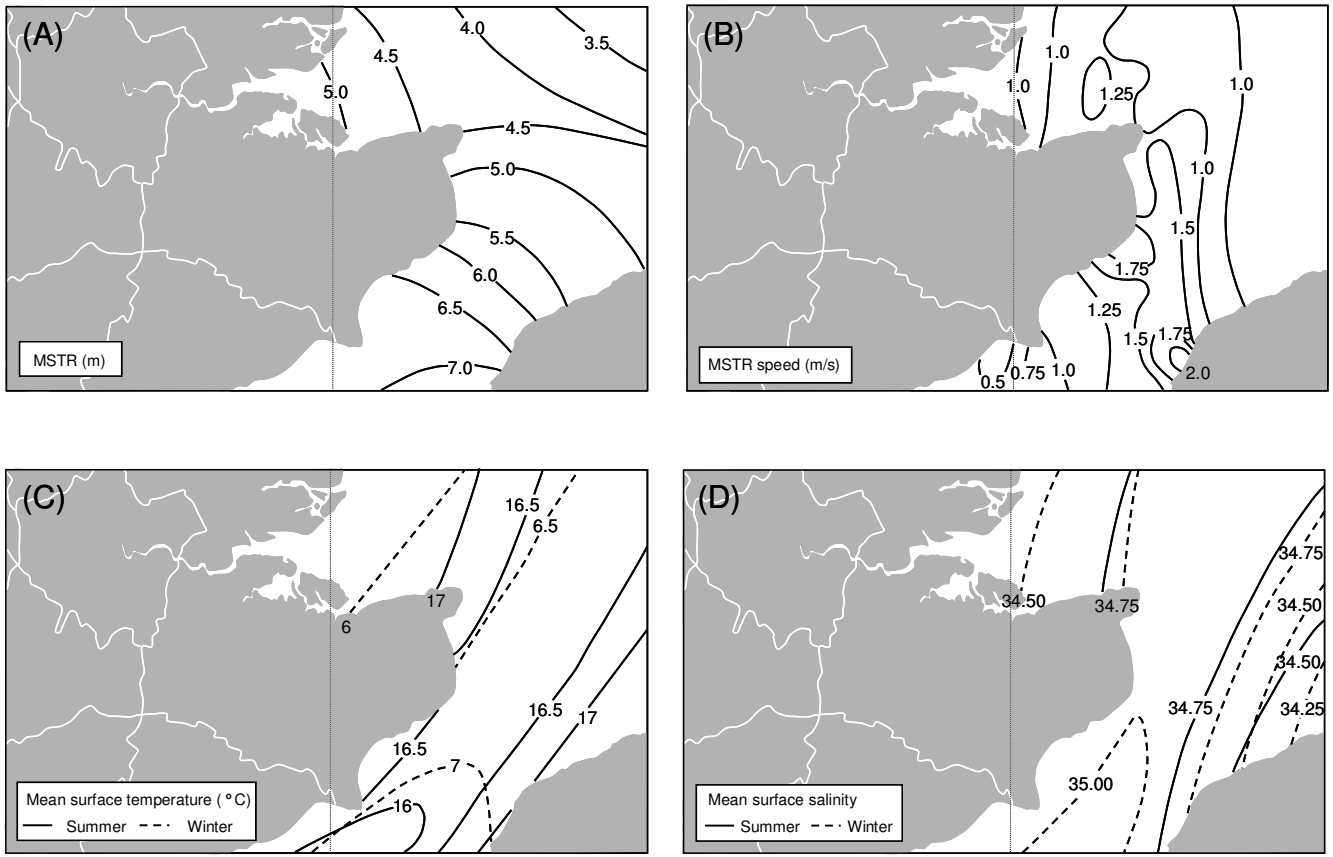

Figure 3.2.2 (A), Tidal range (m) at mean spring tides (Source: Lee & Ramster (1981) © Crown copyright); (B), Maximum tidal current speed (in m s^{-1}) at mean spring tides (Source: Sager & Sammler (1968)); (C), Mean surface water temperature in summer and winter, ℃ (Source: Lee & Ramster (1981) © Crown copyright); (D), Mean surface salinity of seawater in summer and winter (Source: Lee & Ramster (1981) © Crown copyright). These contours are redrawn with modifications from Barne et al. (1998a).

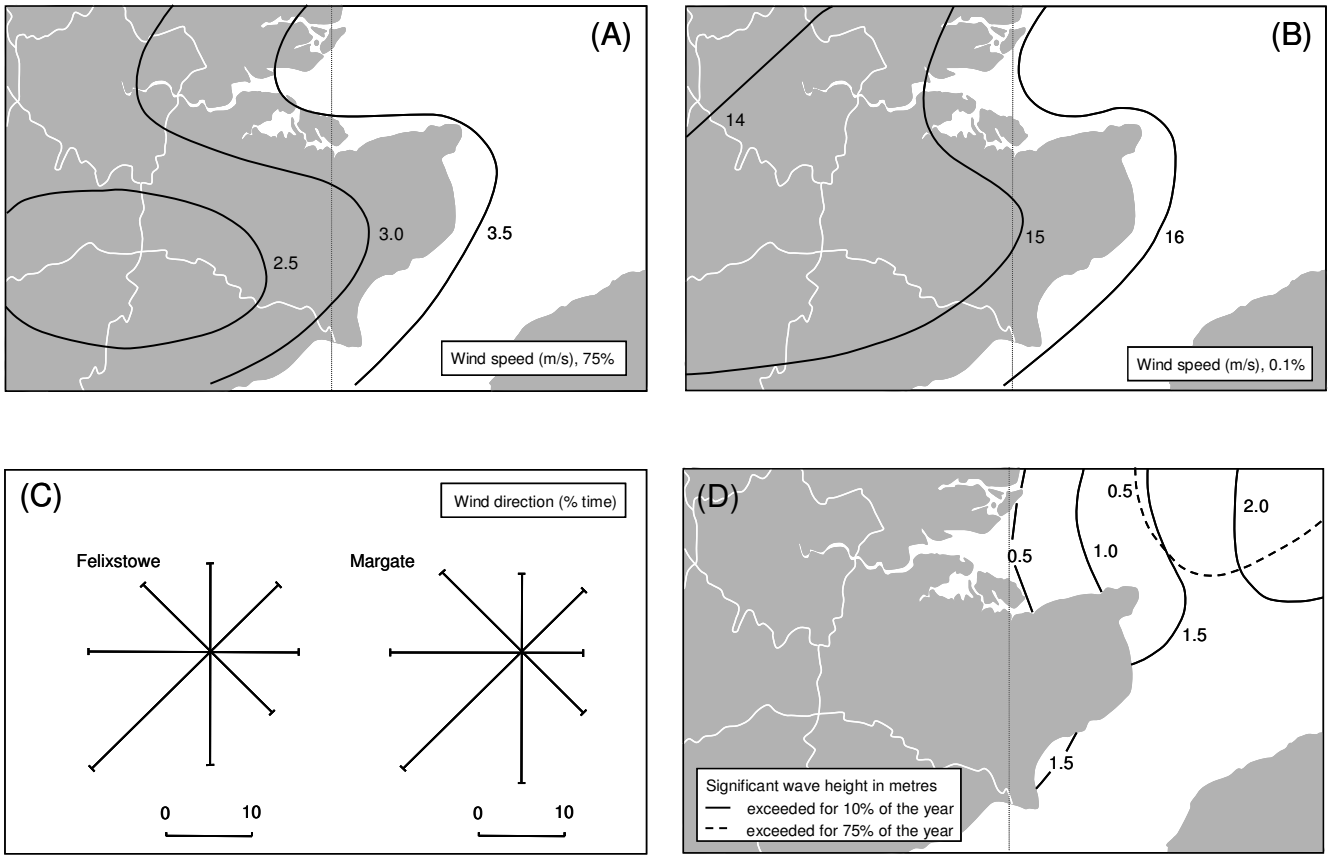

Figure 3.2.3 (A), Hourly means of wind speed (in m s^{-1}) exceeded for 75% of the time: 1965-1973 (Source: Caton (1976)); (B), Hourly means of wind speed (in m s^{-1}) exceeded for 0.1% of the time: 1965-1973 (Source: Caton (1976)); (C), Wind directions at Felixstowe and Margate (Sources: Hydrographic Department (1985)); (D), Significant wave height (m) exceeded for 10% and 75% of the year (Source: Draper (1991)). These contours are redrawn from Barne et al. (1998a).

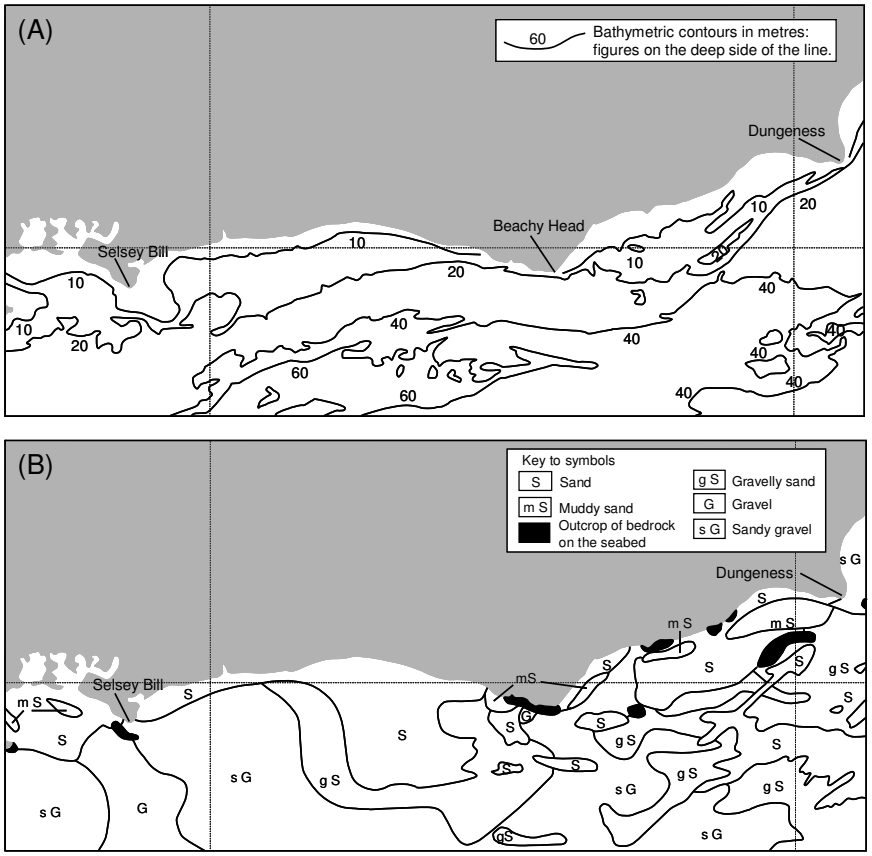

Figure 3.3.1 (A), Bathymetry (Source: British Geological Survey (1987)); (B), Seabed sediments (Source: British Geological Survey (1987); sediment classification modified after Folk (1954)). These contours are redrawn with modifications from Barne et al. (1998b).

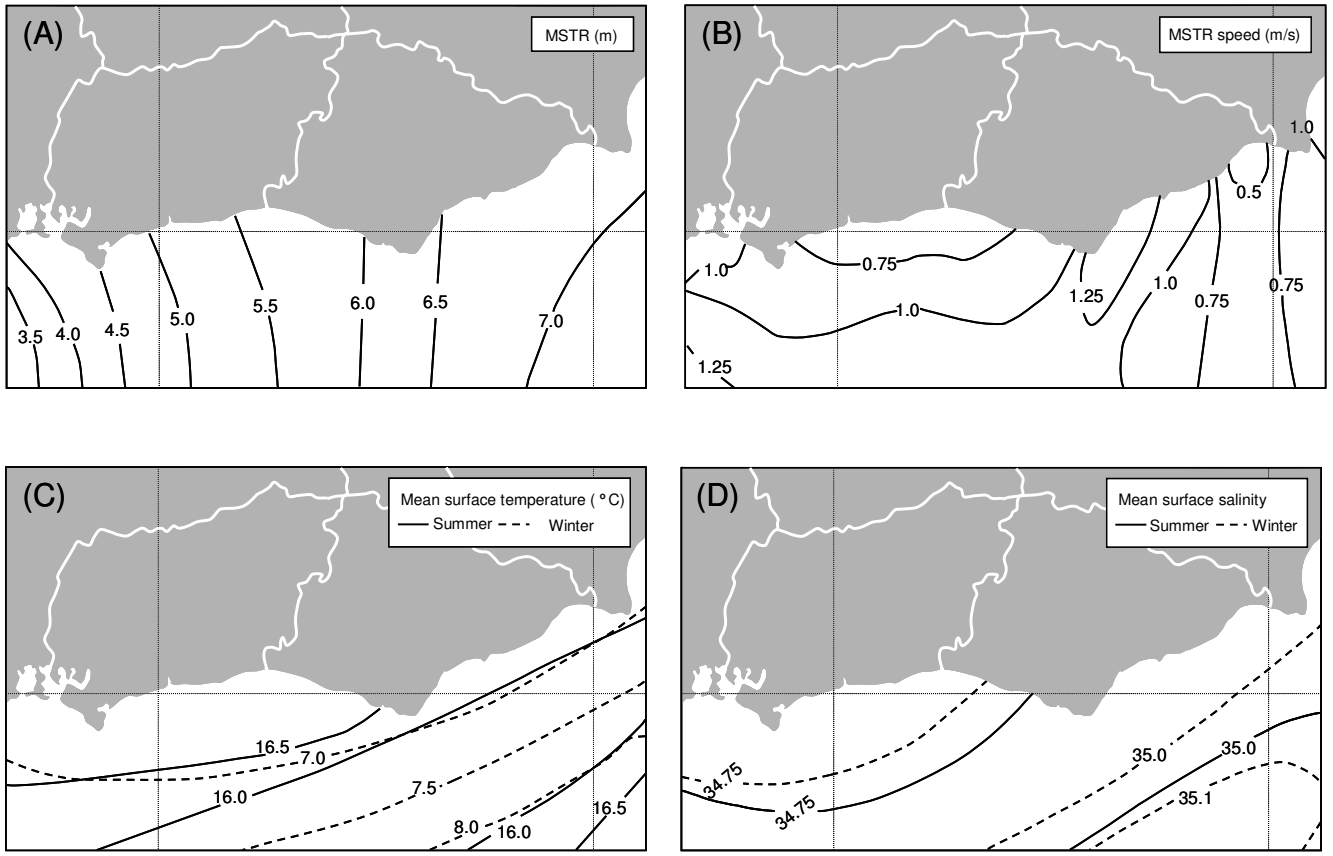

Figure 3.3.2 (A), Tidal range (m) at mean spring tides (Source: Lee & Ramster (1981) © Crown copyright); (B), Maximum tidal current speed (in m s^{-1}) at mean spring tides (Source: Sager & Sammler (1968)); (C), Mean surface water temperature in summer and winter, °C (Source: Lee & Ramster (1981) © Crown copyright); (D), Mean surface salinity of seawater in summer and winter (Source: Lee & Ramster (1981) © Crown copyright). These contours are redrawn with modifications from Barne et al. (1998b).

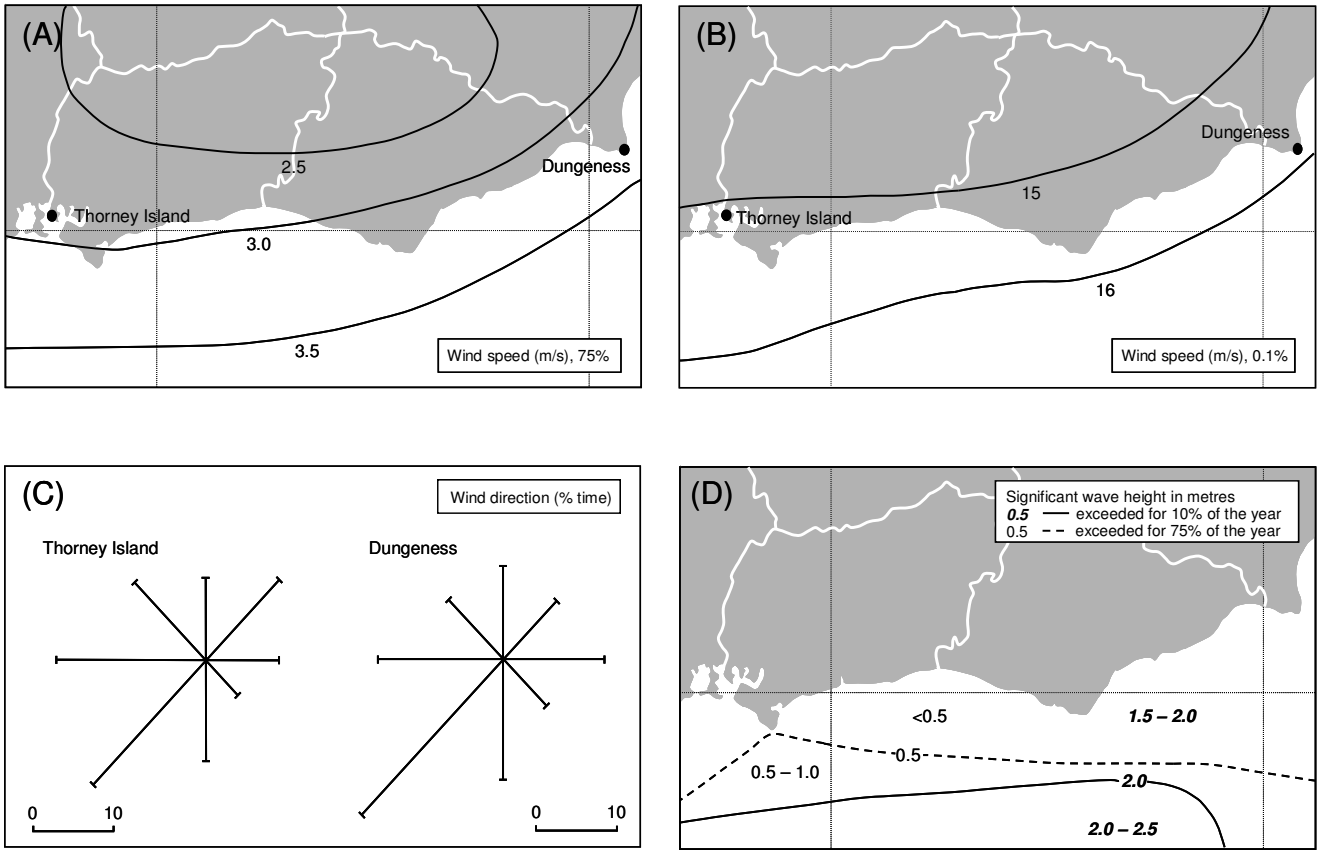

Figure 3.3.3 (A), Hourly-mean wind speed (in m s^{-1}) exceeded for 75% of the time; (B), Hourly-mean wind speed (in m s^{-1}) exceeded for 0.1% of the time: 1965-1973 (Source: Caton (1976)); (C), Wind directions at Dungeness (1941-1970) and Thorney Island (1943-1959) (Sources: Hydrographic Department (1985), Shellard (1968)); (D), Significant wave height (m) exceeded for 10% and 75% of the year (Source: Draper (1991)). These contours are redrawn with modifications from Barne et al. (1998b).

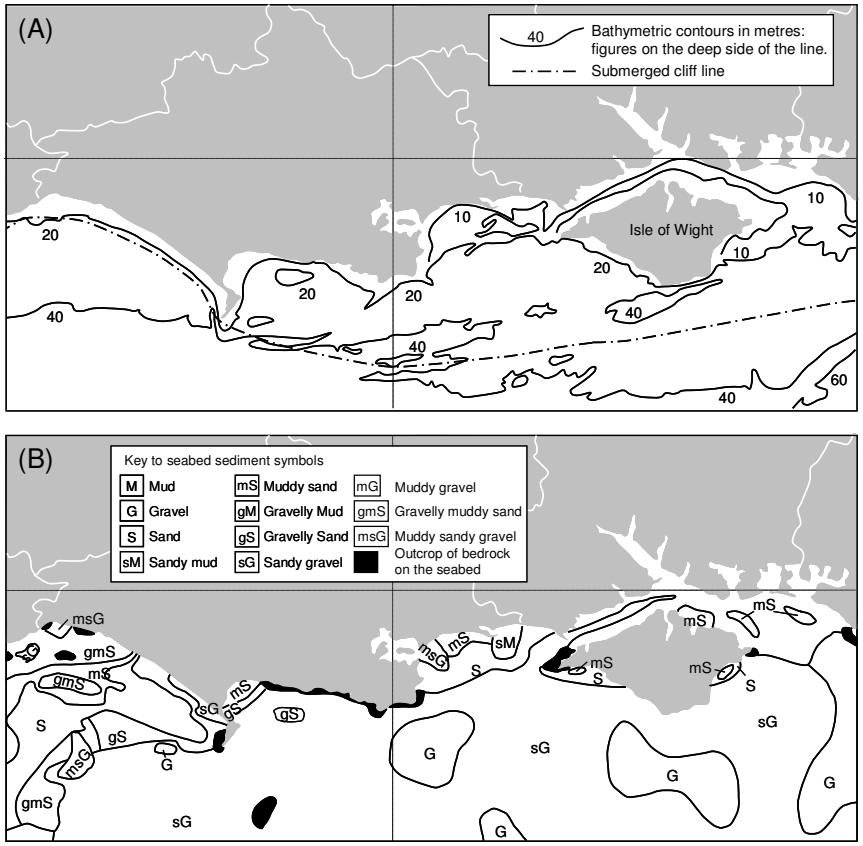

Figure 3.4.1 (A), Bathymetry - 10 m contour not shown where it lies close to the shore (Source: British Geological Survey (1987)); (B), Seabed sediments (Source: British Geological Survey (1991); sediment classification modified after Folk (1954)). These contours are redrawn with modifications from Barne et al. (1996a).

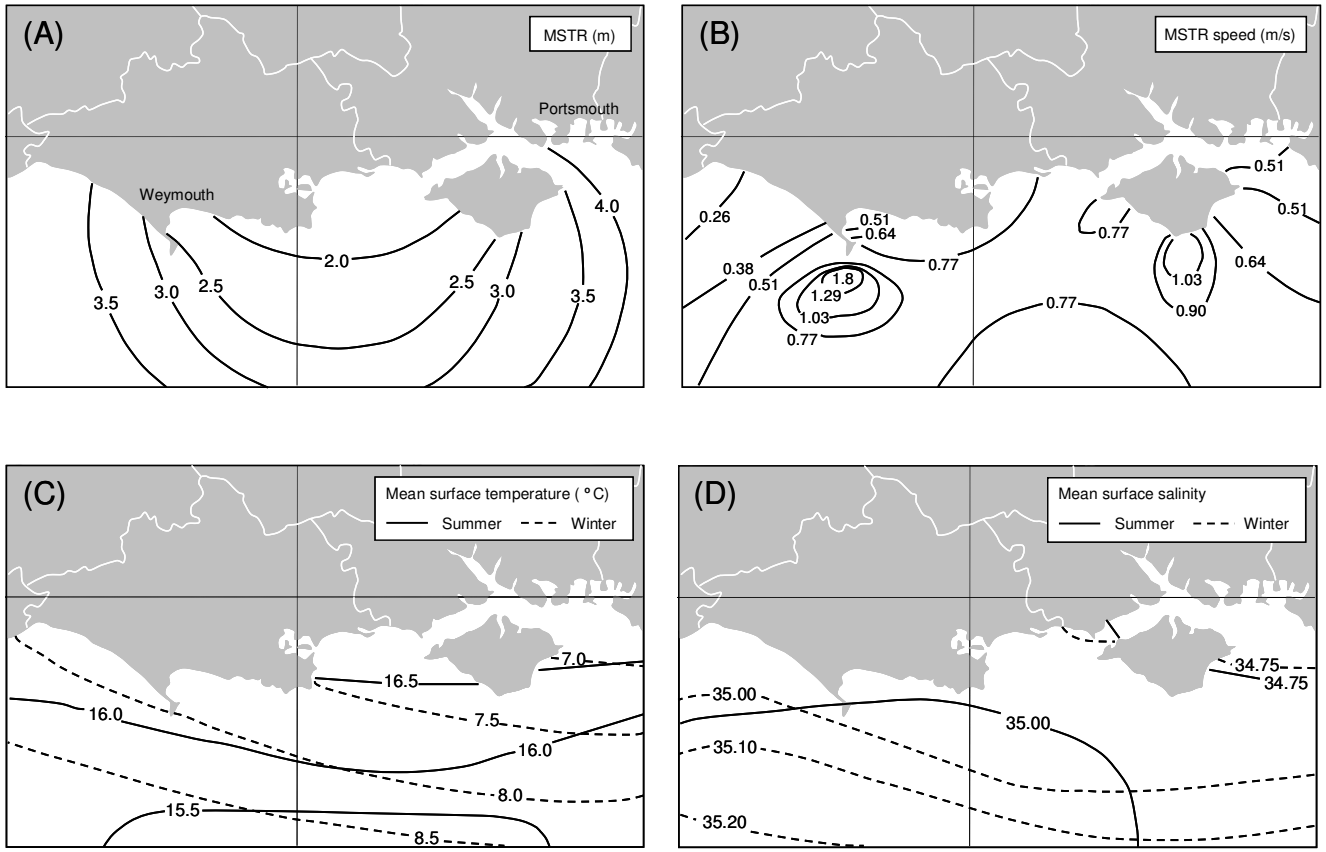

Figure 3.4.2 (A), Tidal range (m) at mean spring tides (Source: Lee & Ramster (1981) © Crown copyright); (B), Maximum tidal current speed (in m s^{-1}) at mean spring tides (Source: Sager & Sammler (1968)); (C), Mean surface water temperature in summer and winter, °C (Source: Lee & Ramster (1981) © Crown copyright); (D), Mean surface salinity of seawater in summer and winter (Source: Lee & Ramster (1981) © Crown copyright). These contours are redrawn with modifications from Barne et al. (1996a).

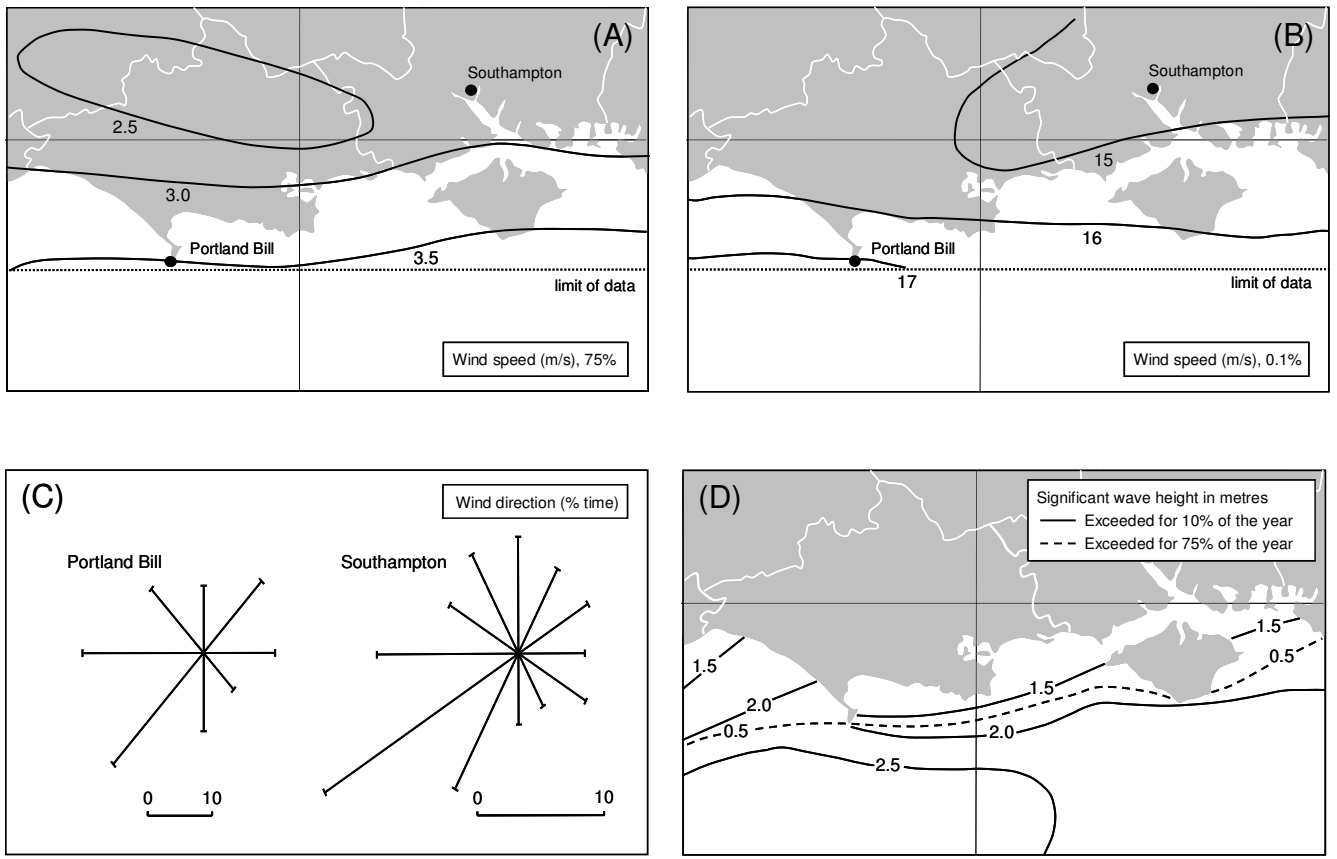

Figure 3.4.3 (A), Hourly-mean wind speed (in m s^{-1}) exceeded for 75% of the time: 1965-1973; (B), Hourly mean wind speed (in m s^{-1}) exceeded for 0.1% of the time: 1965-1973 (Source: Caton (1976)); (C), Wind directions at Portland Bill and Southampton (1916-1950) (Source: Hydrographic Department (1960a)); (D), Significant wave height (m) exceeded for 10% and 75% of the year (Source: Draper (1991)). These contours are redrawn with modifications from Barne et al. (1996a).

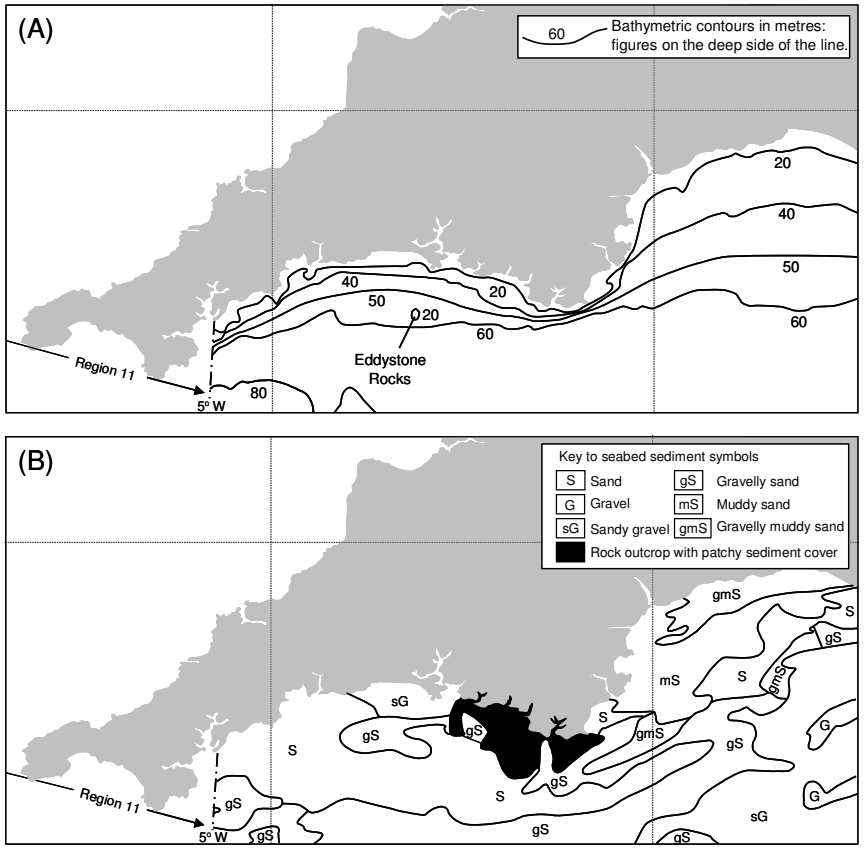

Figure 3.5.1 (A), Bathymetry (Source: British Geological Survey (1991)); (B), Seabed sediments (Source: British Geological Survey (1991), sediment classification modified after Folk (1954)). These contours are redrawn with modifications from Barne et al. (1996b).

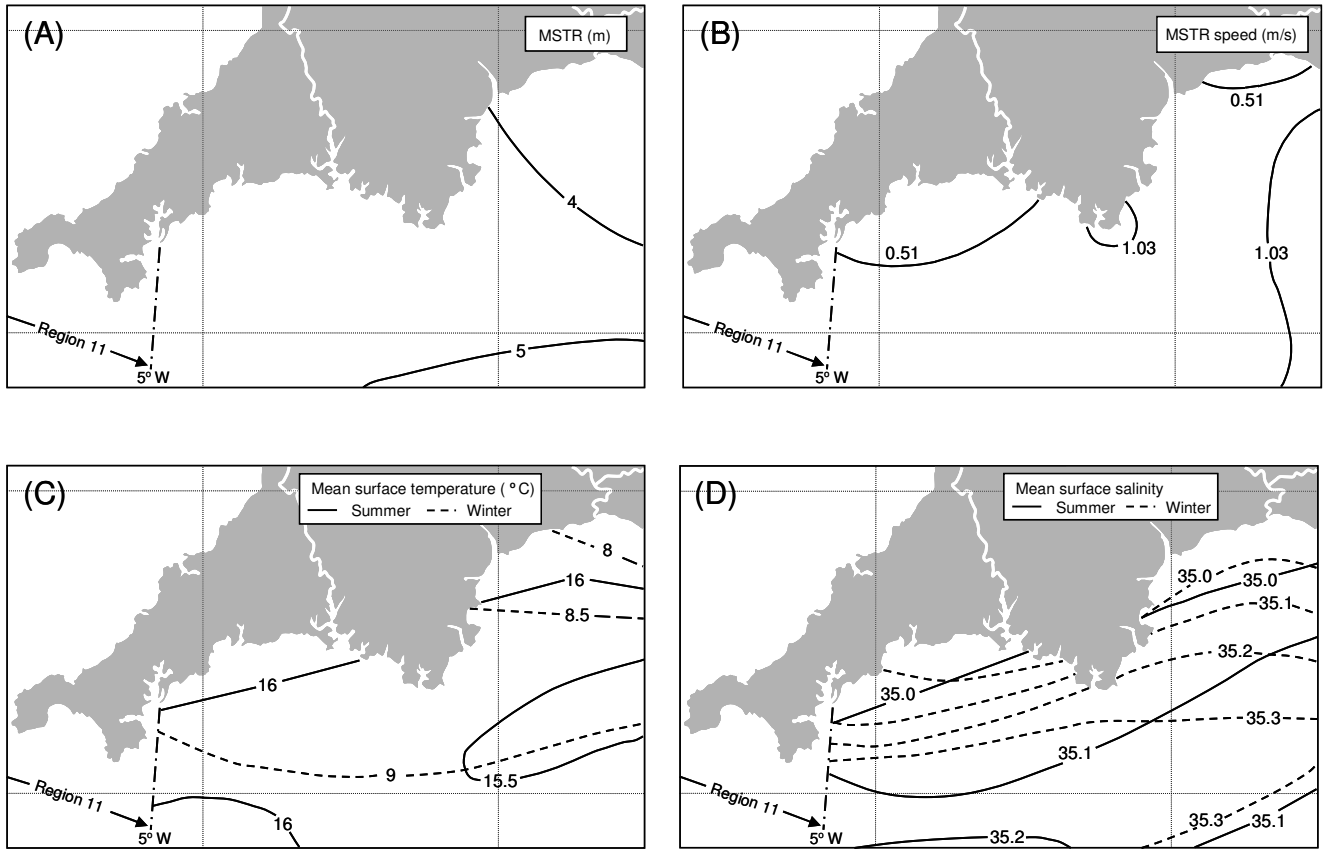

Figure 3.5.2 (A), Tidal range (m) at mean spring tides (Source: Lee & Ramster (1981) © Crown copyright); (B), Maximum tidal current speed (in m s^{-1}) at mean spring tides (Source: Sager & Sammler (1968)); (C) Mean surface water temperature in summer and winter, °C (Source: Lee & Ramster (1981) © Crown copyright); (D), Mean surface salinity of seawater in summer and winter (Source: Lee & Ramster (1981) © Crown copyright). These contours are redrawn with modifications from Barne et al. (1996b).

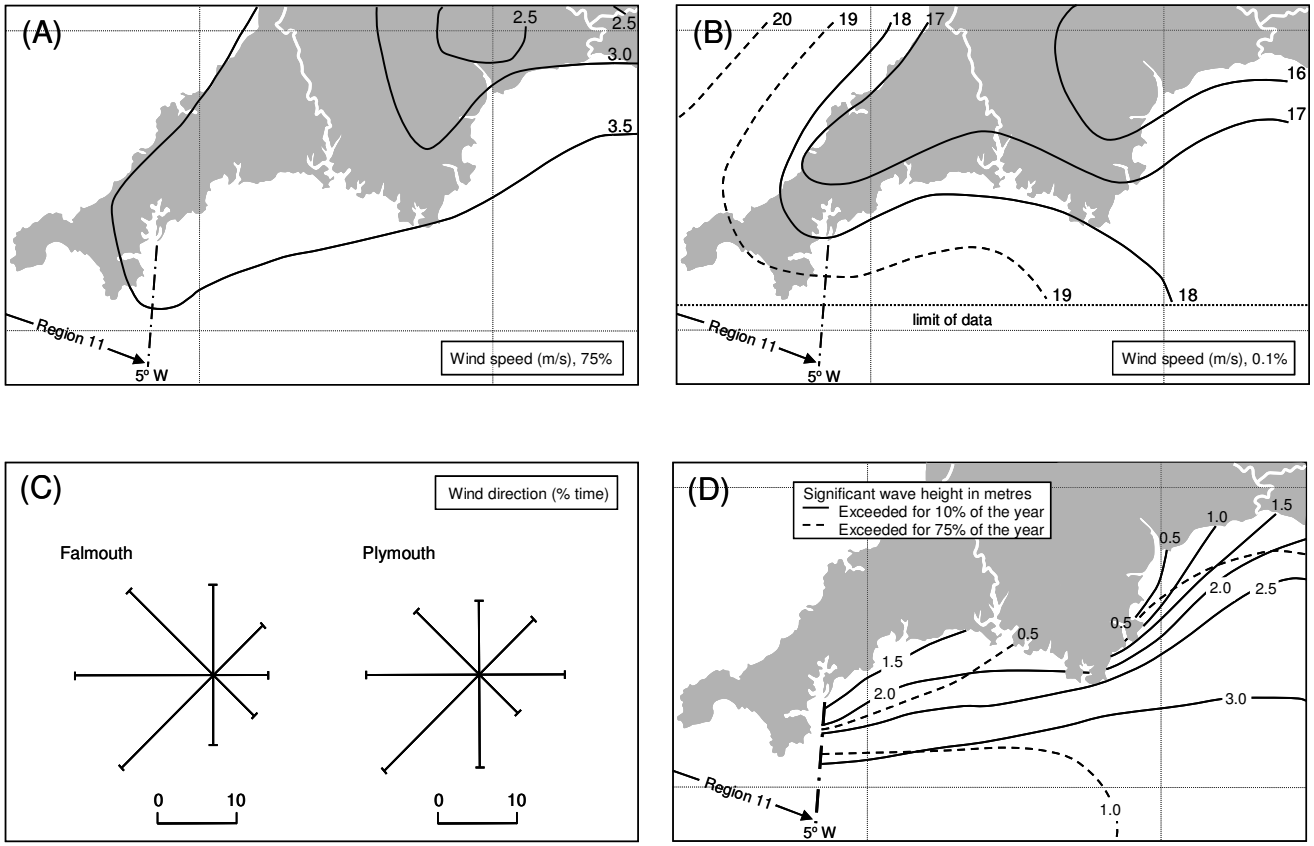

Figure 3.5.3 (A), Hourly-mean wind speed (in m s^{-1}) exceeded for 75% of the time: 1965-1973; (B), Hourly-mean wind speed (in m s^{-1}) exceeded for 0.1% of the time: 1965-1973 (Source: Caton (1976)); (C), Wind directions at Plymouth and Falmouth (1913-1950) (Source: Hydrographic Department (1984)); (D), Significant wave height (m) exceeded for 10% and 75% of the year (Source: Draper (1991)). These contours are redrawn with modifications from Barne et al. (1996b).

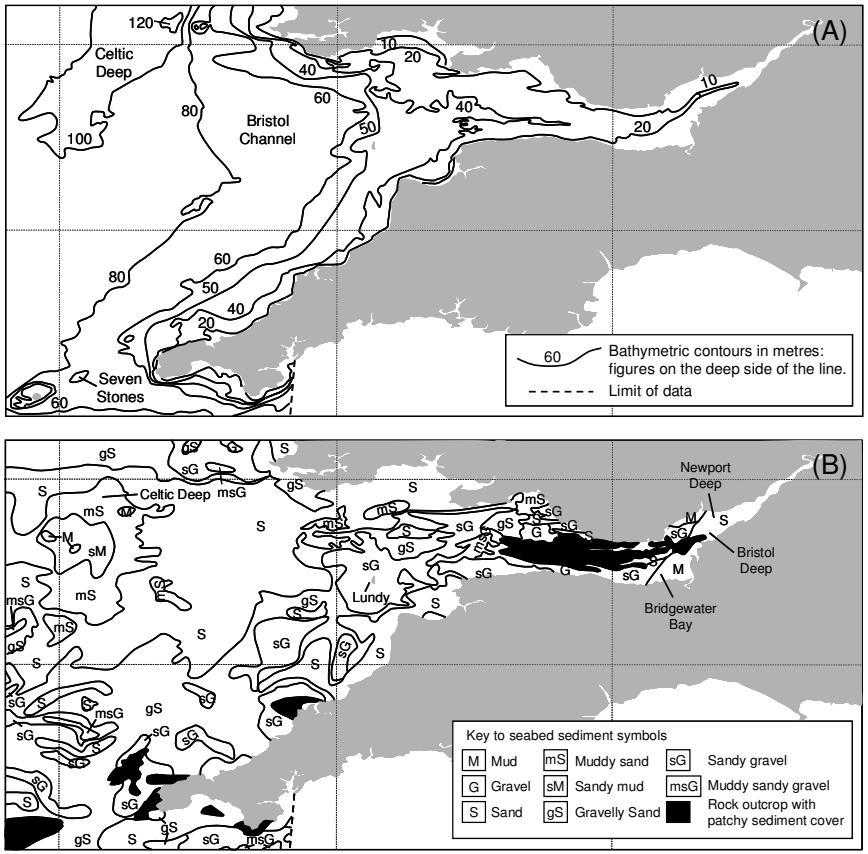

Figure 3.6.1 (A), Bathymetry (Source: British Geological Survey (1987)); (B), Seabed sediments (Source: British Geological Survey (1987), sediment classification modified after Folk (1954)). These contours are redrawn with modifications from Barne et al. (1996c).

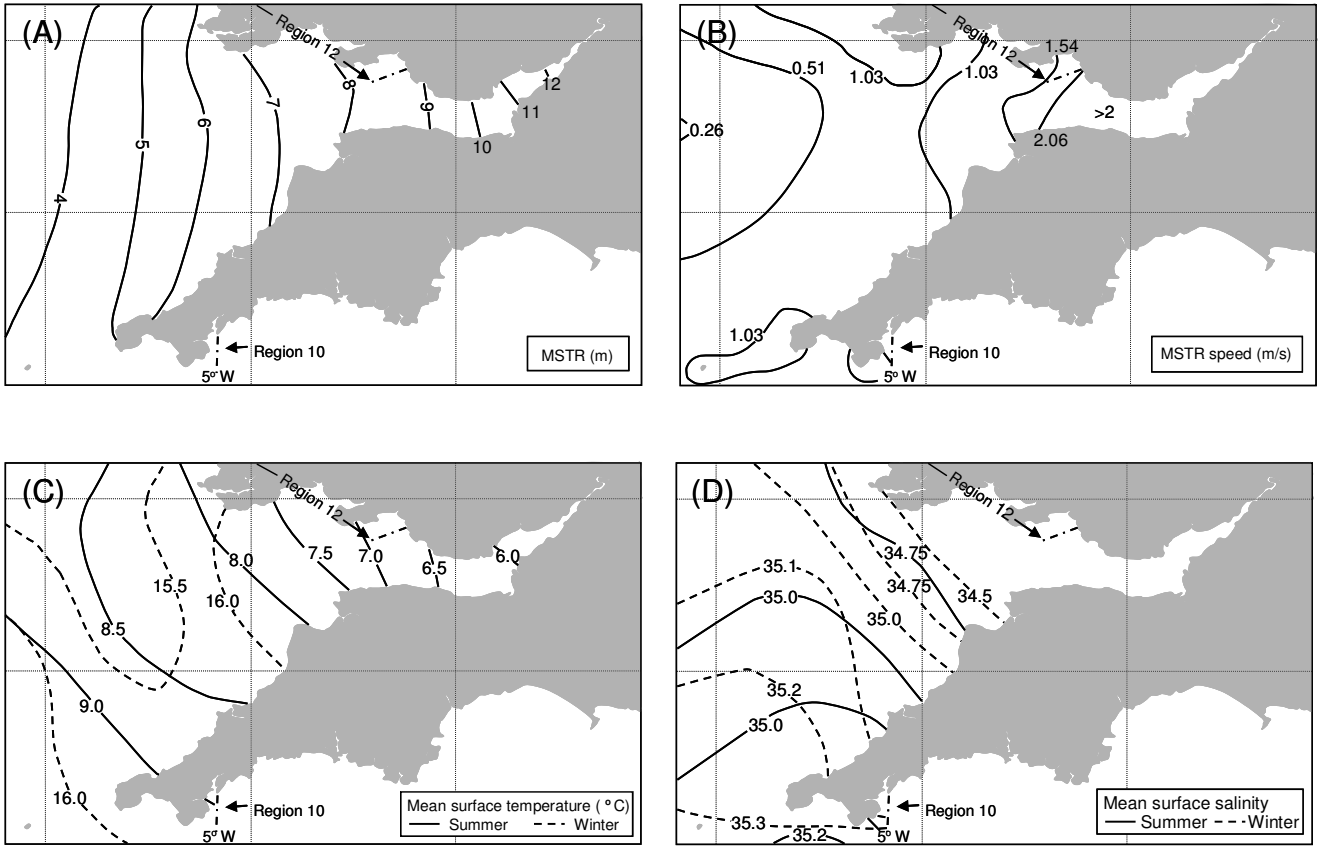

Figure 3.6.2 (A), Tidal range (m) at mean spring tides (Source: Lee & Ramster (1981) © Crown copyright); (B), Maximum tidal current speed (in m s^{-1}) at mean spring tides (Source: Sager & Sammler (1968)); (C), Mean surface water temperature in summer and winter, ºC (Source: Lee & Ramster (1981) © Crown copyright); (D), Mean surface salinity of seawater in summer and winter (Source: Lee & Ramster (1981) © Crown copyright). These contours are redrawn with modifications from Barne et al. (1996c).

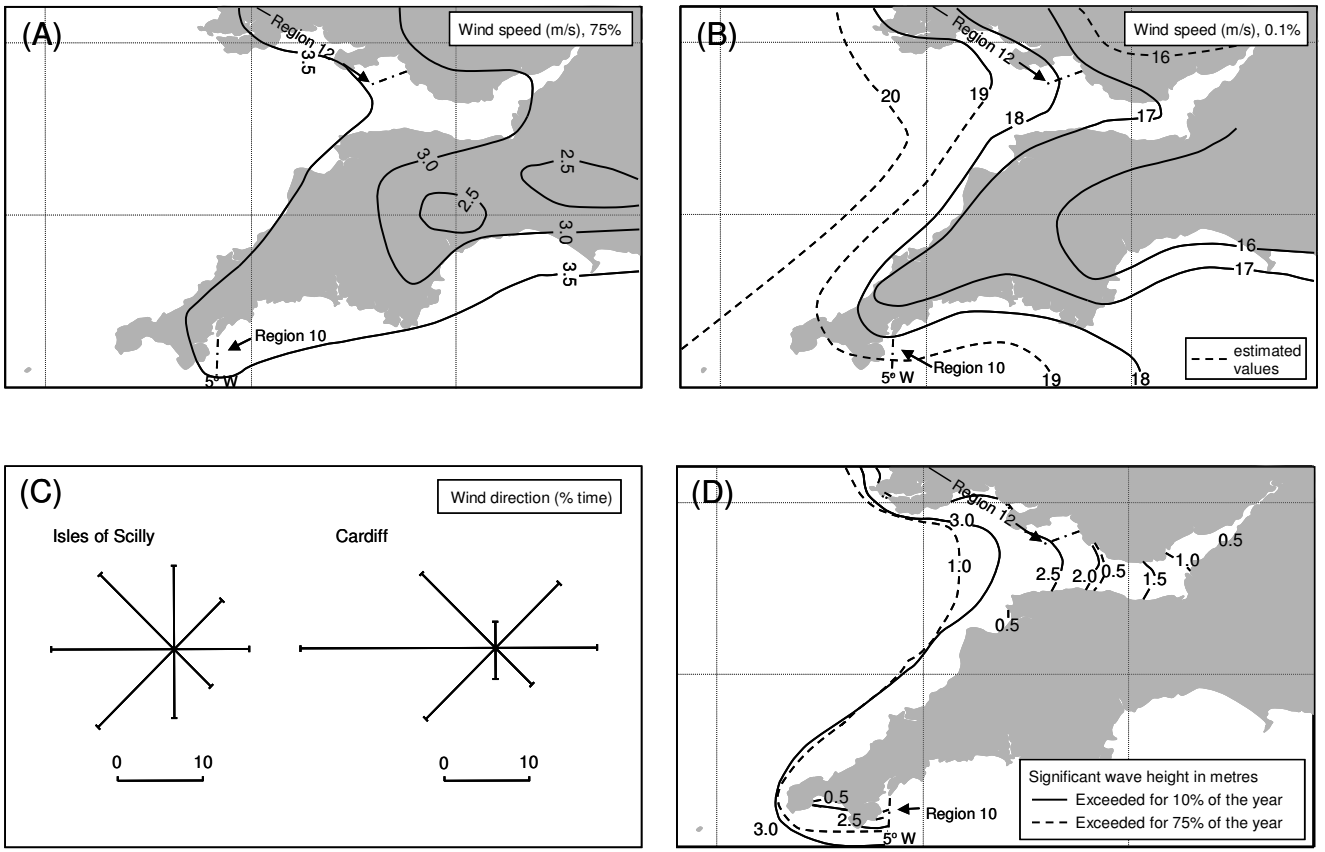

Figure 3.6.3 (A), Hourly-mean wind speed (in m s^{-1}) exceeded for 75% of the time: 1965-1973; (B), Hourly-mean wind speed (in m s^{-1}) exceeded for 0.1% of the time: 1965-1973 (Source: Caton (1976)); (C), Wind directions at Cardiff and on the Isles of Scilly shown as % of observations during the years 1916 - 1950. Flat calm (% of observations) = Cardiff (13.5%); Isles of Scilly (18%) (Source: Hydrographic Department (1960b)); (D), Significant wave height (m) exceeded for 10% and 75% of the year (Source: Draper (1991)). These contours are redrawn from Barne et al. (1996c).

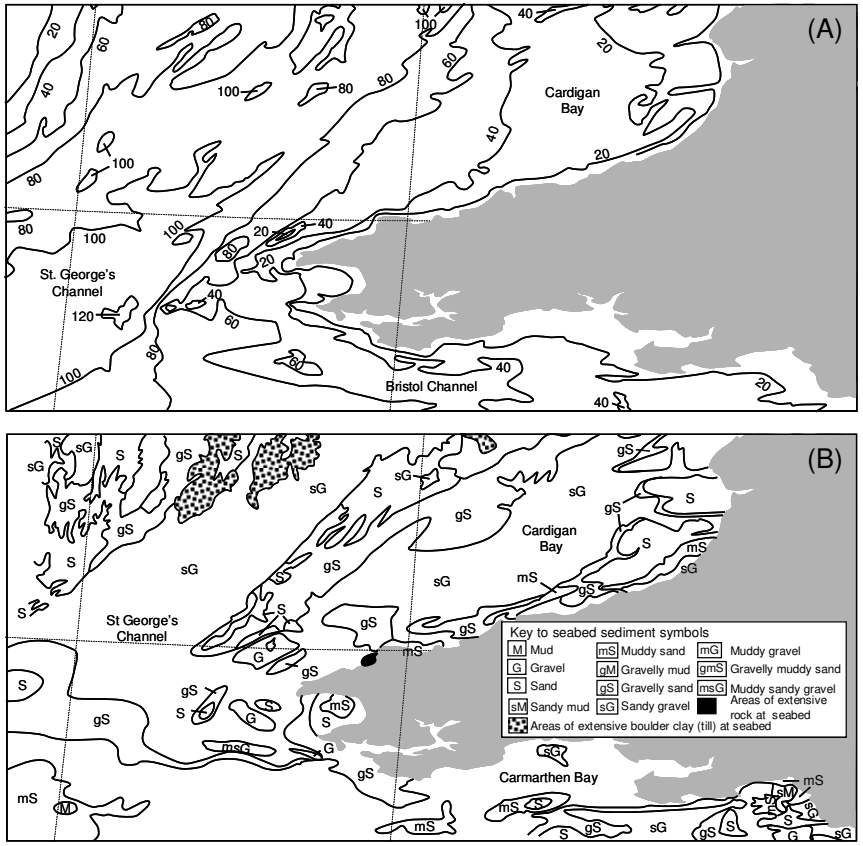

Figure 3.7.1 (A), Bathymetry (Source: British Geological Survey (1987)); (B), Seabed sediments (Source: British Geological Survey (1991), sediment classification modified after Folk (1954)). These contours are redrawn from Barne et al. (1995).

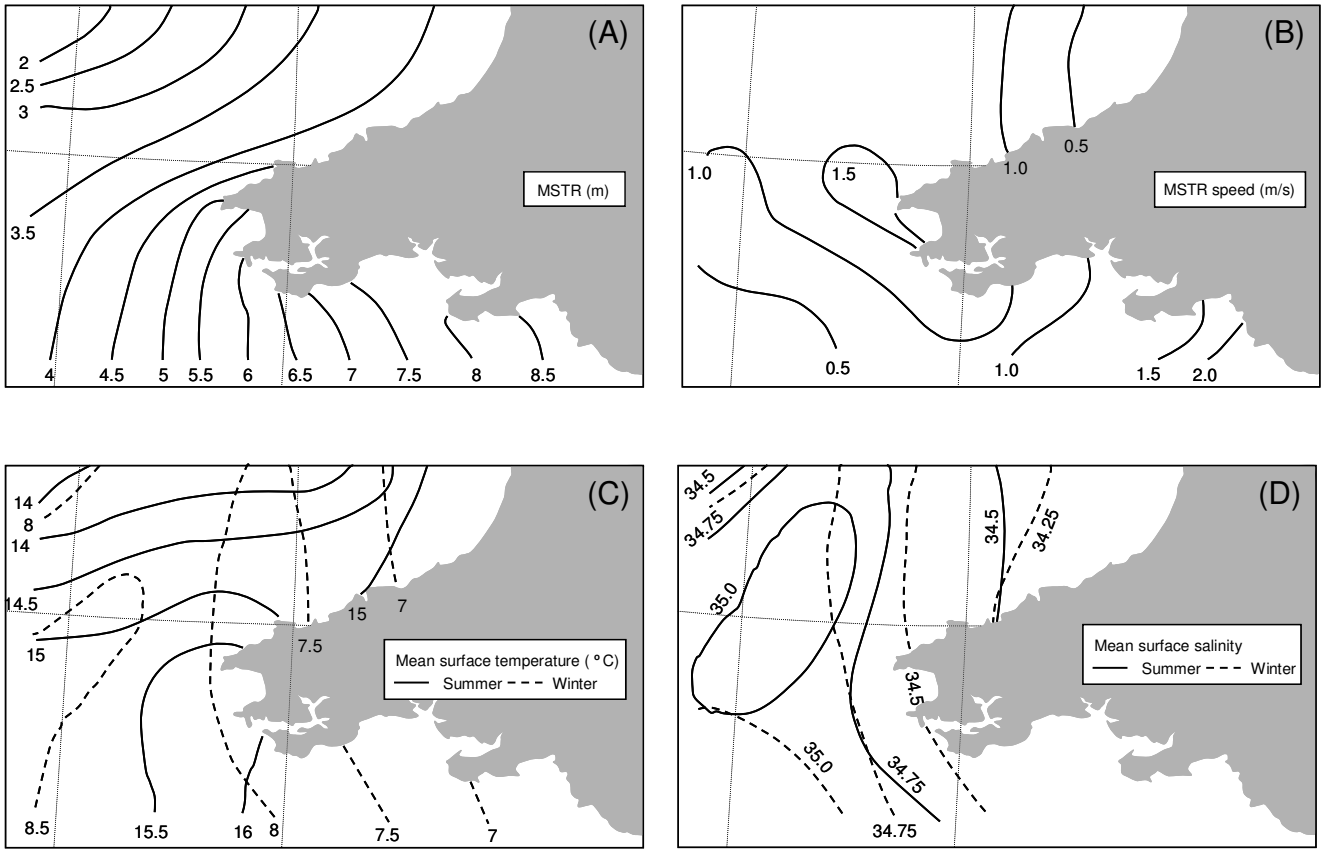

Figure 3.7.2 (A), Tidal range (m) at mean spring tides (Source: Lee & Ramster (1981) © Crown copyright); (B), Maximum tidal current speed (in m s^{-1}) at mean spring tides (Source: Sager & Sammler (1968)); (C), Mean surface water temperature in summer and winter, °C (Source: Lee & Ramster (1981) © Crown copyright); (D), Mean surface salinity of seawater in summer and winter (Source: Lee & Ramster (1981) © Crown copyright). These contours are redrawn from Barne et al. (1995).

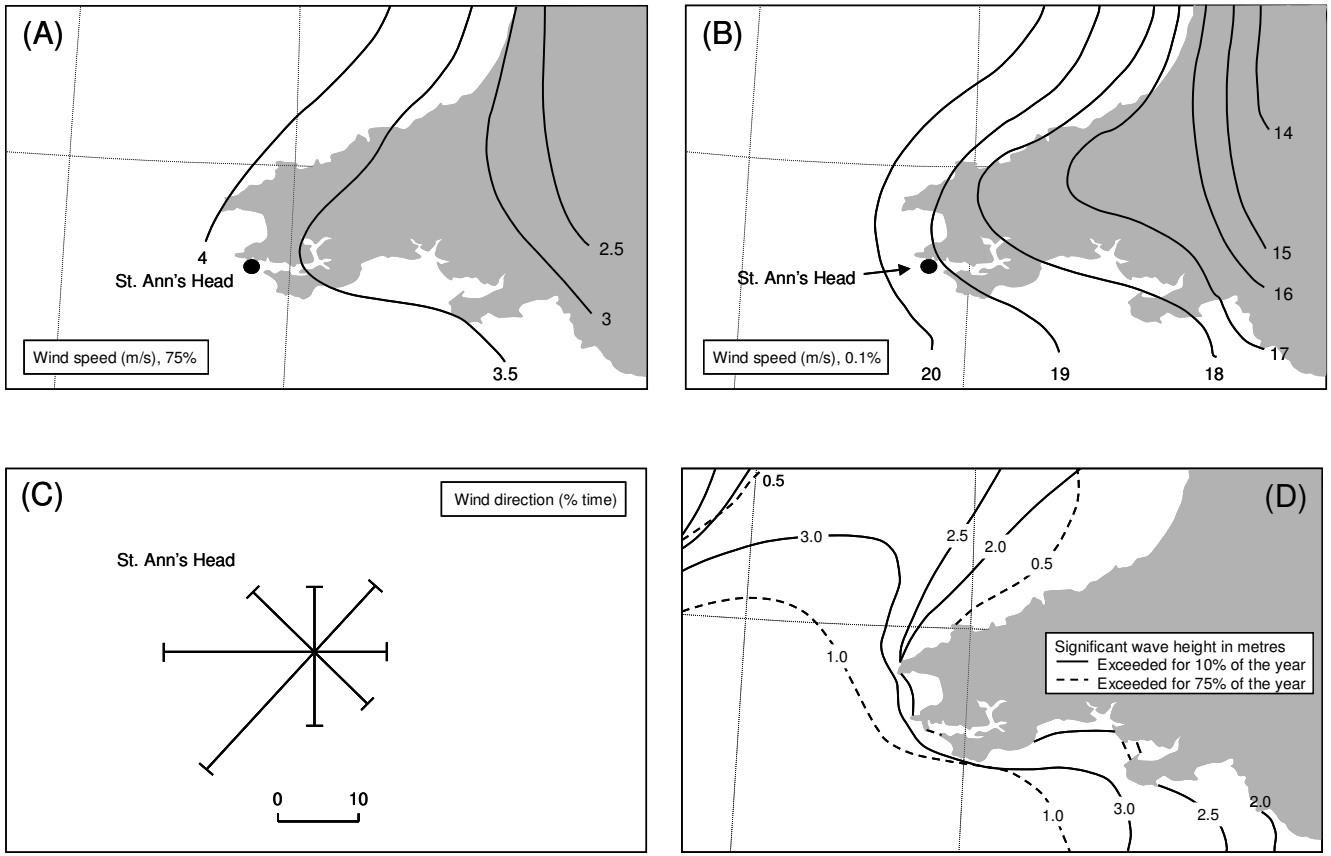

Figure 3.7.3 (A), Hourly-mean wind speed (in m s^{-1}) exceeded for 75% of the time: 1965-1973; (B), Hourly-mean wind speed (in m s^{-1}) exceeded for 0.1% of the time: 1965-1973 (Source: Caton (1976)); (C), Wind directions at St Ann's Head shown as % of observations through the years 1916 -1950 (Source: Hydrographic Office (1960b)); (D), Significant wave height (m) exceeded for 10% and 75% of the year (Source: Draper (1991)). These contours are redrawn from Barne et al. (1995).

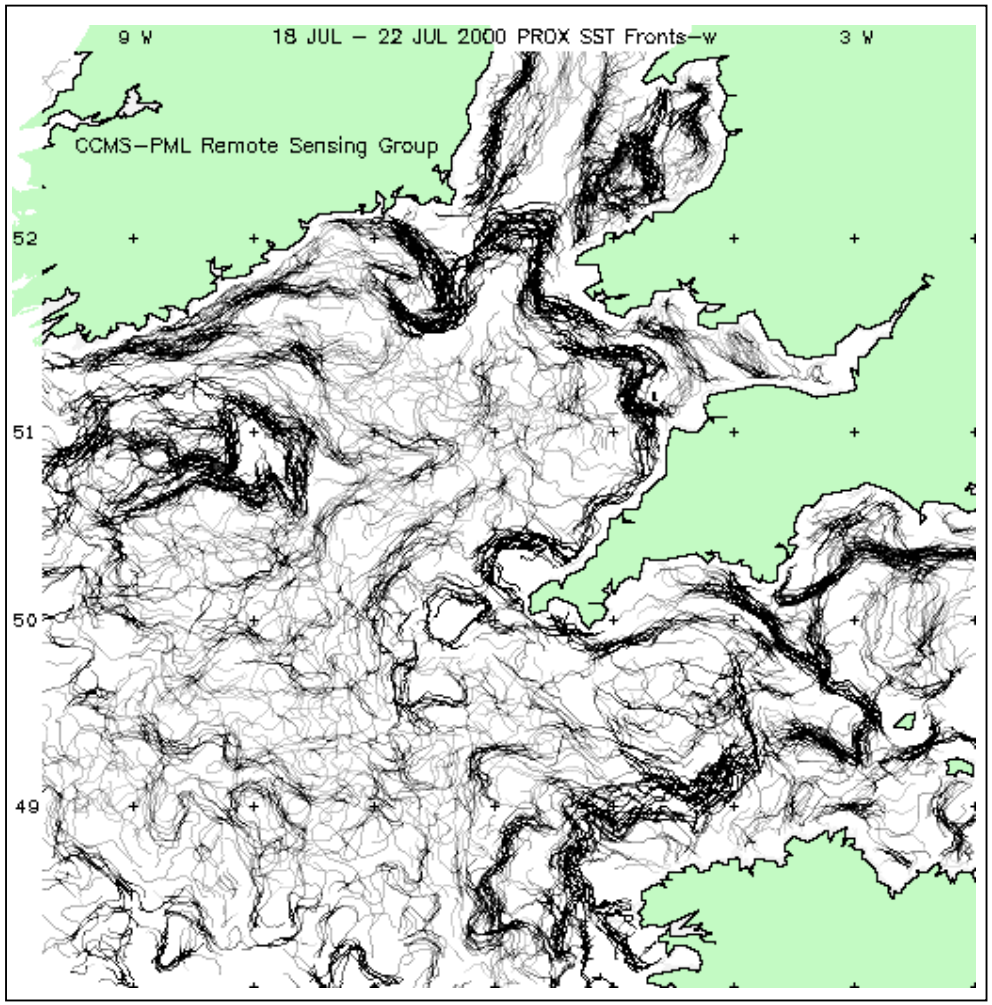

Figure 4.5, An example of a composite-front map of sea surface temperature that shows the frontal situation for the UK Western Approaches and much of the SEA8 region during 18 – 22 July 2000. (See also Figure 2.10 (A, B)). Reproduced by courtesy of Dr. Peter Miller, Remote Sensing Group, Plymouth Marine Laboratory, Plymouth PL1 3DH, UK.